



## Review

# Carbonaceous adsorbents in the removal of aquaculture pollutants: A technical review of methods and mechanisms

Jessica H. Taylor, Salman Masoudi Soltani\*

Department of Chemical Engineering, Brunel University London, Uxbridge UB8 3PH, UK



## ARTICLE INFO

## Keywords:

Adsorption  
Activated carbon  
Aquaculture  
Water treatment  
Antibiotic  
Heavy metal

## ABSTRACT

Carbonaceous adsorbents (CAs) are becoming increasingly popular owing to their low-cost, ease of preparation, and versatility. Meanwhile, aquaculture is becoming a fundamental food industry, globally, due to a wide range of advantages such as economic and nutritional benefits, whilst protecting the depletion of natural resources. However, as with any farming, the technique is known to introduce a plethora of chemicals into the surrounding environment, including antibiotics, nutrients, fertilisers and more. Therefore, the treatment of aquaculture effluent is gaining traction to ensure the sustainable growth of the industry. Although the existing mitigation techniques are somewhat effective, they suffer from degradation of the water quality or harm to local environments/organisms. This article aims to identify the sources and impacts of various aquaculture pollutants. After which the authors will provide an environmentally friendly and novel approach to the treatment of aquaculture effluent using carbonaceous adsorbents. The article will detail discussions about the product life span, including, synthesis, activation, modification, applications in aqueous media, regeneration and End-of-Life (EoL) approaches, with a particular focus on the impacts of competitive adsorption between pollutants and environmental matrices. Some research gaps were also highlighted, such as the lack of literature applying real-world samples, the effects of competitive adsorption and the EoL applications and management for CAs.

## 1. Introduction

Fish consumption is expanding annually across the globe, accounting for over a third of animal production, globally in 2013 (Anderson et al., 2017). This is due to the high nutritional values of fish, which contributes an average of 16.5% of all animal protein consumed in the human diet (Thilsted et al., 2016). However, the combination of the increasing demand for fish and the ever-increasing population, leads to sustainability issues with many natural resources becoming exhausted due to intensive traditional fishing methods. Therefore, alternative solutions have been implemented to prevent mass depletion or extinction of wild fish populations and irreversible damage to natural marine environments – the solution being aquaculture. The Food and Agricultural Health Organisation (FAO) defines aquaculture as “the farming of aquatic organisms including fish, molluscs, crustaceans and aquatic plants”.

Like other farming techniques, a “chemical cocktail” is administered to promote growth and prevent infection, consisting of a range of antibiotics, nutrients, hormones, and pesticides (Romero et al., 2021; Boyd and McNevin, 2015; Pauly and Froese, 2012; Lulijwa et al., 2020;

Dawood and Koshio, 2016; Watts et al., 2017). In Europe, there are extensive restrictions on the application of these chemicals. For example, antibiotics are typically administered therapeutically (only treating diseased animals), whereas in developing countries they are likely to be administered metaphylactically (group treatment) or prophylactically (preventative treatment), having detrimental impacts on surrounding environments (Rico et al., 2012; Miranda et al., 2018; Chen et al., 2015).

Despite the negative aspects associated with the aquaculture industry, there are many positive attributes, such as preventing the depletion of natural resources (Ahmed and Lorica, Apr 1, 2002; Pradeepkiran, 2019; Drakeford BM.). Additionally, the FAO has estimated that 12 million full time jobs were created in Asia in 2004, as a direct consequence as of the industry’s rapid expansion, and this figure has continued to rise with the expansion of the industry (Subasinghe et al., 2009). Therefore, to allow for the sustainable growth of the industry, research must be implemented to limit the pollution to surrounding environments, which is the basis of this article.

There are a range of techniques available to remediate both organic and inorganic pollutants in aqueous media, some examples being adsorption, precipitation, coagulation, flocculation, membrane

\* Corresponding author.

E-mail address: [Salman.MasoudiSoltani@brunel.ac.uk](mailto:Salman.MasoudiSoltani@brunel.ac.uk) (S. Masoudi Soltani).

Nomenclature			
CA	carbonaceous adsorbent	SDZ	sulfadiazine
AC	activated carbon	HM	heavy metal
ACF	activated carbon fibre	MG	malachite green
CF	carbon fibre	PAN	polyarylonitrile
CNT	carbon nanotube	DOM	dissolved organic matter
SWCNT	single walled carbon nanotube	IR	impregnation ratio
MWCNT	multiwalled carbon nanotube	HTC	hydrothermal carbonisation
FQ	fluoroquinolone	CVD	chemical vapour deposition
CIP	ciprofloxacin	MW	microwave
TC	tetracycline	S <sub>BET</sub>	Brunauer, Emmett and Teller surface area
OTC	oxytetracycline	q <sub>e</sub>	equilibrium adsorption capacity
SA	sulfonamides	C <sub>0</sub>	initial concentration
ERY	erythromycin	C <sub>e</sub>	equilibrium concentration
SMX	sulfamethoxazole	PZC	point of zero charge
TMP	trimethoprim	MTZ	mass transfer zone
SDM	sulfadimethoxine	Log K <sub>ow</sub>	octanol-water partition coefficient
		SPE	solid-phase extraction

filtration solvent extraction and more, each with their advantages and disadvantages (Table 1). However, many of the listed techniques aren't industrially viable due to high costs and disposal issues.

Of the remediation techniques, adsorption, is attractive owing to its low cost and simplicity, particularly when waste or recycled materials are employed as the adsorbent precursor. Adsorption processes can be classified into two categories, physisorption and chemisorption. Physisorption is a readily reversible process which occurs via weak intermolecular forces such as hydrogen bonding and van der Waals forces between the adsorbent surface and adsorbate molecule. On the other hand, chemisorption is more specific and irreversible, involving the

**Table 1**

Summary of the advantages and disadvantages associated with water treatment techniques.

Process	Advantages	Disadvantages
Adsorption	Cheap and simple High removal capacities Fast reaction kinetics Low energy Applicable to batch and continuous flow Non-selective	Regeneration can be expensive and reduces adsorption capacity Non-selective pH sensitive
Precipitation	Cheap and simple	Hazardous sludge produced Not suitable at low concentrations (<100 mg/L) (Chai et al., 2021).
Flocculation	Low operating costs Efficient removal of suspended solids and colloidal particles Bacterial inactivation capability	Hazardous sludge produced non-reusable flocculants and coagulants.
Membrane filtration	Simple and small-scale process No chemicals required Quick process Generates low volumes of solid waste.	Energy intensive Rapid membrane fouling High costs Limited flow rates.
Solvent extraction	Suitable for large scale operations with high contaminant load Simple process controls & monitoring.	Hazardous waste stream High capital cost Possible cross-contamination of aqueous streams
Biological	Rapid (aerobic digestion) High efficiency Natural breakdown of pollutants yields cleaner waste effluent	High energy input Large amounts of bio-waste Not suitable for some chemicals such as pharmaceuticals Slow (anaerobic digestion)

formation of covalent or ionic bonds, arising due to various functional groups on the adsorbent's surface (Chai et al., 2021).

Carbonaceous adsorbents (CAs) are extensively applied in process industries due to their versatility, coming in a range of forms including powdered, granular, fibrous etc. and are particularly attractive in adsorption fields owing to their high surface areas, tuneable porosity and surface chemistry, and exceptional chemical stability (Lee et al., 2014; Marsh and Rodríguez-Reinoso, 2006a; Świątkowski, 1999). Each type of carbon exhibits its own advantages and disadvantages; granular activated carbons (GACs) are the oldest CA having been commercially available since the early 1900 s, owing to simplicity of production. They may, however, suffer from slow reaction kinetics, poor selectivity and inaccessible porous networks (Yue and Economy, 2017a). Powdered activated carbons (PACs) benefit from increased surface areas and readily accessible porosity which can be attributed to the smaller particle size. The application of PAC at scale, however, is adversely associated with comparatively higher pressure drops. Additionally, disposal of PACs can create secondary environmental issues and would require additional waste management strategies.

CAs can also come in fibrous or tubular forms which when activated, benefit from enhanced surface area to aspect ratios which correlate with increased adsorption capacities (Lee et al., 2014). Additionally, they are easier to recover from solution. However, they are typically more expensive to produce, owing to more complex synthesis routes (Section 3).

When synthesising CAs for applications in aqueous media, there are a few key properties that must be considered to enhance adsorption capacity. Typically, high surface areas (> 700 m<sup>2</sup>/g) and ordered mesoporosity (i.e. pores with a diameter between 2 and 50 nm) are attractive for aqueous-phase adsorption due to enhanced diffusion of pollutants, which is often the rate limiting step (Ighalo et al., 2021; Hadi et al., 2015; Gang et al., 2021). In some cases, a hierarchical porous network may be desirable, since macropores (with diameters of > 50 nm) allow large molecules to enter the internal structure, mesopores facilitate the mass transfer of molecules and micropores (with diameters < 2 nm) enhance the surface area and subsequently increase the abundance of active sites for adsorption, particularly when smaller molecules are present (Yu et al., 2016). In addition to surface structure, surface functionality (i.e. surface chemistry) is also of particular importance since it determines the mechanism of adsorption (e.g. physisorption vs chemisorption). CAs contain a range of heteroatoms including oxygen, nitrogen and sulphur which exist as surface functional groups. Carboxyl, carbonyl, phenol, lactone and quinone groups are considered to be key in the uptake of both organic and inorganic pollutants and therefore, it is

imperative to introduce these groups into the structure via modification techniques (Bhatnagar et al., 2013) as detailed in Section 5.3 in this paper.

### 1.1. Motivation and summary of the paper

With the rapid expansion of aquaculture, there is growing concern about environmental pollution due to the “chemical cocktail” administered within the industry, creating human health and environmental hazards. This has led to a rise in Scopus indexed publications, from 5 to 624 between 1970 and 2022 (Fig. 1). This work aims to identify the key chemicals applied within the aquaculture industry, assess their environmental fate and persistence.

There after the authors aim to identify suitable techniques to remediate key pollutants using carbonaceous adsorbents (CAs), with the aim of creating a novel technology for in-situ removal of pollutants from an aquaculture setting. This will be achieved by discussing current synthesis, activation and modification techniques of CAs. Followed by scrutinising the literature for adsorption technologies which target antibiotics and heavy metals (HMs), in aqueous media; the importance of which can be observed by the dramatic rise in Scopus indexed publications from 11 to 4927 over the assessed 52-year period (Fig. 1).

In order to achieve this, over 200 Scopus-indexed articles, book chapters and governmental specifications have been studied. Forty-one articles relate to aquaculture practices, and the introduction of pollutants into natural environments. Whilst the remainder of the articles were used to examine the synthesis, activation, modification and adsorption practices of CAs.

## 2. The aquaculture industry

Seventy years ago, the aquaculture industry was sparsely heard of; however, due to pressures on natural environments, the industry has rapidly expanded at a rate of approximately 7.93% per annum, in comparison to traditional capture fisheries which have only expanded at a rate of 2.34% (Fig. 3, FishStat, FAO). This has made aquaculture the most rapidly expanding food sector globally, which is largely attributed to the widespread expansion in Asia (Fig. 2).

In 2013, aquaculture exceeded capture fisheries in production rates and has since continued to expand on a steep upward trajectory. Extrapolating the current data, it can be predicted that the total live weight of aquatic organisms produced by aquaculture could reach almost 200 million kg by 2050, due to the ever-increasing global demand for fish – being a highly nutritious food source. Combined with the limitations associated with capture fisheries such as the known pressures on wild fish populations - causing many populations to exceed their biological limits - the WWF has estimated that one-third of the assessed fisheries, globally have already exceeded these limits, leading to

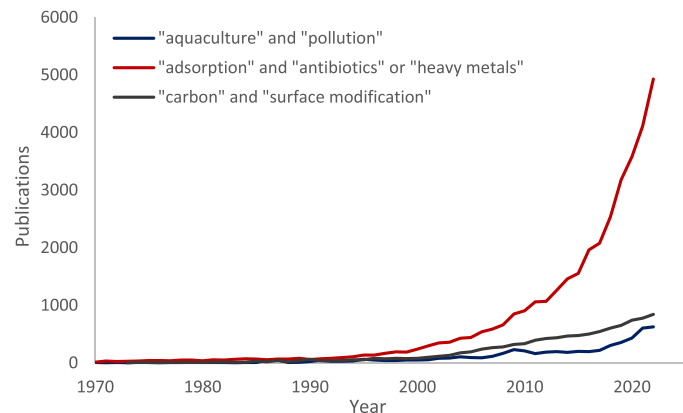


Fig. 1. – Scopus indexed publications per annum, between 1970 and 2022.

governmental legislation on fishing quotas which were first introduced in the 1970 s. This trend can be observed in Fig. 3, where there was a distinct decrease in the expansion rate of capture fisheries after 1970, and the industry has largely plateaued since the mid-1990 s. In comparison, aquaculture involves the breeding and farming of species in captivity, which eliminates pressures on wild populations, allowing for stable expansion rates.

Additionally, capture fisheries have been identified as one of the leading sources of marine litter, due to equipment being lost or discarded overboard whereas, aquaculture is carried out in a controlled environment with mostly fixed equipment, limiting the chances of litter. Finally, many traditional fishing techniques cause widespread damage to the environment, an example being trawling which consists of dragging nets anchored by heavy chains along the seabed, subsequently destroying the natural seabed and having detrimental impacts on bottom-dwelling plants and animals. Additionally, the disruption of the seabed also causes pollutants stored within the sediments, to become remobilised into the water column, leading to subsequent damages. In comparison, aquaculture cages are static, limiting damage to the seabed.

In addition to the environmental advantages, aquaculture also provides a range of social and economic benefits. For example, fish farming provides controlled access to target species of fish, ultimately reducing the cost, which allows developing countries to gain wider access to nutritious food sources. A key example where these positive impacts can be observed is salmon farming – one of the largest contributors within the aquaculture industry. Prior to the 1980 s, salmon was classed as a luxury product, but farmed salmon has since superseded the quantities of wild salmon caught across many continents, leading to quite dramatic drops in retail price, with some even referring to it as “the chicken of the sea” (Hannesson, 2003). Fig. 4 shows the global trends in salmon aquaculture versus capture fisheries. Salmon aquaculture has been rapidly expanding across Europe since the 1980 s and a similar trend has been observed in South America since 2010, both having significantly exceeded the amount of salmon produced by capture fisheries.

Despite the wide range of advantages, aquaculture comes with a host of disadvantages which must be considered and improved, to enable the sustainable growth of the industry. Aquaculture involves the farming of large numbers of fish in close proximity, which has a range of negative consequences such as, promoting the growth and spread of diseases as well as introducing large quantities of fish waste which contributes to eutrophication. In order to prevent mass deaths of fish, broad-spectrum antibiotics and herbicides are widely applied to combat infections and algae development, respectively. A host of nutrients and hormones are also administered to promote growth, allowing fish to reach maturity at faster rates and in turn, favouring increased profits. In addition to nutrients and hormones, selective breeding is a common practice within the industry to produce populations with desirable qualities such as increased growth rates, size and reproductivity. Over generations this can produce farmed populations with significantly different genetics when compared to wild populations; creating issues when farmed, potentially invasive species escape from aquaculture facilities.

Furthermore, the high density of fish within an aquaculture environment can cause a change to the surrounding water chemistry, which can vary significantly depending on the species, location and environmental conditions (Table 2) (Ahmad et al., 2021). Without proper management of water quality, environmental concerns are raised around reduced oxygen demand, organic pollution, eutrophication, excessive nutrients and chemical pollution. In order to limit these impacts, some countries such as Hawaii, Thailand and Taiwan have introduced water quality standards for aquaculture effluents such as pH, total suspended solids, biochemical oxygen demand and chemical oxygen demand.

### 2.1. Chemical use in aquaculture

This section will discuss the commonly applied chemicals within the

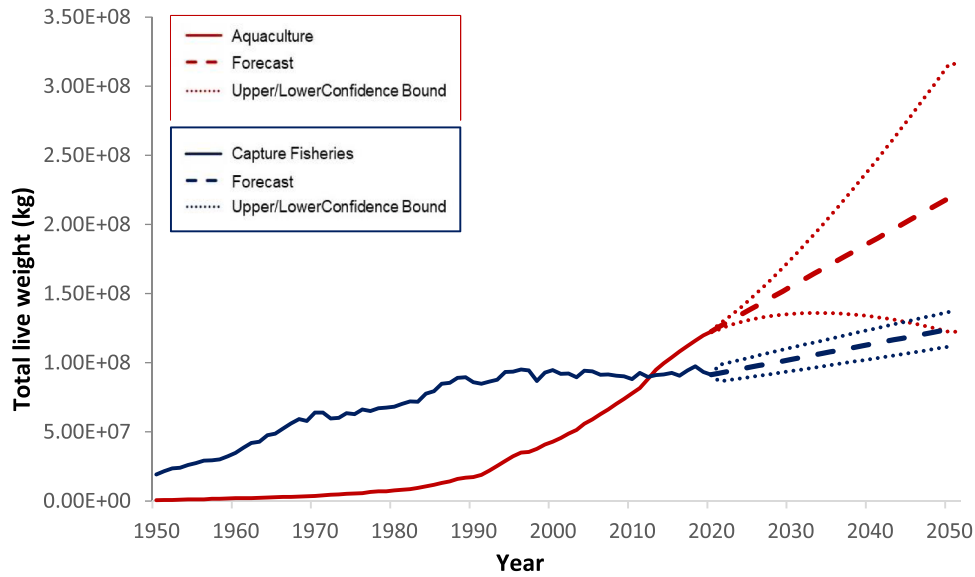


Fig. 3. Total live weight (kg) of products produced between 1970 and 2020, extrapolated to 2050, within aquaculture and capture fisheries.

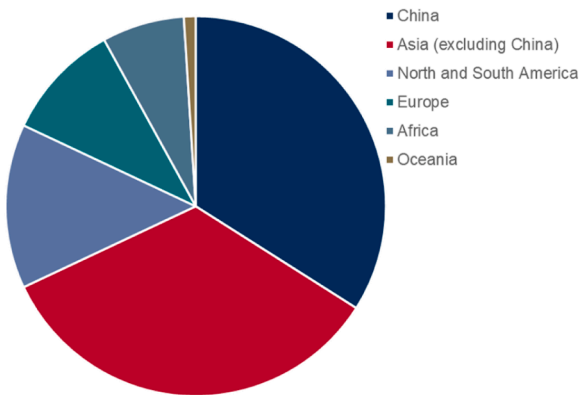


Fig. 2. Global contribution to aquaculture.

aquaculture industry and the subsequent impacts on the health of farmed animals and humans. Additionally, the environmental fate and persistence will be discussed.

2.1.1. Antibiotics

Aquaculture conditions typically create the ideal breeding ground for bacterial infections, owing to the large numbers of fish living in close proximity, this has led antibiotics to become one of the most widely applied chemicals within the industry. Antibiotic administration can vary globally depending on governmental regulations. The drugs can be administered prophylactically (preventive) metaphylactically (control) or therapeutically (curative). Typically, the former two methods are administered in the form of feed, bathing, or pond sprinkle, whereas therapeutic treatments are commonly in the form of injection.

Antibiotics can be grouped into three subcategories, namely, natural, semi-synthetic and synthetic. In the past, natural antibiotics such as chloramphenicol, erythromycin (ERY), tetracycline (TC) and oxytetracycline (OTC) were widely used in aquaculture; however, overtime, the effectiveness was reduced due to the development of resistance genes.

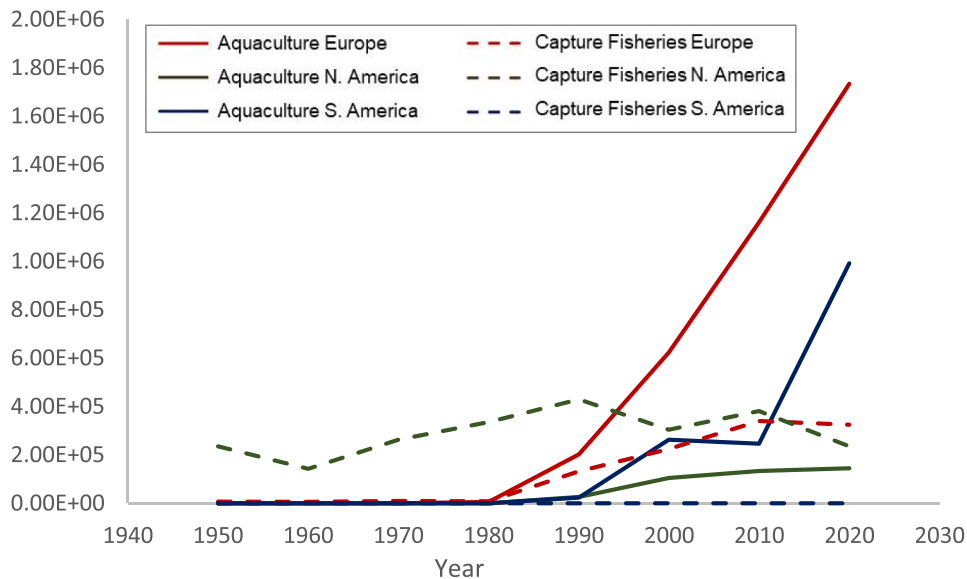


Fig. 4. Global trends in salmon aquaculture between 1950 and 2020.

**Table 2**  
Typical characteristics of aquaculture effluents.

Characteristic	Range
pH	6.30 – 8.78
Temperature (°C)	22.50 – 28.23
Dissolved oxygen (mg/L)	1.44 – 7.82
Chemical oxygen demand (mg/L)	10.00 – 140.2
TSS (mg/L)	347.68
Turbidity (NTU)	0.41 – 83.50
TDS (mg/L)	350.00 – 641.39
NO <sub>3</sub> -N (mg/L)	0.05 – 40.67
NO <sub>4</sub> -N (mg/L)	0.13 – 17.00
NH <sub>4</sub> -N (mg/L)	2.35 – 5.32
N <sub>2</sub> (mg/L)	1.59 – 53.15
PO <sub>4</sub> (mg/L)	3.60 – 19.26
Conductivity (µs/cm)	179.39 – 2883.55
Alkalinity	255.58
Salinity (ppt)	10.85

This has led to the wider application of semi-synthetic (many  $\beta$ -lactams) and synthetic (florfenicol, quinolones, and nitrofurans) antibiotics (Sun et al., 2020). Typically, quinolones are applied to treat skin diseases and septicemia in fish. Sulfonamides (SAs) and TCs are typically applied as prophylactics or therapeutics to treat bacterial infections.

Salmon farming consumes large quantities of antibiotics due to the susceptibility of the species to bacterial infections. ERY use is prevalent within the industry, to treat bacterial kidney disease. Additionally, TC and OTC are commonly administered to treat infections such as furunculosis and vibrio.

There have been several review articles that have summarised the antibiotic use in aquaculture globally over the decades. It has been observed that there has been an increase in the antibiotic classes applied in aquaculture between 1990 and 2018, despite the increasing governmental restrictions in some countries. Sapkota et al. found that there was an average of 7 antibiotic classes used between 1990 and 2007 (Sapkota et al., 2008), this number had increased to 67 antibiotic compounds by 2018, identified in the review article by Lulijwa et al (Lulijwa et al., 2020). This increase has been attributed to the widespread application of prophylactic drugs in Vietnam and China, which are two of the major producing countries in the aquaculture industry. It has been estimated that 105,000 tonnes of antibiotics are produced annually in China for animal consumption. Despite an overall increase in antibiotic consumption, there has been a reduction in antibiotic use in several countries, including Norway, UK, USA, Japan, and Thailand, due to improved administration techniques and therapeutic treatments such as probiotics. In the EU, TCs followed by SAs are the most prevalent antibiotics in aquaculture (Lulijwa et al., 2020). However, in general, information regarding antibiotic application globally is scarce; at present there are no databases regarding antibiotics use globally within the aquaculture industry, leading limited knowledge on exact figures. Despite widespread bans of certain antibiotics, they can still be detected in foodstuffs over a decade after the ban was introduced. For example, Vietnam introduced a ban on enrofloxacin in 2009; however, residues of the antibiotic in aquaculture products are still frequently detected to date. This can be attributed to the high stability of FQs due to their poor water stability and high log  $K_{ow}$  (> 1).

It has been reported that up to 90% of antibiotics administered in aquaculture are excreted as the parent compound or degradation products. Due to the open nature of aquaculture, these residues are readily transported into the surrounding environment. In intensive farming, up to 70% of all antimicrobials administered diffuse into the surrounding environment, having the ability to accumulate in sediments, animal tissue and more, leaving a negative impact on wild populations and ecosystems. Once in an environment, there are numerous physical, chemical, or biological degradation pathways for antibiotics, which are highly dependent on the physio-chemical properties, particularly the water solubility and octanol-water partition

coefficients of a compound (Table 3). Quinolone-type antibiotics in particular, are known to have high stability in aquatic environments, leading them to become identified as “pseudo-persistent” (Sun et al., 2020). Lulijwa et al., identified 14 antibiotics which exceeded maximum residue limits, with enrofloxacin and oxytetracycline most commonly exceeding the limits, particularly in Brazil, China Korea and Vietnam (Lulijwa et al., 2020). Many antibiotics have unidentified intermediate products during the degradation process which have unknown effects on ecosystems.

As mentioned above, intensive use of antibiotics in aquaculture leads to increased quantities of antibiotic residues in food for human consumption, from both wild and farmed fish populations, creating human health concerns. Antibiotic residues in the human diet can lead to adverse effects such as the development of AMR, toxicity through bioaccumulation and adverse drug reactions. AMR is of particular concern, with The World Health Organisation (WHO) identifying it as one of the top 10 threats of our generation (World Health Organisation, 2021). It has been estimated that AMR directly caused 1.27 million deaths worldwide, in 2019, and was associated with an additional 4.95 million deaths (Murray et al., 2022).

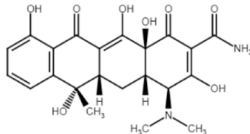
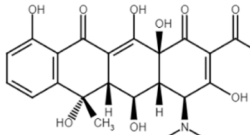
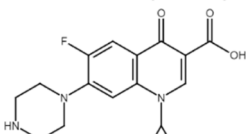
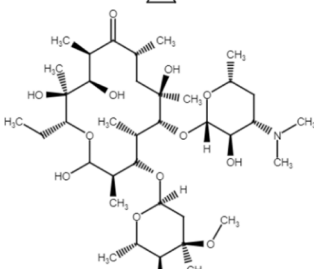
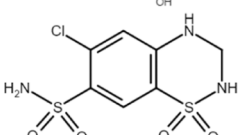
Commonly the impacts of antibiotic residue consumption are assessed using estimated daily intake as a percentage of acceptable daily intake combined with maximum residue levels (MRLs) to determine chronic effects; figures which are typically determined by the WHO and the Food and Agriculture Organisation (FAO) typically range between  $\mu\text{g}/\text{kg}$  –  $\text{ng}/\text{kg}$  (Monteiro et al., 2015). In the majority of cases, cultured products and surrounding wildlife were below the permissible levels posing low or no risk to human health. However, there are a number of cases where antibiotic residues exceed the recommended levels for human consumption, particularly in Brazil, China, Korea, and Turkey which have been discussed below.

Monteiro et al. applied liquid chromatography-mass spectrometry (LC-MS) to determine the quantities of antimicrobial residues in Nile tilapia (*Oreochromis niloticus*), reared via cage farming in Brazil (Monteiro et al., 2015). The study simultaneously assessed 12 common antimicrobials, including florfenicol, OTC and TC. Of the 12 assessed antimicrobials, OTC was found to be the most detected molecule, being found in nine fish samples across two of the four assessed farms. OTC levels ranged from 15.6 to 1231.8  $\mu\text{g}/\text{kg}$ , with one farm exceeding the MRL proposed by the EU of 100  $\mu\text{g}/\text{kg}$  (EMA, 1996a, 1996b). TC was identified in three samples; however, quantities were not specified in this study. Florfenicol was found at levels ranging between 521.2 and 528.0  $\mu\text{g}/\text{kg}$ ; below the MRL values set by the EMA (1000  $\mu\text{g}/\text{kg}$ ).

China is known for its extensive application of antibiotics, leading to a number of studies regarding the occurrence of antimicrobials in food stuffs. In 2015, a study was conducted to determine the occurrence, bioaccumulation and human dietary exposure of antibiotics in marine aquaculture farms surrounding Hailing Island, South China (Chen et al., 2015). Thirty-seven antibiotics were investigated from five different classes, including fluoroquinolones, TCs, sulphonamides, macrolides and ionophores. Water samples were collected, and the concentrated assays were obtained via solid-phase extraction (SPE). Whilst seafood samples were extracted using a combination of acetonitrile and citric acid buffer, followed by purification with SPE. The resultant samples were analysed using rapid resolution LC-MS. Fourteen out of the 37 antibiotics were identified in water samples, with salinomycin, sulfamethoxazole and trimethoprim being present in all samples. When analysing seafood, it was found that antibiotic concentrations in molluscs were relatively low with antibiotics only being identified in three samples. However, antibiotics were present in much higher quantities in crustaceans, particularly shrimp, having been identified in nine samples. Finally, antibiotics sulfamethoxazole (SMX) and trimethoprim (TMP) were detected in all young fish samples. Overall, fish were found to have the greatest EDI which was attributed to antibiotics being easily accumulated in fish tissues.

As can be seen from the discussion above, it is imperative to limit the

**Table 3**  
Chemical characteristics of antibiotics commonly applied in aquaculture.

Antibiotic	MW (g/mol)	pK <sub>a</sub>	K <sub>ow</sub>	Structure
Tetracycline	444.435	pK <sub>a1</sub> 3.30 pK <sub>a2</sub> 7.68 pK <sub>a3</sub> 9.69	-1.37	
Oxytetracycline	460.434	pK <sub>a1</sub> 3.27 pK <sub>a2</sub> 7.32 pK <sub>a3</sub> 9.11	-0.90	
Ciprofloxacin	331.346	pK <sub>a1</sub> 5.9 pK <sub>a2</sub> 8.9	0.28	
Erythromycin	733.93	8.88	3.06	
Sulfonamide	172.21	5.9	-0.09	

use of antimicrobials in aquaculture, and where required, to ensure that the parent compounds and subsequent residues are prevented from entering natural waters. Therefore, water treatment technologies need to be significantly improved in aquaculture settings.

Among existing technologies, adsorption is a potentially viable candidate to reduce the number of antimicrobials released into the environment, without introducing harmful by-products into the surrounding environment; having successfully been applied to a number of different antibiotic compounds, ranging from lab-scale to industrial effluents (Section 6).

### 2.1.2. Heavy metals

Heavy metals (HMs) can be defined as elements having an atomic mass and atomic density greater than 20 and 5 g/cm<sup>3</sup>, respectively (Raychaudhuri et al., 2021). They have unique chemical characteristics and can readily change valance depending on factors such as temperature, pH, salinity and oxygen content, typically existing as a divalent metal ion HM<sup>2+</sup>, or various hydroxide complexes HM(OH)<sub>x</sub>, at environmentally relevant conditions. HMs can be introduced into aquaculture via several different pathways such as nutrient sources, antifoulants, fertilizers and pesticides, which will be the subject of this section (Emenike et al., 2021a; Chanda et al., 2015).

There are approximately 15 HMs which can be classified as essential elements including copper, zinc, iron, manganese and cobalt, which are considered to be biologically important, being required in low concentrations (Table 4) to maintain physiological functions of cells. Fish have the ability to absorb the required minerals through their gills and skin; however, in cramped farming conditions the natural concentrations may not meet the total requirement, in which case, the elements are acquired

**Table 4**  
Dietary requirements of essential elements in fish (Chanda et al., 2015).

Metal	Dietary requirement (mg/kg)
Copper	3 – 5
Zinc	15 – 80
Iron	30 – 170
Manganese	2 – 30
Cobalt	0.05 – 1

through supplementary feed (Chanda et al., 2015; WEBSTER CD, LIM C. NUTRITION AND FISH HEALTH, 2019). Chanda et al. have summarised the deficiency syndromes which may be observed in different species of fish if these HMs are not present in high enough concentrations, which include conditions such as increased mortality, anaemia, haemoglobin suppression, poor hatching rates, skeletal abnormalities, reduced growth, muscular dystrophy and more (Chanda et al., 2015). Despite their biological importance, if the permissible level is exceeded, toxic effects may be observed.

Another common source of HMs in aquaculture are copper-based coatings for antifouling which are fundamental to extending the life of the cage nets. A key concern of net-biofouling is reduced water flow which can result in a reduction in oxygen supply and limited removal of waste within the fish cage. This ultimately makes the farmed animals more vulnerable to diseases; increasing the requirement for antibiotics, as discussed above. The most used antifoulants are copper (I) oxide and copper thiocyanate, which are sometimes combined with additives such as zinc or copper pyrithione (Emenike et al., 2021a). Despite being effective antifoulants, these compounds leach into the surrounding

environment overtime, readily accumulating in the surrounding water column and sediments, causing toxicity in non-target organisms. It has been estimated that copper and zinc concentrations are approximately 2 – 3 times higher in aquaculture areas where antifouling nets have been applied, when compared to those without.

HM application in aquaculture is of huge concern, causing detrimental impacts on human and environmental health. This is due to their environmental persistence combined with their ability to readily bioaccumulate in organisms, causing toxic effects even at low concentrations. In fact, it has been well documented that HMs can impact fish in a variety of ways, including neurotoxic and genotoxic effects, damage to the respiratory, circulatory and reproductive systems and reduced growth rates and development, all of which ultimately lead to reduced life spans and higher rates of mortality.

### 2.1.3. Pesticides and Herbicides

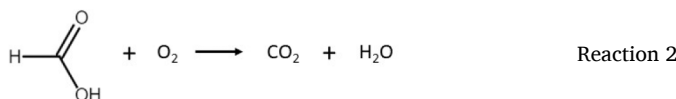
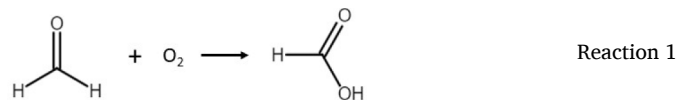
Pesticide treatments are common in intensive aquaculture to prevent the growth of common parasites. Treatments can be administered using several techniques such as application directly to a tank, where in some cases a curtain may be temporarily installed to retain the chemicals, bathing fish or in some cases it is administered in feed (Boyd and McNevin, 2014). Common pesticides in aquaculture include formalin, copper sulphate and hydrogen peroxide with the former compound being the most widely applied globally.

Formalin is an aqueous solution consisting of formaldehyde (37 – 40%) in methanol (10 – 15%) and water. It is a particularly attractive, due to its versatility in effectively treating a range of fin, skin and gill diseases whilst also controlling parasites due to the high chemical reactivity of formalin with biological macromolecules (e.g. DNA, RNA, polysaccharides etc.) (Boyd and McNevin, 2014; Tavares-Dias, 2021; Leal et al., 2018; Bills et al., 1977). Studies have suggested that formalin reacts with macromolecules via inter- and intra-molecular crosslinking, resulting in a change in the physicochemical properties, ultimately denaturing the macromolecule. Once in an environment, formalin is decomposed via chemical and biological processes, with an estimated half-life ranging from 1 to 400 days. Due to the short half-life, studies have confirmed that formalin does not accumulate in the edible tissue of aquatic animals and therefore, posing little threat for human consumption. However, it is widely agreed that formalin is toxic or fatal to humans at high concentrations, posing health concerns for those administering the treatment.

Unfortunately, formalin has a range of disadvantages, such as formaldehyde being extremely toxic to fish and aquatic plants, with toxicity increasing with rising concentration and prolonged exposure times; however, toxicity limits can vary significantly between species, the lethal concentration of formalin on a range of species has been reported elsewhere (Boyd and McNevin, 2014; Tavares-Dias, 2021; Leal et al., 2018). The most reported consequences of formalin application to fish are permanent damage to the gills and mucous cells; however, impacts to the blood and hypochloraemia have also been reported (Leal et al., 2018). Several factors can have a significant impact on the toxicity of formalin to fish including, water hardness, temperature, dissolved oxygen, salinity and DOM. Bills et al. found soft water (pH 9.5) caused formalin to become more toxic to fish, than hard waters with lower pH, meaning lower concentrations of formalin should only be applied when water hardness is less than 100 mg/l of calcium carbonate (Leal et al., 2018; Bills et al., 1977). Similarly, higher levels of salinity cause a decrease in toxicity of formalin due to the associated increased levels of calcium and magnesium.

A significant issue associated with the widespread application of formalin on fish health is oxygen depletion. This phenomenon occurs due to the conversion of formaldehyde to formic acid via oxidation (Reaction 1), which then undergoes additional reactions mediated by microorganisms to produce carbon dioxide and water (Reaction 2) (Leal et al., 2018). Some studies have suggested that applying 5 mg/L of Formalin to an aquatic environment removes 1 mg/L of dissolved

oxygen, which is a major concern since the average dissolved oxygen in freshwater typically ranges between 6.5 and 8 mg/l, and between 7 and 8 mg/L in saline conditions. Furthermore, formalin is a known algaeicide, resulting in further reductions in dissolved oxygen levels due to reduced photosynthesis.



Copper sulphate is another common algaeicide used in aquaculture. It is typically used to treat blue-green algal blooms. Blue-green algae can omit odorous compounds such as geosmin and methylisoborneol which are readily absorbed by fish, leading to undesirable flavours in products. Copper sulphate treatments are common practice in the United States to treat pond-reared fish such as channel catfish and shrimp. At present, there are no exact figures on the total quantities of copper sulphate applied in aquaculture. However, Boyd et al. have estimated that approximately 2400 tonnes of copper sulphate (612 t copper) may be applied annually in catfish farming in the US. The impacts of copper on human and environmental health have been previously discussed in Section 1.1.3.

Malachite green (MG) is a common dye, effective at treating protozoal and fungal infections leading to extensive application within the aquaculture industry. This is particularly concerning due to the toxicity and bioaccumulative potential to aquatic animals; this ultimately poses risks to human health via food consumption since malachite green is a multi-organ toxin.

## 3. Synthesis of carbonaceous adsorbents for applications in aqueous media

This section discusses several carbonaceous materials commonly discussed within literature, providing a timeline about how precursors are processed via pyrolysis, synthesis, activation, and modification to create adsorbents suitable for applications in *aqueous media*. The wide range of carbonaceous materials available leads to significant variation in chemical and mechanical properties, in turn, leading to differing activation and modification conditions, as discussed in Sections 5.2 and 5.3.

### 3.1. Synthesis of carbonaceous adsorbents

Carbonaceous materials exist in a variety of forms with a range in physicochemical properties. Carbonaceous materials are typically grouped according to their particle size and shape (e.g. powdered, granulated, fibrous, spherical etc.) and are the *precursors* for the synthesis of carbonaceous adsorbents. There are several factors that must be considered during precursor selection, for example, waste materials (e.g. food and plant waste etc.) are particularly attractive due to their increased sustainability and low cost. However, waste materials are more likely to have impurities present which may hinder adsorption capacity, or require further processing steps, such as acid washing. Whereas non-waste materials such as CFs and CNTs benefit from higher purity but are typically more expensive. Overall waste or recycled materials are more attractive owing to their increased sustainability, despite a potentially lower adsorption capacity – however this is highly dependent on the techniques employed during synthesis, activation and modification.

Furthermore, the physicochemical properties of various carbonaceous materials will dictate the methods employed in their conversion to CAs, which have been reviewed in the following sections.

Carbonaceous materials are often carbonised prior to activation to increase the percentage of fixed carbon within the material, whilst also improving thermal and chemical resistance (Hassan et al., 2020). Carbonisation is a common thermal decomposition technique, applied to develop a rigid, cross-linked carbonaceous framework. This is achieved by applying pyrolysis techniques, which cause volatiles and other non-carbon species such as heteroatoms to be burnt off in the form of carbon monoxide, oxygen, hydrogen, nitrogen, methane, and water (Hassan et al., 2020). Additionally, during this process, the structure undergoes a series of dehydrogenative condensations leaving a planar, graphene-like structure consisting of largely aromatic ring systems with graphite-like interstices between the sheets (Fig. 5). These spaces are often blocked with various products and tar during the decomposition process. The key parameters to consider when determining the carbonisation methodology are temperature, hold time and heating rate, which can vary quite significantly for different carbonaceous materials (i.e. precursors) due to their differing structures and mechanical stability.

In the following sections three types of CAs have been discussed in depth, namely, activated carbons (ACs), activated carbon fibres (ACFs) and carbon nanotubes (CNTs), because they have been widely applied in liquid-phase adsorption. Additionally, synthesis routes are relatively simple and low-cost in comparison to other CAs, such as graphene.

### 3.1.1. Activated carbons

Activated carbons (ACs) have been synthesised from a wide range of materials such as bamboo, peat, petroleum pitch, sewage sludge and many more. Precursor selection is an important aspect in the production of ACs since it has a large impact on the physical and chemical properties of the resultant ACs (Lewis, 1982). The ideal AC precursor used in carbonisation, is widely available, at a low cost, consisting of a carbon-rich framework with a low inorganic content - making biomass a very attractive precursor (Dqbrowski, 1999). The carbonisation would then lead to a porous, carbon-rich structure. This resultant porous structure, however, would normally require further treatment to enhance the porosity - a process referred to as *activation*.

Prior to carbonisation, the raw material normally goes through some pre-treatment stages, (e.g. grinding/milling). The extend of the grinding/milling process largely depends on the application, having a notable impact on the properties of the to-be-prepared AC. For example, smaller particle sizes have an increased surface area to volume aspect ratio, ultimately impacting the adsorption kinetics, with studies showing

that a smaller particle size (1 – 2 mm) can reach the equilibrium adsorption capacity in a third of the time when compared to larger particles (2.8 – 4 mm) (Lua and Guo, 2001). Additionally, particle hardness and density can have an impact on adsorption capacity, with coarser particles typically having slightly lower surface areas, due to the requirement of harsher conditions to etch pores into the carbon surface (Şentorun-Shalaby, Jan 21 et al., 2006). For example, wood-based carbons typically have a low hardness and density, resulting in large pore volumes; characteristics that make them attractive for aqueous phase applications (Świątkowski, 1999).

Pyrolysis is most commonly used for the carbonisation of AC precursors, which is conducted in an inert atmosphere (usually N<sub>2</sub> or Ar), typically at temperatures below 800 °C (Amer and Elwardany, 2020; Strezov et al., 2007; Ighalo et al., 2022). The process breaks down organic matter such as biomass into carbon-rich biochar and waste products, namely: carbon dioxide, carbon monoxide, hydrogen, short chain hydrocarbons and liquid products (bio-oil and tar). Pyrolysis can be divided into three sub-categories depending on the heating rate, namely, slow-pyrolysis, intermediate-pyrolysis and fast-pyrolysis, with the slower techniques having a lower heating rate (Table 5). Pyrolysis temperature and heating rate have significant impacts on the resulting products. Excessively increasing temperature is unfavourable for adsorbent preparation since it results in decreased solid and increased vapour yields, which are subsequently condensed and are subsequently converted to liquid waste. However, as the temperature is raised, volatile matter is expelled from the solid structure resulting in biochars of greater quality, particularly for application as adsorbents (Ioannidou and Zabaniotou, 2007).

Recently, attention has turned to hydrothermal carbonisation (HTC), which is carried out in the presence of subcritical liquid water. The technique benefits from lower temperatures (180 – 250 °C) and reduced residence times; however, the process requires a pressurised vessel, typically ranging between 1 and 40 bar (Bevan et al., 2021). A key difference between HTC and traditional pyrolysis techniques, is the ability to process biomass with a higher moisture content (75 – 90%) which significantly reduces energy consumption, which would be used to dry the feedstock. However, there is lack of knowledge regarding the chemistry and mass transfer mechanisms of HTC, preventing its widespread application in industry (Heidari et al., 2019).

### 3.1.2. Carbon fibres

According to The International Union of Pure and Applied

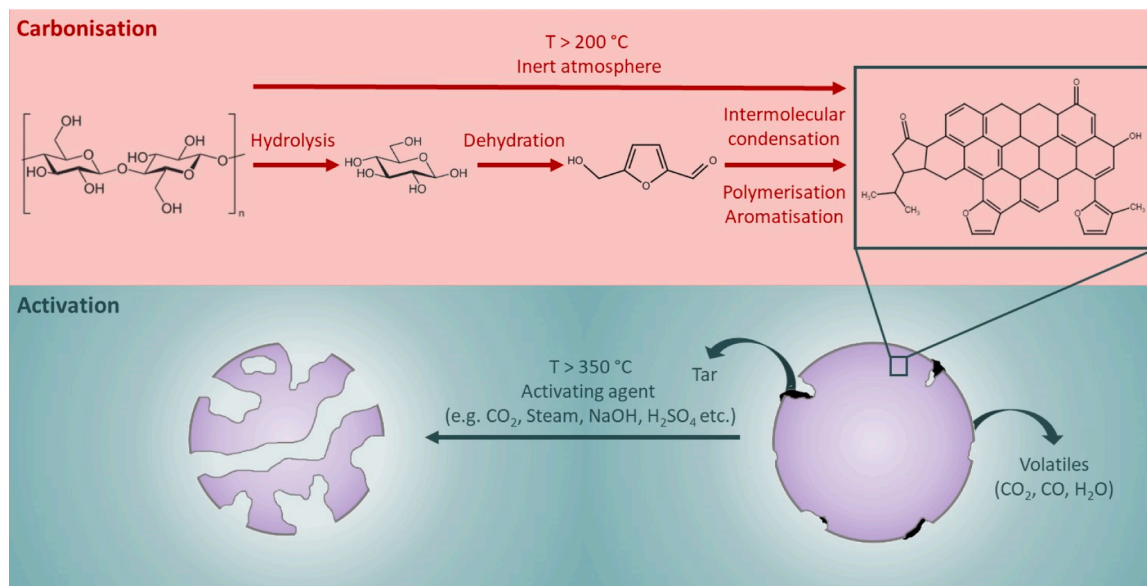


Fig. 5. Schematic to demonstrate the changes to a high-cellulose content precursor throughout the carbonisation and activation stages of a CA preparation.



**Table 5**  
Comparison between carbonisation technologies.

Process	Temperature (°C)	Hold Time (min)	Pressure (bar)	Heating Rate (°C/min)	Product distribution (weight %)		
					Solid	Liquid	Gas
Slow pyrolysis	300 – 700	5 – 720	1	≤ 5	25 – 35	20 – 50	20 – 50
Intermediate pyrolysis	350 – 450	4	1	≤ 10	30 – 40	35 – 45	20 – 30
Fast Pyrolysis	450 – 800	< 1	1	≤ 15	10 – 25	50 – 70	10 – 30
HTC	180 – 250	30 – 480	10 – 40	-	50 – 80	5 – 20	2 – 5

**Table 6**  
Molecular sizes of water and steam.

Molecule	Molecular Size (Å)
Water	2.75
CO <sub>2</sub>	3.3

Chemistry, carbon fibres (CFs) are fibrous shaped materials with a diameter between 5 and 10 μm, with a carbon content more than 92%. CFs can be synthesised from a range of synthetic precursors such as, polyacrylonitrile (PAN), pitch or rayon, with approximately 90% of CFs being produced from the former precursor (Bhatt and Goe, 2017). CFs are typically synthesised via four steps; polymerisation, spinning, stabilisation and carbonisation (Hassan et al., 2020; Bhatt and Goe, 2017). Alternatively, CFs can be prepared from natural fibres such as cellulose or any biomass with a high hemicellulose, lignocellulose, or lignin content (Hassan et al., 2020; Chen, 2016). Natural fibres benefit from only requiring stabilisation and carbonisation steps since the materials already possess a fibrous form, consisting of polymeric units.

Spinning method is an important factor since it impacts the final morphology of the CFs. Typically, wet spun fibres are characterised with micro-grooves along the fibre axis, whereas dry-jet wet spun fibres have a smooth surface. At present, there are two industrialised spinning techniques namely, melt spinning, and solution spinning, where the later can be further divided into wet and dry spinning.

Melt spinning consists of melting the precursor in an extruder which is then pumped into a spin pack which filters solid particles from the melt (Edie and Dunham, 1989). Afterward, the melt is passed through a spinneret containing large numbers of individual capillaries. As the melt is passed through the capillaries, it cools, forming a filament. Melt spinning process benefits from simplicity, high material utilisation, and low environmental impacts (Xu et al., 2020). However, this method is not readily applicable for PAN-based fibres due to the polar nitrile groups within the structure, causing PAN homopolymers to undergo thermally induced cyclisation prior to reaching the melting point (Frank et al., 2012). In order to prevent the cyclisation process, a plasticiser must be applied to reduce the nitrile-nitrile interactions, subsequently, increasing the environmental impacts.

Yue et al. have summarised the stabilisation mechanism for PAN-based CFs, consisting of three key stages namely, cyclisation of nitrile groups, dehydration of saturated carbon bonds, and oxidation (Fig. 6) (Yue and Economy, 2017b).

The processing techniques for other types of CF precursors, such as pitch or cellulose-based materials, can be more complex, requiring a pre-treatment step. For pitch-based fibres, this step is known as infusibilisation which typically increases the oxygen content allowing the formation of more stable oxygen-bridge structures, ultimately preventing the fibre from softening/melting during the carbonisation process. This process involves heating the fibres to 150 – 400 °C in an oxidising atmosphere such as air or ozone (Yue and Economy, 2017b). The method

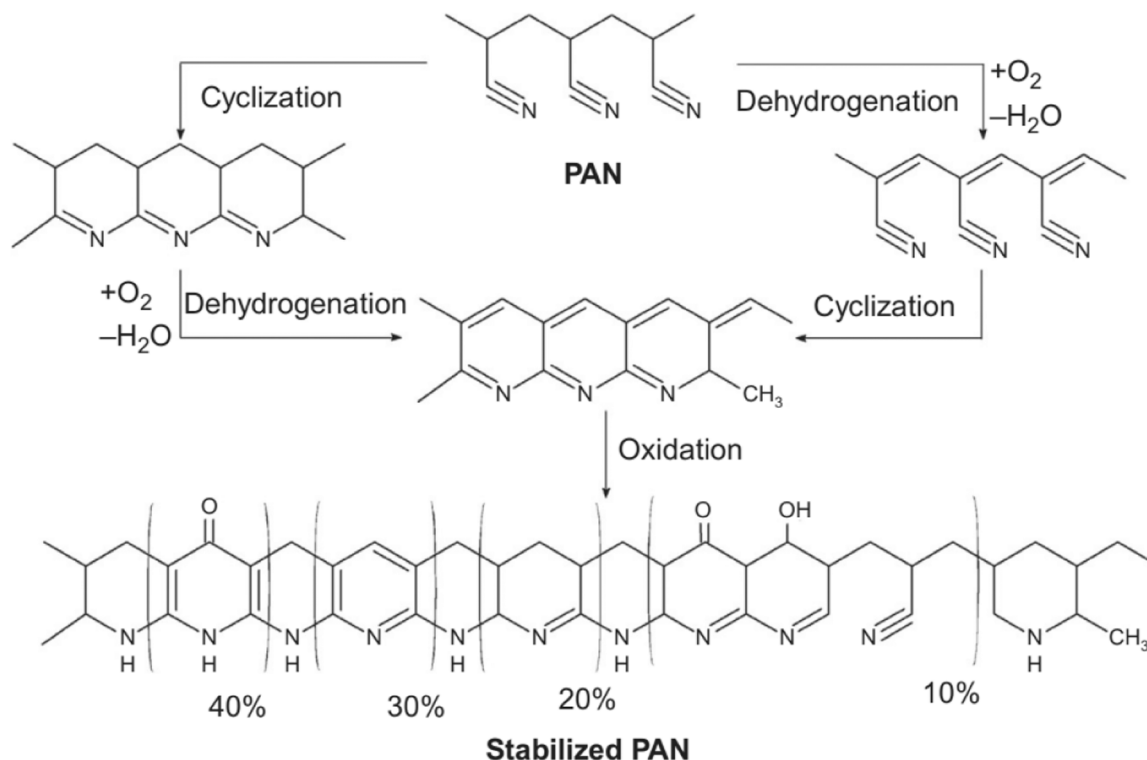


**Fig. 6.** Stabilisation process of PAN CFs (Yue and Economy, 2017b).

causes a series of exothermic reactions, ultimately converting the fibre from a thermoplastic to a thermosetting. Similar to carbonisation, infusibilisation involves oxygenation, cyclisation, and dehydrogenation, releasing biproducts of carbon monoxide, carbon dioxide and water.

Cellulose-based fibres typically contain hydroxyl groups, so do not require an infusibilisation step. However, they typically have a much lower carbon content when compared to PAN or pitch-based fibres which results in significant structural changes, weight loss, and shrinkage during the carbonisation process.

### 3.1.3. Carbon nanotubes

Carbon nanotubes are typically synthesised using either chemical vapour deposition (CVD), electric-arc discharge and laser vaporisation, with the former technique being widely considered as the best and most applied, due to the higher purity and longer tube lengths obtained, in comparison to other techniques. CVD consists of heating a substrate (> 500 °C) in a low pressure, inert gas (commonly Ar) atmosphere. Once the target conditions are met, a carbon bearing gas is introduced into the reaction chamber, which then decomposes to produce CNTs, as discussed below (Shah and Tali, 2016).

Within the bracket of CVD, synthesis techniques can be further divided into a wide variety of sub-sections, including but not limited to aerogel assisted, catalytic, hot filament, microwave assisted, plasma enhanced and etc.

The most common method is catalytic CVD, which applies a hydrocarbon gas precursor (commonly methane or acetylene) and a metal oxide catalyst mounted on a support, which provides an active site for the nucleation and growth of CNTs. Here, the reaction mechanism can be divided into five stages, namely: transportation, adsorption, reaction, diffusion, nucleation, and growth, which have been discussed below (Shah and Tali, 2016; Kumar and Ando, 2010):

1. Transportation of the gaseous precursor to the metal catalyst.
2. Adsorption of the gaseous precursor onto the metal catalyst surface
3. Reaction between the gaseous precursor and hot metal, which causes the precursor to decompose into carbon and hydrogen species. The carbon atoms then dissolve, forming metastable carbide.

4. Diffusion of the carbon species into the pores of the metal catalyst
5. Nucleation and growth, occurs when the liquid carbide concentration reaches the carbon-solubility limit, causing the carbon to precipitate into the form of a cylindrical network.

The process has the ability to maintain itself, due to the thermal gradient that is created between the exothermic hydrogen decomposition reaction and the endothermic precipitation of carbon (Kumar and Ando, 2010).

There are several key parameters that must be considered during CVD, namely, the temperature, precursor flow rate and reaction time. Venkatesan et al. reported that the former two parameters are directly proportional to CNT diameter (Kumar and Ando, 2010). Whereas, reaction time is inversely proportional to diameter size. Furthermore, the catalyst-substrate interaction has a significant impact on CNT growth. When there is a weak interaction between the catalyst and substrate (i.e. the catalyst has an acute contact angle) the tip growth model is favoured (Fig. 7a). In comparison, a strong interaction between the catalyst and substrate (i.e. an obtuse contact angle) results in a base growth model (Fig. 7b).

### 3.1.4. Biosorbents

Biosorbents such as alginate and chitosan are interesting precursors for applications as CAs in an aquaculture setting, as they may be byproduct within the aquaculture industry which could prevent the need to purchase carbonaceous precursors. To produce chitosan, chitin (a component of the exoskeleton of crustaceans) must first be extracted which typically occurs via a two-step process, involving demineralization and deproteination (Varun et al., 2017). Demineralisation can be achieved by mixing 2 M HCl with chitin in a 1:15 ratio (solid:solvent) for 2 h under stirring (150 rpm). After drying the subsequent sample is then deprotonated and demineralised at 50 °C with 2 M NaOH in a 1:20 ratio for 2 h under stirring (150 rpm). Chitosan can then be produced from chitan via deacetylation which is achieved by mixing the chitin with 50% NaOH for 1 h at 121 °C at a pressure of 15 psi. The subsequent product is then washed and dried. A key drawback of this technique is the pressurised vessel which subsequently increases start-up costs and

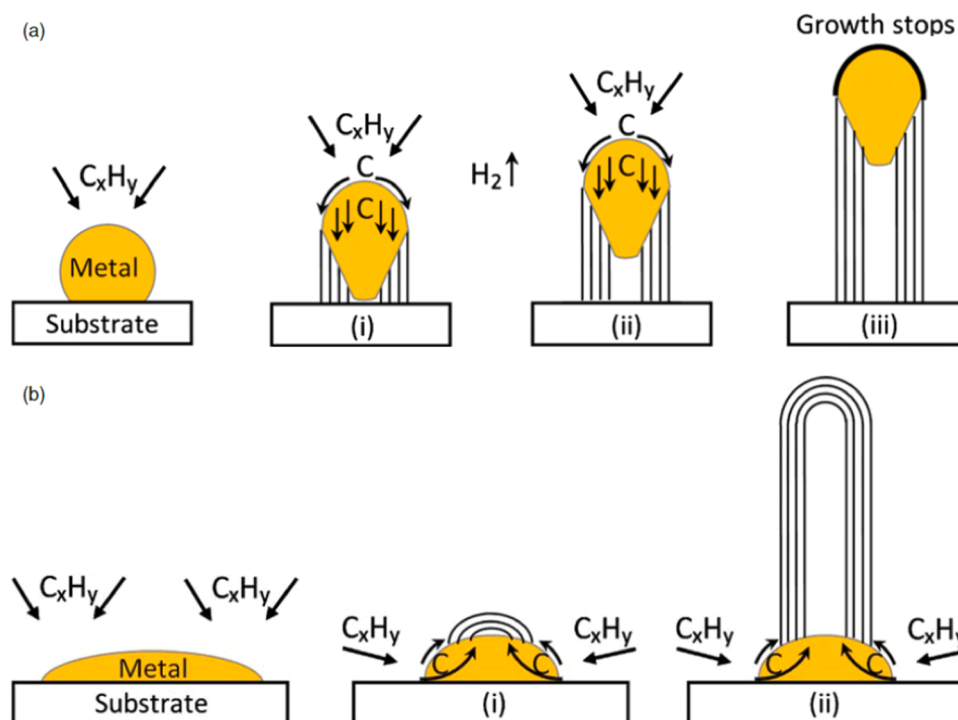


Fig. 7. Widely-accepted growth mechanisms for CNTs: (a) tip-growth model, (b) base-growth model (Kumar and Ando, 2010).

health and safety hazards.

Chitosan is particularly attractive for adsorbent synthesis, being the most abundant biopolymer in nature after cellulose. Furthermore, chitosan is biodegradable, non-toxic and hydrophilic, with the additional benefit of antimicrobial activity. Numerous studies have shown chitosan-based adsorbents to be efficient when removing pharmaceuticals or HMs (Doyo et al., 2023; Vakili et al., 2019; Zhang et al., 2016; Adriano et al., 2005; Karimi-Maleh et al., 2021; Nazraz et al., 2019).

Magnetic chitosan-based adsorbents for mercury adsorption have been produced via the co-precipitation method, where 4 g of chitosan powder was dissolved in 150 ml of acetic acid solution (10% w/v) (Elwakeel and Guibal, 2015). The resulting precursor was combined with 150 ml of deionised water, 6.479 g of  $\text{FeCl}_3 \cdot 6 \text{H}_2\text{O}$ , 3.334 g of  $\text{FeSO}_4 \cdot 7 \text{H}_2\text{O}$  and 2 ml of HCl and stirred for 30 min. Once complete dissolution of the Fe salts was achieved the magnetic chitosan was precipitated by adding 20 ml of NaOH (50% v/v) dropwise at 30 °C under vigorous stirring. The final solid product was obtained by centrifuging followed by freeze-drying. The resulting material was then modified with glycidyl-methacrylate and diethylenetriamine grafting, which has been discussed in Section 3.4.

Alginate is a hydrocolloid which is extracted from algae or seaweed. Fenoradosa et al., extracted sodium alginate, via the following method (Fenoradosa et al., 2010). Firstly, dried alginate was soaked in 2% formaldehyde for 24 h at ambient conditions, the subsequent solid was washed with water, followed by HCl and left for 24 h, after which the samples were washed with water again. The alginate was then extracted by heating to 100 °C for 3 h with 2% sodium carbonate. The solid fraction was then separated via centrifugation and the alginate was precipitated using 95% ethanol. Finally, the alginate was washed with acetone and dried. For further purification the sample was then dissolved again in water followed by precipitation with ethanol.

Devesa-Rey, R, studied the synthesis of calcium alginate beads with entrapped ACs for the clarification of winery wastewaters. This was achieved by combining sodium alginate (1 – 5%) with AC (0.5 – 2%) the subsequent suspension was then added dropwise to calcium chloride solution (0.05 – 0.900 M) which acts as the crosslinking agent. The precipitated beads were then separated via filtration. The study found the optimum synthesis conditions for winery wastewater purification to be 2% AC immobilised with 3% calcium alginate and 0.485 M calcium chloride, reducing the absorbance of the wastewater by up to 96%. However, the authors suggest that a similar DoE would be repeated that is applicable to pharmaceuticals and/or HMs to achieve maximum removal efficiency.

CA precursors can vary significantly from high-value products such as CFs and CNTs to waste or by-products such as chitosan, plant matter and sewage sludge. CFs and CNTs benefit from high purity and fixed carbon content, however, this comes at a significantly higher cost. Where possible the authors suggest that waste materials are used for the synthesis of CAs, reducing costs and creating a more sustainable production pathway. For purification of aquaculture practices chitosan is a particularly attractive precursor, being a potential by-product of the industry. However, waste materials typically have higher levels of impurities which may reduce adsorption capacities or require pre-treatment prior to synthesis.

Carbonisation is a particularly important stage within the CA synthesis process, since the pyrolysis parameters impact the amount of fixed carbon within the structure. For adsorbent synthesis, HTC is attractive since it yields a significantly higher solid content when compared to traditional pyrolysis techniques. However, the technique requires a pressurised vessel (10–40 bar) significantly increasing equipment costs and health and safety hazards. Where HTC is not possible, intermediate pyrolysis is recommended due to the relatively high solid yield.

### 3.2. Activation of carbonaceous adsorbents

The methodologies for activating CAs for applications in aqueous

media have been well established and typically consist of either a physical or chemical activation agent which etches at the carbonaceous network, creating a porous structure. During this process, typically the non-carbonised regions of the carbonaceous framework are burnt off in the form of volatiles (commonly  $\text{CO}_2$ , CO,  $\text{H}_2\text{O}$  or low molecular weight hydrocarbons) and any tar, blocking the porous framework, is removed from the structure. Typically, chemically activated CAs show more attractive textural parameters, increased specific surface areas and pore volumes by approximately two-to-threefold.

Despite the variations observed between the different CAs, there are typically similarities between the activation methods. Although, when selecting activation conditions, the precursor material must be considered. CAs with high mechanical stability, such as CFs and CNTs require harsher conditions to achieve significant development of surface area and porosity, such as increased temperatures, impregnation ratios (IRs) or hold times (Table 7 and 10).

Activation techniques have been extensively studied using design of experiment techniques (DoE) to determine significant parameters and gain an insight into the activation mechanism, this has been discussed in depth in the authors' recent work (Gorbounov et al., 2022). Typically, these studies have aimed to optimise textural properties such as surface area and pore volume, and physicochemical properties (adsorption capacity), through the investigation of key parameters such as, activation temperature, IR, hold time, ramp rate and more. The former two parameters have commonly been identified as having the most significant impacts on surface area and subsequently adsorption capacities. Harsher conditions such as increased activation temperatures and impregnation ratios favour increased surface areas due to increased etching and burn-off of the carbonaceous framework, creating a porous network. However, this is only beneficial up to a point, after-which, the pore walls begin to collapse, and the surface area diminishes, hence the necessity for the optimisation of the process via appropriate techniques. The following sections will review some of the main activation techniques in preparing carbonaceous adsorbents.

#### 3.2.1. Physical activation

Physical activation is a well-established technique. The method involves heating the precursor (i.e. CA) to temperatures typically above 700 °C, in the presence of a gaseous activation agent. The most common activation agents are carbon dioxide and steam since the processes are endothermic and therefore, easier to control, when compared to other agents such as oxygen which are highly exothermic (Marsh and Rodríguez-Reinoso, 2006a; Zhao et al., 2007; Rio et al., 2006; Choi et al., 2019; Sajjadi et al., 2019). The mechanism of physical activation is still debated although some researchers have suggested that it occurs via two processes. Firstly, disorganised carbon is expelled from the structure resulting in approximately 10 – 20 wt% burn-off, the gaseous activation agents then diffuse into the internal network of the carbonaceous structure, resulting in the widening of inaccessible pores (Sajjadi et al., 2019; Yang et al., 2021; Ruiz-Fernández, Alexandre-Franco, Fernández-González, Gómez-Serrano). Furthermore, the mechanism can differ depending on the gaseous activation agent due to varying molecule sizes and reactivity which has been extensively discussed elsewhere (Marsh and Rodríguez-Reinoso, 2006a; Sajjadi et al., 2019). For example, a water molecule (steam), is smaller than a  $\text{CO}_2$  molecule (Table 6), which facilitates the diffusion into the internal porous structure, resulting in the production of ACs with high surface area.

Steam activation begins with oxygen being exchanged from water to the carbonaceous surface via chemisorption, creating surface oxides (Fig. 8) (Sajjadi et al., 2019). Some surface oxides may be expelled as CO, which in turn enhances the gasification rate by withdrawing further oxygen groups to produce  $\text{CO}_2$ . Carbon gasification is widely accepted as the key stage in all physical activation processes, where carbon is emitted from the carbonaceous network and subsequently porosity develops; the pivotal step being the water gas shift reaction where CO reacts with water to produce  $\text{CO}_2$  and  $\text{H}_2$ . Subsequently, the produced

**Table 7**

Summary of physical activation techniques in literature and the subsequent properties of CAs.

Precursor	Activation Agent	Activation Temp (°C)	Heating atmosphere/Flow rate (ml/min)	Activation Time (h)	Gas/Flow rate (ml/min)	S <sub>BET</sub>	V <sub>micro</sub> /V <sub>tot</sub>	ref
Sewage sludge	Steam	750 – 850 Opt 760		0.5 – 1.5 Opt 30	2500	226	0.083/ 0.269	(Rio et al., 2006)
Palm Shell	Steam	900		4		1104	0.41/0.51	(Mohamed, M, Darzi GN, 2010)
Palm Shell	CO <sub>2</sub>	900		0.5		1360	0.47/0.69	(Kang et al., 2011)
Palm Shell	Steam	820		1	60	1076	0.51/0.81	(Lua and Yang, 2004)
Pistachio shell	CO <sub>2</sub>	900		0.5		896	0.237 (tot)	
Biomass flax fibre	CO <sub>2</sub>	825		1–6				(Illingworth et al., 2022)
MWCNTs	Steam	800	N <sub>2</sub> /100			85.8		(Zhao et al., 2007)
methane CVD		850	N <sub>2</sub> /100			0.80		
MWCNTs	CO <sub>2</sub>	750	N <sub>2</sub> /100			113.6		
		800	N <sub>2</sub> /100			144.0		
		850	N <sub>2</sub> /100			97.3		
Pitch-based CF	Steam	800	N <sub>2</sub> /100			850		
		850	N <sub>2</sub> /100			870		
		900	N <sub>2</sub> /100			1900		
PAN- based CF	Steam	850		0.75	200	1041.9	0.42/0.49	(Choi et al., 2019)
PAN-CF	CO <sub>2</sub>	900		2	CO <sub>2</sub> /30	576	0.34	(Park and Kim, 2001)
Polyethylene CF	Steam	900	N <sub>2</sub> /300	0.66	H <sub>2</sub> O 0.5	1750	0.60/0.99	(Kim et al., 2021)

**Table 8**

Surface functional groups of ACFs determined by Boehm titration (Silva et al., 2018).

Material	Surface Functional Groups				Total	Basic Groups	PZC	Ref (Silva et al., 2018)
	Acidic Groups	Lactonic	Phenolic					
ACFs	Carboxylic 0.386	0.290	0.454		1.13	0.569	2.1	

**Table 9**

Physiochemical properties of alkali metals.

Element	Ionisation Energy (KJ/mol)	Atomic Radii (Å)
Lithium (Li)	-520.2	1.67
Sodium (Na)	-495.8	1.90
Potassium (K)	-418.8	2.43
Rubidium (Rb)	-403.0	2.65
Caesium (Cs)	-375.7	2.98

CO<sub>2</sub> further activates the surface, in contrast, there is some debate that the H<sub>2</sub> produced may inhibit further steam gasification by deactivating active sites on the carbon surface via dissociative hydrogen adsorption, reverse oxygen exchange or scavenging of surface oxides; a concept introduced by Hermann and Hüttinger (Sajjadi et al., 2019; Hermann and Hüttinger, 1986).

The first step of CO<sub>2</sub> activation involves the Boudouard reaction, where CO<sub>2</sub> undergoes dissociative chemisorption with the carbonaceous framework, forming surface oxides and CO (Fig. 8) (Marsh and Rodríguez-Reinoso, 2006a; Sajjadi et al., 2019). The surface oxides are then expelled from the structure in the form of CO, further developing the network. CO within the reactor can then partake in carbon gasification and subsequently the water gas shift reaction where the full extent of porosity is developed. Notably, CO production in the Boudouard reaction is not favoured at temperatures < 700 °C and therefore, elevated temperatures are desirable to promote increased burn-off of the carbonaceous framework.

Various CAs, prepared from a wide range of carbonaceous materials have been activated using CO<sub>2</sub>. Oil palm stones which were firstly carbonised at 600 °C in N<sub>2</sub> with a flow rate of 150 ml/min for 2 h (Aik Chong Lua, 2001). The activation was carried out at temperatures between 500 and 900 °C for 10 – 60 min with a CO<sub>2</sub> flow rate of 100 ml/min. The ramp rate was kept consistent at 10 °C/min for both carbonisation and activation. The ACs produced at 900 °C with a hold time of 30 min had the largest surface area (1366 m<sup>2</sup>/min) and

microporosity (958 m<sup>2</sup>/g). Reduced surface areas and porosity was observed at hold times above this range which can be attributed to the destruction of micropores due to pore wall collapse.

PAN-CFs were prepared via carbonisation in an inert atmosphere at 1000 °C for 2 h followed by activation in CO<sub>2</sub> (flow rate 30 ml/min) at temperatures of 700, 800, 900 and 1000 °C for 2 h (Park and Kim, 2001). Similarly, to above, the highest surface area and porosity was achieved at 900 °C after which a reduction in surface area is observed (Fig. 9).

Kang et al. investigated a series of different activation methods of palm shell, including both physical activation techniques (Kang et al., 2011). Prior to activation, the material was carbonised at 500 °C, after which the palm shells were activated at temperatures ranging between 750 and 820 °C for 2 h under steam (flow rate 60 ml/min). The study found that the maximum surface areas and porosity of 1076 m<sup>2</sup>/g and 0.81 ml/g, respectively, were achieved at the maximum temperature, which in turn dramatically increased the adsorption capacity (Fig. 10). However, the yield was significantly reduced at the highest temperature (i.e. by 24.3%), when compared to those at lowest temperature (i.e. by 64.0%), which can be attributed to the increased carbon burn off.

Likewise, PAN-based CFs have been activated under steam with prior carbonisation under vacuum conditions at 200 °C for 8 h (Choi et al., 2019). A range of activation conditions were applied with temperatures ranging between 700 and 850 °C and hold times of 0.5 – 6 h. The flow rate of steam was kept consistent at 200 ml/min. Fig. 11a and b show the impact of temperature and hold time on the surface area and yield. The data is consistent with harsher conditions favouring increased burn off the carbonaceous structure, with activation temperature having the greatest impact. Subsequently the surface area increased whilst the yield decreased. It was found that higher temperatures and shorter hold times enhanced the surface area when compared to lower temperatures with longer hold times; this was attributed to higher temperatures favouring the formation of microporous structures. This study was conducted for gas-phase applications and therefore, concluded that higher temperatures were beneficial. However, for liquid-phase applications, lower

**Table 10**  
Review of chemical activation techniques for CAs.

Precursor	Activation Agent	Activation Temp (°C)	Activation Time (h)	Gas/Flow rate (ml/min)	IR (CA: Chemical)	S <sub>BET</sub>	V <sub>micro</sub> /V <sub>tot</sub>	ref
Watermelon rinds	H <sub>2</sub> SO <sub>4</sub>	150	24	-	1:1	0.357	-	(Jawad et al., 2019)
Acacia erioloba seed	H <sub>2</sub> SO <sub>4</sub>	600	1	-	10%	129.83	0.05/-	(Rahman et al., 2019)
Macadamia nutshell	H <sub>2</sub> SO <sub>4</sub>	650	0.75	-	1:1	426.3	0.19/0.21	(Dao and Le Luu, 2020)
H <sub>2</sub> SO <sub>4</sub>	K <sub>2</sub> CO <sub>3</sub>	650	1	-	1:1	459.8	0.21/0.23	(Dao and Le Luu, 2020)
Kesambi wood biomass	H <sub>2</sub> SO <sub>4</sub>	400	0.5	-	96%	179.05	0.00/2.17	(Neolaka et al., 2021)
Eucalyptus residue	H <sub>3</sub> PO <sub>4</sub>	400	3	N <sub>2</sub>	1:2.5	1545.44	0.04//1.70	(Han et al., 2020)
Sisal hemp pulp fibres	H <sub>3</sub> PO <sub>4</sub>	450	1	-	1:1.25	1801	-/1.02	(Liu et al., 2021)
Kenaf stem short fibre	-	600	0.5	N <sub>2</sub>	1:1 – 1:4	1570	0.54/1.82	(Baek et al., 2019)
Oil palm shell	H <sub>3</sub> PO <sub>4</sub>	700 (W)	0.083	-	1:2	854.42	-/0.74	(Tan et al., 2016)
Agricultural waste	H <sub>3</sub> PO <sub>4</sub>	200 (W)	0.067	N <sub>2</sub> /200	60%	-	-	(Canales-Flores and Prieto-García, 2020)
PAN-rCF	NaOH	700	1	N <sub>2</sub> /100	1:1	-	-	(Taylor et al., 2022)
Cherry stone	NaOH dry	600	0.33	-	-	704	0.32/-	(Pietrzak et al., 2014)
	NaOH impreg 24 h, dried 105	600	0.33	-	-	788	0.36/-	
Non-woven biomass flax fibre	KOH	800	0–3	N <sub>2</sub>	-	1051	0.411/0.533	(Illingworth et al., 2022)
	K <sub>2</sub> CO <sub>3</sub>	800	0–3	N <sub>2</sub>	-	1007	0.399/0.516	
	KOH (vac)	800	0–3	N <sub>2</sub>	-	1197	0.460/0.589	
PAN-CF	KOH	750	1	-	4:1	756	0.31	(Maciá-Agulló et al., 2007)
					5:1	877	0.38	
					8:1	891	0.39	
	NaOH	750	1	-	4:1	391	0.16	
					5:1	674	0.28	
					8:1	855	0.37	
PAN-CF	KOH	850	1	N <sub>2</sub> /50	2:1	780.17	0.35/0.39	(Shen et al., 2011)
	KOH	Pre-ox: 500	1	N <sub>2</sub> /50	2:1	2231.24	0.76/1.16	
		850	1	N <sub>2</sub> /50	-	0.24	-	
PAN-CF	KOH	950	1	N <sub>2</sub> /150	3:1	2889	2.39/1.87	(Alkathiri et al., 2020)
		950	1	CO <sub>2</sub> /250	-	774	-	
PAN-CF	KOH	Pre-treat: 120	12	N <sub>2</sub>	3:1	1896	V <sub>meso</sub>	(Martín-Gullón et al., 2001)
		600	0.5	N <sub>2</sub> /1000	3:1	3388	0.044	
		700	0.5	N <sub>2</sub> /1000	3:1	3034	0.547	
		800	0.5	N <sub>2</sub> /1000	1:1	271	1.098	
		600	0.5	N <sub>2</sub> /1000	1:1	502	0.044	
		700	0.5	N <sub>2</sub> /1000	1:1	2023	0.078	
		800	0.5	N <sub>2</sub> /1000				
PAN-CF	KOH	800	4	Steam: N <sub>2</sub> /1000	1:1	670	0.031	
		800	1	N <sub>2</sub>	1:1	2283	0.634/	(Lu and Zheng, 2001)
		820			1:1	2828	0.876	
		850			1:3	3220	0.526/1.007	
							0.655/1.204	
Pitch based	KOH	750	1	N <sub>2</sub>	2:1	1090	0.49	(Maciá-Agulló et al., 2004)
					4:1	1635	0.78	
					6:1	2225	0.90	
					8:1	2420	0.94	
	NaOH	750	1	N <sub>2</sub>	2:1	1130	0.51	
					4:1	2000	0.81	
					6:1	2541	0.96	
					8:1	3033	1.02	
		890	3	N <sub>2</sub> /100		644	AN	
		890	9	CO <sub>2</sub> /100		1528		
		890	22.5			2487		
MWCNTs	KOH	800	-	N <sub>2</sub> /500	1:4	1028	0.47	(Jorda, 2002)
	KOH	800	-	N <sub>2</sub> /500	1:5	1184	0.50	

temperatures with longer hold times may be beneficial as this may allow for the development of attractive mesoporous structure.

Overall, physical activation techniques benefit from being simple, industrially scalable, and relatively environmentally friendly, without

secondary waste generation/disposals when compared to chemical activation. However, it also suffers from a fair share of disadvantages when compared to other activation techniques. For example, it is more energy intensive due to increased activation times and temperatures.

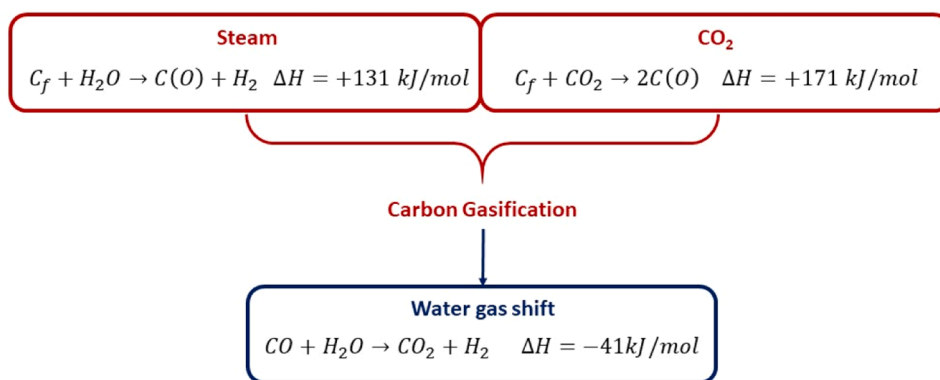


**Fig. 8.** Comparison between steam and CO<sub>2</sub> physical activation mechanisms, where C<sub>f</sub> describes carbon atoms which are free from bonding with surface complexes and are therefore accessible to react with an oxygen molecule and C(O) describes surface oxygen complex.

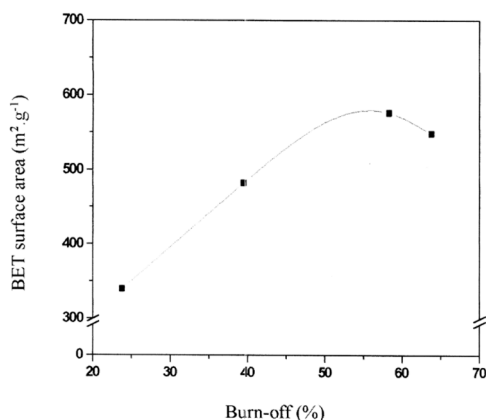


**Fig. 9.** Impact of percentage burn off on the specific surface area of PAN-based activated carbon fibres (Park and Kim, 2001).

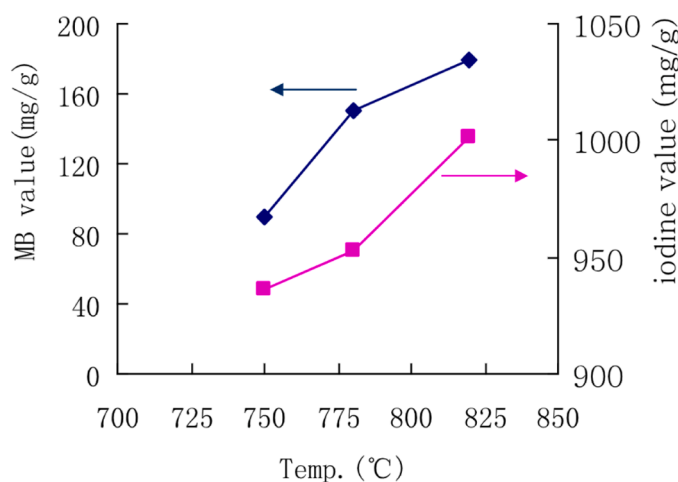


**Fig. 10.** Impact of temperature on methylene blue (MB) and Iodine values (Kang et al., 2011).

Additionally, preparation of commercial CAs via physical activation is a two-step process, where carbonaceous materials typically require carbonisation in a neutral atmosphere before activation.

### 3.2.2. Chemical activation

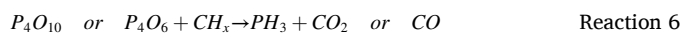
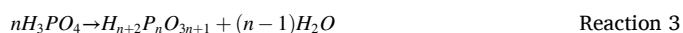
Chemical activation has many benefits when compared to physical activation, such as increased and controlled development of surface

area, porosity and yields at decreased activation temperatures and hold times (Marsh and Rodríguez-Reinoso, 2006b; Rio et al., 2005; Maciá-Agulló et al., 2004; Hoseinzadeh Hesas et al., 2013; Jorda, 2002; Lillo-Ródenas et al., 2003). Additionally, carbonisation and surface functionalisation can occur *simultaneously* during chemical activation processes. However, the technique suffers from limited industrial scalability due to the application of corrosive chemical precursors. Also, adsorbents require an additional washing step which produce toxic waste streams, requiring secondary treatments before disposal (Heidarinejad et al., 2020).

There are multiple parameters that need to be considered for chemical activation processes: chemical agent, impregnation ratio, mixing method, activation temperature, hold time, atmospheric conditions and ramp rate. Selection of chemical agents are key because this strongly influences the ultimate surface morphology, functionalities and overall crystallinity. The most commonly used activation agents include potassium hydroxide (KOH), sodium hydroxide (NaOH), phosphoric acid (H<sub>3</sub>PO<sub>4</sub>), sulphuric acid (H<sub>2</sub>SO<sub>4</sub>), potassium carbonate (K<sub>2</sub>CO<sub>3</sub>), zinc chloride (ZnCl<sub>2</sub>) and more.

**3.2.2.1. Acidic activation.** As previously mentioned, H<sub>3</sub>PO<sub>4</sub> and H<sub>2</sub>SO<sub>4</sub> are the most applied acidic activation agents; however, other activation agents such as H<sub>2</sub>SO<sub>4</sub>, HNO<sub>3</sub> and hypochlorites have been used less frequently. Din et al. conducted a mini review on the various activation techniques of ACs and found that of the aforementioned acidic agents. H<sub>3</sub>PO<sub>4</sub> is preferable since it produces ACs with the highest surface areas (907 – 1033 m<sup>2</sup>/g) whilst maintaining high yields (Din et al., 2017). In comparison, H<sub>2</sub>SO<sub>4</sub> only achieved a maximum surface area of 554 m<sup>2</sup>/g and a reduction in yield. HNO<sub>3</sub> and hypochlorite activation had the lowest yields of all ACs in the study. Based on this, the following section will focus largely on H<sub>3</sub>PO<sub>4</sub> and H<sub>2</sub>SO<sub>4</sub> activation techniques.

There are several variations in the mechanism of H<sub>3</sub>PO<sub>4</sub> activation which are temperature dependent; the overall reaction is summarised in Reaction 1 (Neme et al., 2022). At temperatures of 100 – 400 °C, H<sub>3</sub>PO<sub>4</sub> is dehydrated, resulting in the expulsion of water (Reaction 3). As temperatures are increased (400 – 700 °C), the P<sub>4</sub>O<sub>10</sub> that is formed in Reaction 4, undergoes two concurrent parallel reactions (i.e. Reactions 5 and 6), which subsequently reacts with the carbon surface etching and widening existing pores, whilst simultaneously expelling CO<sub>2</sub> or CO.



Silva et al. studied the chemical activation of CFs produced from

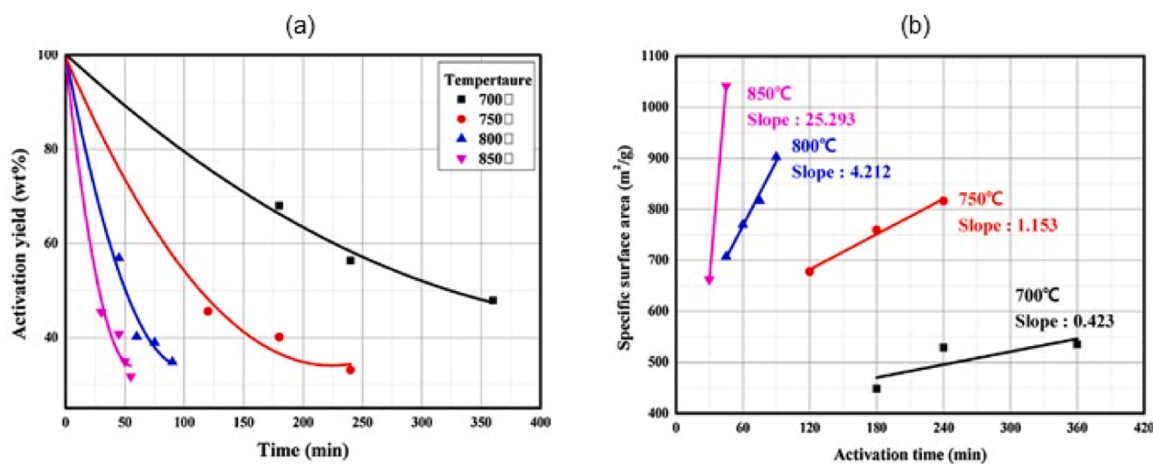


Fig. 11. (a) The yields as a function of time and temperature in physical activation, (b) Correlation between activation temperature/time and SBET [75].

denim fabric waste using phosphoric acid. Firstly, the CFs were impregnated with  $\text{HP}_3\text{O}_4$  in a 1:1 ratio which was heated to  $60^\circ\text{C}$  for 24 h (Silva et al., 2018). The impregnated CFs were then subjected to activation under  $\text{N}_2$  with a flow rate of 100 ml/min, via a three-step heating process. The CFs were heated from room temperature to  $300^\circ\text{C}$  for and held at this temperature for 3 h. After completion of this segment, the CFs were subjected to further ramping to  $500^\circ\text{C}$  with a hold time of 1 h. The CFs were then allowed to cool to  $100^\circ\text{C}$ . Finally, the ACFs were neutralised with 0.1 M NaOH and washed deionised water until a pH of  $\sim 6$  was achieved, followed by drying for 24 h at  $100^\circ\text{C}$ . The resultant ACFs were analysed using  $\text{N}_2$  adsorption/desorption isotherms to determine the BET surface area and pore volume. It was found that the ACFs had a high specific surface area and mesopore volume of  $1582\text{ m}^2/\text{g}$  and  $0.390\text{ cm}^3/\text{g}$ , respectively, which is ideal for aqueous phase adsorption. Additionally, the surface functional groups and point of zero charge (PZC) were determined. The surface was found to be highly acidic, with a  $\text{pH}_{\text{PZC}}$  of 2.1 (Table 8). The resultant fibres were then applied to the adsorption of Remazol Brilliant Blue R (RBBR) textile dye. The highest adsorption capacities were observed at  $\text{pH} < 2$  which can be attributed to the enhanced electrostatic interactions between the positively charged surface and negatively charged sulphonic groups ( $\text{SO}_3^-$ ) of RBBR.

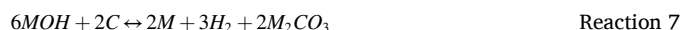
ACs were synthesised from palm tree leaves using a  $\text{H}_2\text{SO}_4$  activation agent, this is particularly beneficial for waste materials since it can impregnate, clean and de-ash the precursor simultaneously (Soliman et al., 2016). The date palm leaves were soaked in a 25% (w/w) solution of  $\text{H}_2\text{SO}_4$  for 24 h at ambient conditions, afterward the material was washed and dried at room temperature. The resulting material was activated at various temperatures ( $250 - 450^\circ\text{C}$ ) for 24 h. The resulting AC was washed with  $\text{NaHCO}_3$  until a constant pH was achieved ( $\sim 6$ ). Finally, the AC was dried, ground, and sieved to obtain a material with a particle size between  $300$  and  $425\ \mu\text{m}$ . The AC was applied to remove Pb (II) ions in aqueous media, achieving a maximum adsorption capacity of  $61.55\text{ mg/g}$  at  $29^\circ\text{C}$ .

In some cases, adsorbents have been synthesised using a combination of agents at low temperatures, for example MWCNT have been activated using a mixture of  $\text{H}_2\text{SO}_4$  and  $\text{H}_2\text{O}_2$  (both 4 M) in a 70:30 volumetric ratio ( $\text{H}_2\text{SO}_4:\text{H}_2\text{O}_2$ ) (Babaei et al., 2016). Where, the MWCNT were combined with the  $\text{H}_2\text{SO}_4:\text{H}_2\text{O}_2$  mixture and heated under reflux for  $120^\circ\text{C}$  for 2 h under stirring; once completed the nanotubes were washed until a pH of  $\sim 6$  was achieved, followed by drying at  $80^\circ\text{C}$ . The resulting MWCNTs were found to have a low surface area and total pore volume of  $221.9\text{ m}^2/\text{g}$  and  $0.716\text{ cm}^3/\text{g}$ , respectively. Additionally, it was observed that the average pore volume in the mesoporous region. The MWCNTs were applied to remove TC antibiotics; despite the low surface area and pore volume, reasonable maximum adsorption

capacities ( $253.38\text{ mg/g}$ ) were observed when compared to other studies, this has been discussed in more detail in Section 6).

**3.2.2.2. Basic activation.** Of the chemical agents, KOH is particularly attractive due to its ability to create high surface areas with a narrow pore size distribution, whilst also being less corrosive and costly when compared to other activation agents such as  $\text{H}_2\text{SO}_4$  and  $\text{H}_3\text{PO}_4$ . Additionally, it is widely agreed that KOH can suppress the generation of tar by accelerating the rate of pyrolysis and subsequently, the removal of non-carbon moieties (Gao et al., 2020). In fact, many studies have highlighted the efficiency of KOH activated carbons in adsorbing a range of pollutants including HMs, antibiotics and pesticides.

The mechanism of activation with hydroxides have been extensively studied, and it is widely agreed that the first step of the mechanism consists of overlapping redox reactions between the hydroxide (Reaction 7):



Alkali metals possess the ability to intercalate between the graphene sheets of a carbonaceous structure, increasing the spacing between the sheets and subsequently the specific surface area and pore volume (Marsh and Rodríguez-Reinoso, 2006b; Gao et al., 2020; Alkathiri et al., 2020). Intercalation is an *electron transfer* process, where the metal donates an electron to the delocalised  $\pi$ -electrons within the conduction band of graphene. Ionic radius has a large impact on intercalation of cations for several reasons. Atoms with a larger number of electron orbitals, require a lower energy to donate electrons due to the reduced electric forces between the nucleus and the valence electron according to Eq. (1).

$$F = \frac{kq_1q_2}{d^2} \quad (1)$$

For this reason, alkali metals with atomic radii  $\leq$  potassium readily form intercalation compounds with carbonaceous adsorbents, independently of structural order (Raymundo-Piñero et al., 2005). However, this is not the case with sodium. By applying density functional theory (DFT), it has been determined that graphite compounds intercalated with  $\text{Na}^+$  ( $\text{NaC}_6$  and  $\text{NaC}_8$ ) cause C-C bonds to stretch, making them thermodynamically unstable (Wang et al., 2021a). For this reason,  $\text{Na}^+$  exhibits increasing intercalation with increasing interlayer distance, which correlates with increased disorder of the carbonaceous structure.

KOH activation has been extensively studied, due to the large surface areas typically produced by hydroxides (Illingworth et al., 2022; Park

and Kim, 2001; Alkathiri et al., 2020; Maciá-Agulló et al., 2007; Shen et al., 2011; Martín-Gullón et al., 2001; Lu and Zheng, 2001; Sun et al., 2006). This phenomenon can be attributed to the redox reaction between  $K^+$  with the carbon surface, producing CO, CO<sub>2</sub>, and H<sub>2</sub>O, (Reaction 8). Typically, the activation process is carried out at between 600 and 850 °C for 0.5 – 3 h under an inert atmosphere. While impregnation ratios vary from 1:1 – 1:10 (CF:KOH). Several articles have studied a direct comparison between physical activation and chemical activation of CFs, all of which concluded that the application of KOH significantly increases surface area and porosity in comparison to physically activated samples (Alkathiri et al., 2020; Shen et al., 2011; Martín-Gullón et al., 2001).

Shen et al. investigated three activation methods of PAN-based CFs (Shen et al., 2011), namely, physical activation in an N<sub>2</sub> atmosphere, chemical activation using KOH and a 1:2 (CF:KOH) impregnation ratio, and chemical activation with pre-oxidation. Each experiment applied the same activation conditions: an activation temperature of 850 °C, a hold time of 1 h in an N<sub>2</sub> atmosphere (flow rate 50 ml/min) and a heating rate of 5 °C/min. The final experiment pre-oxidised the CFs at 500 °C in air for 2 h, prior to activation. The study concluded that chemical activation with pre-oxidation obtains ACFs with significantly higher surface areas than other techniques (>2230 cm<sup>3</sup>/g, Table 10).

Similarly, Alkathiri et al. investigated the activation of PAN-based CFs (Alkathiri et al., 2020). Prior to activation, the CFs were subjected to stabilisation and carbonisation processes (Section 3.1). After which the CFs were activated either physically or chemically. Physical activation involved a heating the CFs to either 850 or 950 °C in an N<sub>2</sub> atmosphere before switching the gas to CO<sub>2</sub> (flow rate 250 ml/min) and holding for 2 h, the resulting surface areas were 173 and 774 m<sup>2</sup>/g, respectively. In comparison, the chemically activated carbon fibres were immersed in a KOH slurry with IRs of either 1:1, 1:2, or 1:3 (CF:KOH), heated to 950 °C, with a hold time of 1 h. The resulting fibres demonstrated significantly higher surface areas when compared to their physically activated counterparts, of 1356, 2470 and 2889 m<sup>2</sup>/g, respectively.

Okman et al. conducted a study to compare KOH and K<sub>2</sub>CO<sub>3</sub> as chemical activation agents for the synthesis of ACs from grape seeds (Okman et al., 2014). The biomass was impregnated with either activation agent for 24 h at impregnation ratios ranging from 0.25:1 – 1:1 (chemical:AC), then dried at 105 °C. The resulting material was then carbonised at 600 or 800 °C for 1 h under N<sub>2</sub> (flow rate 30 ml/min). After activation, the samples were refluxed in concentrated HCl, followed by washing with deionised water until chloride ions were not detected, then dried at 105 °C for 24 h. The highest BET surface area was observed when activating the samples at 800 °C with K<sub>2</sub>CO<sub>3</sub> (IR 0.5:1, Fig. 12). Whereas the highest surface area for KOH activation was achieved at 800 °C using an IR of 0.25:1, due to the increased etching effect of KOH which will cause destruction of the pore walls at higher IR.

### 3.2.3. Microwave activation

Microwave (MW) activation has become increasingly popular over conventional heating techniques for a range of reasons, including decreased activation times and energy consumption, uniform temperature throughout a sample and improved diffusion processes (Ewis and Hameed, 2021). The technique involves bombarding a sample with electromagnetic radiation, with wavelengths ranging between 0.001 and 1 m (MW region) (Babaei et al., 2016). MW activation typically produces adsorbents with enhanced morphology and physicochemical properties in comparison to traditional heating techniques, which can be attributed to the absorption of electromagnetic energy on a molecular level which heats the internal structure by dipole rotation causing friction within the structure, which is then transferred outwards (Fig. 13) (Njoku et al., 2014). Carbonaceous materials are particularly effective at absorbing MW radiation, resulting in excellent development of physicochemical properties (Tan et al., 2016).

Tan et al. investigated MW activation of activated carbon synthesised from oil palm shells using H<sub>3</sub>PO<sub>4</sub> impregnation techniques achieving a maximum S<sub>BET</sub> of 854.42 m<sup>2</sup>/g (Tan et al., 2016). This was achieved by firstly submerging the precursor in H<sub>3</sub>PO<sub>4</sub> using an IR of 1:1 – 1:3 (w/w); the resulting mixture was then dried at 100 °C for 24 h. The impregnated samples were then subjected to MW treatment with a radiation power of 700 W for 5 – 8 min. Finally, the samples were washed until neutral and dried. The resulting ACs were applied to investigate the adsorption of cadmium ions, with the harshest conditions (1:3 IR, 8 min irradiation) favouring the highest adsorption capacities (> 78.32 mg/g). This was attributed to the increased concentrations of H<sub>3</sub>PO<sub>4</sub> causing the linkages between cellulose and lignin to rupture during the impregnation stages; after which a series of recombination reactions occur, leading to the formation of larger, strong, cross-linked units (Tan et al., 2016; El-Hendawy et al., 2008).

Similarly, Ge et al., applied MW irradiation to simultaneously carbonise and activate rayon-based CF felts for applications as adsorbents to remove TC antibiotics (Ge et al., 2020). Firstly, the CF felts were soaked in a water bath for 2 h containing an 8% (NH<sub>4</sub>)<sub>2</sub>HPO<sub>4</sub> solution in a 1:100 (CF:(NH<sub>4</sub>)<sub>2</sub>HPO<sub>4</sub>) ratio. The impregnated CFs were then carbonised in a MW oven under air, using a temperature and radiation of 500 °C and 1200 W, respectively. Once carbonised, the fibres were activated at temperatures ranging between 600 and 700 °C and MW power of 720 – 2160 W under CO<sub>2</sub> (flow rate 75 – 100 ml/min). The harshest conditions led to the greatest development of surface area (1982 m<sup>2</sup>/g) and porosity (1.0110 cm<sup>3</sup>/g) and subsequently achieved significantly higher adsorption capacities (315.2 mg/g), in comparison to the other samples in this study. This was attributed to the increased pore diameters which allowed TC to more readily enter the porous network.

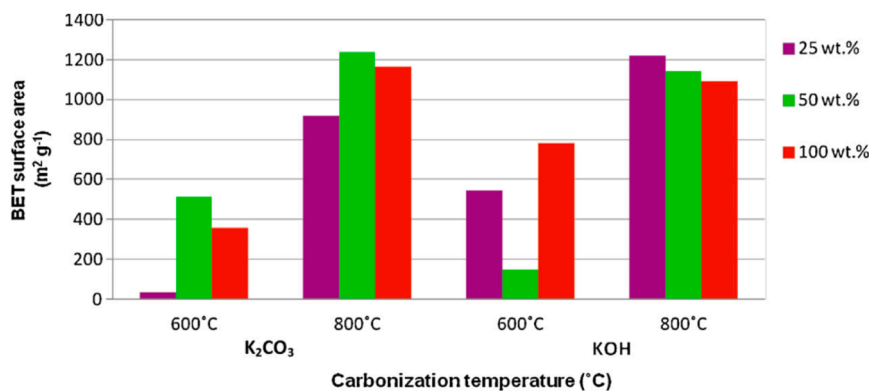


Fig. 12. BET surface areas of activated carbons produced from the chemical activation (either K<sub>2</sub>CO<sub>3</sub> or KOH) of grape seeds in relation to carbonization temperature (Okman et al., 2014).



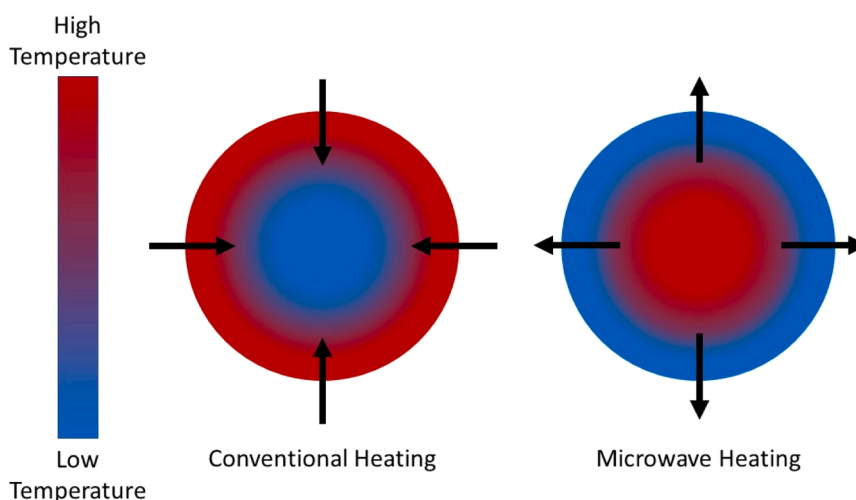


Fig. 13. Conventional heating vs. Microwave heating  
Adapted from Babaei et al. (2016).

### 3.2.4. Summary of activation of carbonaceous adsorbents

Selection of activation technique is paramount since it determines the physiochemical characteristics of the adsorbent produced. When selecting activation techniques, the application must be considered, for example the pollutants in question and the adsorption conditions (i.e. pH, temperature, DOM etc.). In general, for aqueous phase adsorption the authors suggest that chemical activation techniques are particularly attractive, since they enhance the hydrophilic nature of the adsorbent and introduce surface functional groups, which act as active sites for adsorption (Section 4). Furthermore, chemical activation benefits from being a one-step synthesis and activation process, since carbonisation occurs in tandem with activation. Where possible, less corrosive activation agents should be selected to limit health and safety hazards and waste disposal costs. However, the method does suffer from limited scalability due to the hazardous chemical feedstock. Additionally, the technique requires an additional washing step to remove remnant activation agents.

In some cases, physical activation may be preferred, particularly when working with hydrophobic adsorbates, since physical activation expels heteroatoms from the structure, enhancing the hydrophobic character of the material, therefore enhancing the hydrophobic interactions between the CA and adsorbate. However, the method is energy intensive requiring higher activation temperatures and longer hold times, as well as a prior carbonisation step.

Of all of the activation techniques, MW activation is particularly attractive, achieving high  $S_{BET}$  at significantly reduced hold times (i.e. minutes in comparison to hours), therefore reducing energy consumption. Furthermore, the technique can be coupled with chemical activation, enhancing the hydrophilic nature of the CA. However, a key drawback is the start-up cost, with microwave systems typically being more expensive than traditional furnaces. Therefore, this method may not be applicable in developing countries, which are typically contributing to more pollution within the aquaculture industry.

### 3.3. Characterisation

Adsorption isotherms are a fundamental characterisation technique which aim to describe the physisorption of gas molecules on a solid surface, to determine surface area ( $S_{BET}$ ), pore size distribution and pore volume of adsorbents. Nitrogen, argon and carbon dioxide are typically applied, with the former being the most commonly cited in literature. Standard BET analysis using nitrogen is conducted at 77 K ( $N_2$  boiling temperature at relative pressures ranging between 0 and 1). Brunauer-Emmet-Teller (BET), modified the Langmuir adsorption theory to

account for multilayer adsorption, whilst assuming the layers do not interact with each other. The BET equation identifies the relationship between adsorption and partial pressure:

$$\frac{P}{V(P_0 - P)} = \frac{C - 1}{V_m C} \frac{P}{P_0} + \frac{1}{V_m C} \quad \text{Eq. 2}$$

Where,  $P$  is the total equilibrium pressure of the adsorbed gas (in the system),  $P_0$  is the vapor pressure of the adsorbed gas at the temperature of adsorption;  $V$  is the actual (multi-layer) adsorption amount of the sample,  $\text{cm}^3/\text{g}$ ;  $V_m$  is the single-layer saturated adsorption amount/capacity per unit mass of adsorbent (i.e. monolayer capacity),  $\text{cm}^3/\text{g}$ ;  $C$  is the constant reflecting heat of adsorption (Bardestani et al., 2019; Fu et al., 2021).

Multi-point BET consists of measuring  $N_2$  uptake at a minimum of three data points with  $P/P_0$  ranging between 0.025 and 0.30, since this range is suitable for multilayer adsorption, whilst preventing the onset of capillary condensation, when the relative pressure is too high.

FTIR is commonly applied to define the presence of polar surface functional groups. Typical peaks for CAs are listed in Table 11. Raman is less commonly applied to assess the hybridisation of a network via the analysis of the ratio between the D and G bands at  $1350 \text{ cm}^{-1}$  and  $1580 \text{ cm}^{-1}$ , respectively (Biru and Iovu, 2018; Melanitis et al., 1996a, 1996b). The D-band corresponds to disordered  $sp^3$  hybridised carbon, whilst the G-band relates to crystalline, ordered  $sp^2$  hybridised carbons. Other common characterisation techniques include scanning electron microscopy energy-dispersive X-ray spectroscopy (SEM-EDS) to determine the surface morphology and surface composition.

Table 11  
Commonly assigned FTIR peaks for CAs.

FTIR peak ( $\text{cm}^{-1}$ )	Peak assignment
3700 – 3200	O-H stretch N-H stretch
1775–1690	C=O stretch
1690–1640	C=N stretch
1678–1610	C=C stretch
1550–1500	N-O stretch
1465–1390	C-H bend
1440–1310	O-H bend
1342–1266	C-N stretch (aromatic)
1310–1250	C-O stretch (aromatic)
995–985	C=C bend
1000	C-O-N
900–700	C-H

### 3.4. Modification of carbonaceous adsorbents

Excluding surface area and porosity, modification of surface chemistry of the adsorbent could be considered as one of the most important aspects of adsorbent preparation. The technique aims to improve the adsorption capacity by increasing the selectivity of the adsorbent toward target pollutants. This is achieved by altering the chemical characteristics to increase the abundance of active sites on the surface of the adsorbent.

Similar to activation, modification can be grouped into physical or chemical techniques. Traditionally, acidic, or basic treatments have been applied to introduce heteroatoms such as oxygen, nitrogen, sulphur and phosphorous into the carbonaceous matrix. Due to the aromatic nature of carbonaceous materials, it is widely accepted that when functionalised, their chemical properties would resemble that of their aromatic hydrocarbon counterparts and therefore can readily generate reactive acidic or basic surfaces due to the presence of delocalised electrons (Fig. 14) (Rehman et al., 2019). Acidic and basic surfaces are advantageous for applications in aqueous media because they increase the hydrophilicity of the surface. In recent decades attention has turned to more energy efficient techniques such as microwave, plasma, or ozone treatments.

Despite all the positive aspects of adsorbent modification, it also comes with drawbacks. Introducing surface functionalities can result in pore blocking, ultimately reducing the surface area of the adsorbent. Regardless of this phenomenon, increasing surface functionalities does not correlate with decreasing adsorption capacity, due to the increased active sites for adsorption. However, functionality selection is paramount, since bulkier groups have a larger impact on pore blocking.

When selecting modification techniques, it is fundamental to first consider the characteristics of the adsorbate system in question. pH has a dramatic effect on the speciation of pollutants which may exist in cationic, anionic or zwitterionic forms, as discussed in Sections 1.1 – 1.3. Moreover, the pH will impact the surface charge of an adsorbent. Therefore, when selecting modification techniques, the functionalities present must be compatible with each other, either by physical or

chemical interactions, at the desired experimental conditions.

A key characterisation technique used to determine the behaviour of an adsorbent is the point of zero charge ( $\text{pH}_{\text{PZC}}$ ), which identifies the pH at which the net charge of an adsorbent's surface is zero. There are several techniques in literature which are commonly applied to determine  $\text{pH}_{\text{PZC}}$ , including, mass titrations, potentiometric titrations, and the salt addition method. Mass titrations consist of preparing solutions of varying pH by the addition of NaOH or  $\text{HNO}_3$  to deionised water. Known amounts of CA are then added to the mixture and allowed to equilibrate for a minimum of 24 h under nitrogen atmosphere, followed by measurement of the solution pH.  $\text{pH}_{\text{PZC}}$  is determined by plotting the solid fraction (wt%) against the pH, the point where all points converge, as the mass fraction is increased is the  $\text{pH}_{\text{PZC}}$  (Fig. 15a) (Noh and Schwarz, 1990; Kodama and Sekiguchi, 2006; Peng et al., 2018; Qin et al., 2018). The technique benefits from being simple and cheap which has led to numerous citations in literature; however, the method is very sensitive to traces of acids or bases. Potentiometric titrations consist of titrating NaOH with a solution containing CAs and  $\text{NaNO}_3$  and measuring the pH after each addition, where the equivalence point constitutes the  $\text{pH}_{\text{PZC}}$  (Fig. 15b) (Okman et al., 2014). Finally, salt addition consists of combining CAs with 0.1 M NaCl of varied pH (2 – 12) adjusting the solution using HCl or NaOH, the suspension is then allowed to equilibrate for a minimum of 24 h prior to recording the pH.  $\text{pH}_{\text{PZC}}$  is determined by plotting the final pH final vs. the initial pH, where the point of intersection corresponds to the  $\text{pH}_{\text{PZC}}$  (Fig. 15c) (Abatal et al., 2020; Mahmood et al., 2011; Al-Degees et al., 2008).

Furthermore, the total acidity and basicity of an adsorbent can be determined using Boehm titrations. Goertzen and Ockele et al. have published several articles to standardise the methodology of the technique (Goertzen et al., 2010; Oickle et al., 2010). In summary, CAs are combined with one of three 0.05 M reaction bases ( $\text{NaHCO}_3$ ,  $\text{Na}_2\text{CO}_3$  or NaOH). After which the CA-containing solutions were acidified using HCl. The subsequent mixtures were then back titrated using standardised 0.05 M NaOH. Non-acidified solutions were titrated directly with 0.05 M HCl. For back-titrations, the number of acidic groups is calculated by Eq. (3), whereas for direct titrations Eq. (4) is used.

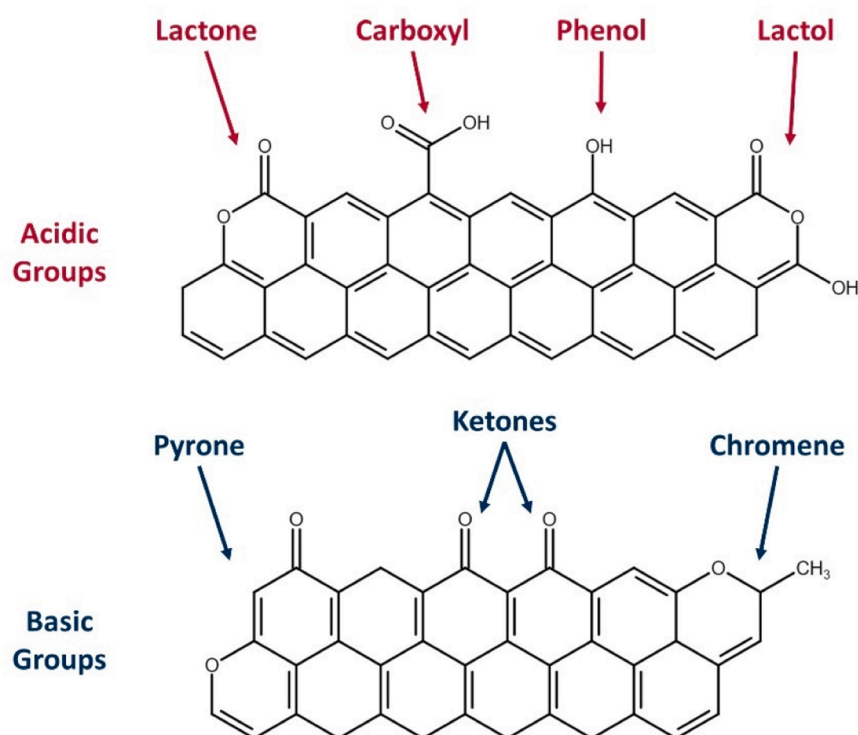


Fig. 14. Acidic and basic surface groups of carbonaceous adsorbents.

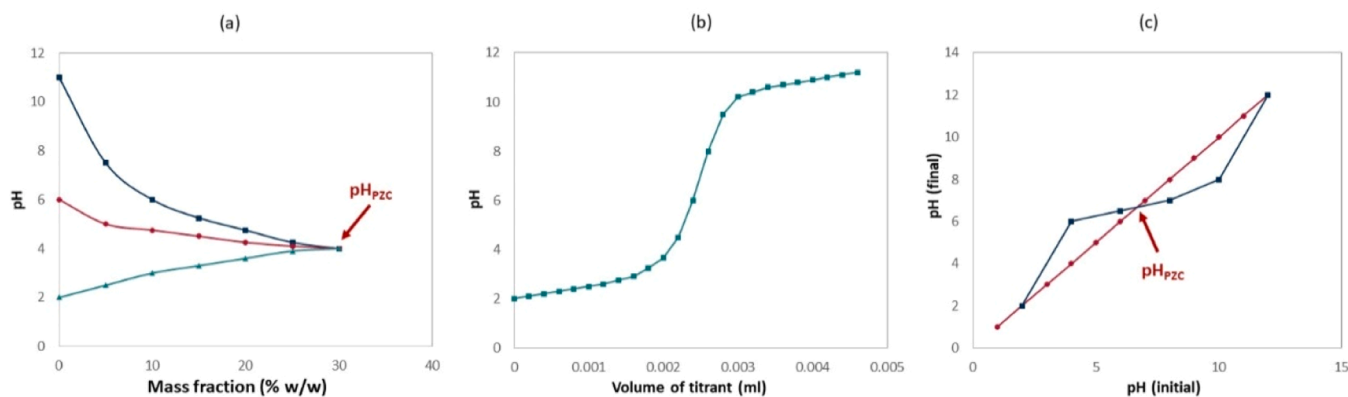


Fig. 15. Examples of PZC determination using (a) mass titration, (b) potentiometric titration and (c) salt addition techniques.

$$n_{CSF} = \frac{n_{HCl}}{n_B} [B]V_B - ([HCl]V_{HCl} - [NaOH]V_{NaOH}) \frac{V_B}{V_a} \quad (3)$$

$$n_{CSF} = [B]V_B - [HCl]V_{HCl} \frac{V_B}{V_a} \quad (4)$$

In the above equations,  $n_{CSF}$  is the number of moles of surface functional groups on the CA,  $[B]$  ( $\frac{n_{HCl}}{n_B}$ ) is the molar ratio of HCl to reaction base,  $V_B$   $[HCl]$   $[M]$  and  $V_{HCl}$   $[ml]$  are the concentrations and volumes of the base and HCl, respectively.  $V_a$  is the volume of the aliquot taken from  $V_B$ . The various acid functionalities (phenolic, lactonic and

carboxylic) are calculated via the differences in  $n_{CSF}$ , since NaOH reacts with all acidic groups,  $Na_2CO_3$  reacts with carboxylic and lactonic groups and  $NaHCO_3$  only reacts with carboxylic groups (Goertzen et al., 2010).

In order to increase the acidic nature of a surface, heteroatoms with proton donor capabilities are introduced to the structure. Oxidation of the carbonaceous structure using nitric acid or sulphuric acid has been the most extensively studied. Depending on the modification agent, modification temperature may or may not have an impact. With regards to nitric acid modification there is a strong positive correlation between increasing temperature and increasing oxygen-containing surface

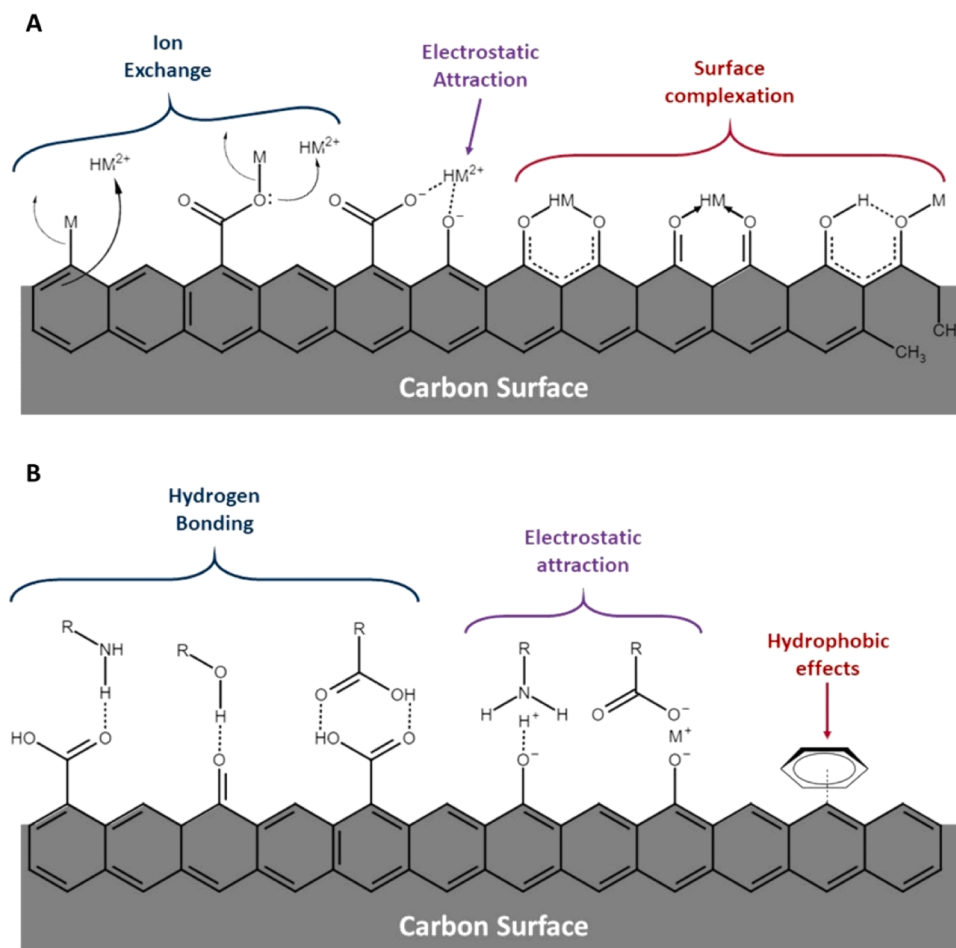


Fig. 16. Common chemisorption mechanisms for (A) heavy metals and (B) antibiotics. Where, HM and M indicate heavy metals and alkali or alkaline earth metals, respectively.

functionalities (Rivera-Utrilla et al., 2011). Oxidation is a particularly attractive technique when considering the adsorption of HMs from water since divalent metal cations readily react with deprotonated oxygen containing groups via several pathways, the formation of chelation complexes, ion exchange reactions and electrostatic interactions (Fig. 16) (Neolaka et al., 2023).

Adsorption mechanisms of organic molecules can be more complex due to the vast range of chemical functionalities and molecular sizes. The interactions may be hydrophilic or hydrophobic in nature depending on the adsorbate-adsorbent system (Fig. 16). Hydrophilic interactions include surface complexation, covalent bonding, electrostatic interactions, and hydrogen bonding (Neolaka et al., 2023). Hydrophobic effects include  $\pi$ - $\pi$  interactions and hydrophobic effects (aggregation). For antibiotics, hydrophilic interactions are more common due to Lipinski's rule of five which states that the octanol-water partition coefficient should not exceed 5 in order to prevent bioaccumulation via hydrophobic interactions with fatty tissues. However, this is highly dependent on pH since a neutrally charged molecule will favour  $\pi$ - $\pi$  interactions. Since both HMs and antibiotics tend to interact with hydrophilic entities, increasing the overall acidity/basicity of an adsorbent will be the subject of this section.

Nitric acid modification has been extensively applied to enhance the adsorption of both antibiotics and HMs (Qin et al., 2018; Huang and Su, 2010; Zhao et al., 2018; Demiral et al., 2021; Khan et al., 2019). ACF felt have been modified to enhance the adsorption  $\text{Cd}^{6+}$  ions. This was achieved by combining ACFs with 3.65 M  $\text{HNO}_3$  in a thermostat oscillator for 2 h (Zhao et al., 2018). The subsequent m-ACFs were washed and dried. It was observed that modification resulted in an increase in oxygen-containing functional groups and  $\text{sp}^3$  hybridised carbon, which were confirmed using FTIR; indicating the presence of carboxyl, hydroxyl and carbonyl groups. When applied as electro-assisted adsorbents, m-ACFs had significantly higher maximum adsorption capacities, when compared to commercial ACs and ACFs (Fig. 17). This can be attributed to the increased surface area, pore volume and active sites for adsorption.

Correct selection of modification conditions are imperative, as too harsh conditions may result in the destruction of the porous network, as observed in the study conducted by Qin et al. High temperatures (90 °C), concentrated  $\text{HNO}_3$  (10 M) and prolonged hold times (12 h), were applied in the modification procedure, resulting in a 96.6% reduction in

$S_{\text{BET}}$  of the m-ACs. Despite the significant reduction in surface area, the acidic surface groups present in the structure quadrupled, and the basic groups doubled, resulting in increased adsorption capacities of Cu(II) and TC, due to enhanced electrostatic attraction. The overall adsorption capacities in this study could be further improved through the application of optimisation of the modification process, to maintain a high surface acidity, whilst preventing the depletion of the surface area.

Turk Sekulic et al. functionalised ACs by combining them with 50% (w/v)  $\text{H}_3\text{PO}_4$ , in a 1:1 ratio (Turk Sekulic et al., 2019). The impregnated material was then subjected to a two-phase functionalisation procedure, where it was first heated to 180 °C for 45 min. The temperature was then increased to 500 °C and held at this temperature for 1 h. Using FTIR, the modified ACs were found to have newly formed phosphor-containing groups, in addition to increased oxygen containing groups. A novel approach to CA development, is introducing metals into a CA structure, which act as both adsorbents and catalysts, by degrading organic pollutants via non-selective oxidation through the production of free radicals (Peng et al., 2018; Zhou et al., 2021). Peng et al. investigated the adsorption of fluoroquinolone antibiotics onto amine functionalised magnetic ACs. Prior to modification, the ACs were chemically activated using  $\text{H}_3\text{PO}_4$ . The modification consisted of a two-step process. Firstly, the ACs were soaked in a solution of 0.25 M  $\text{FeSO}_4$  and 0.50 M  $\text{FeCl}_3$  for 2 h at room temperature, under nitrogen atmosphere. Afterward,  $\text{NH}_3 \cdot \text{H}_2\text{O}$  was added to the reaction mixture and heated to 70 °C and held for 4 h. 20 ml of epichlorohydrin and N,N-dimethylformaldehyde (1:1 ratio) were added to the container which was stirred at 90 °C for 2 h, followed by the addition of 3 ml of ethylenediamine for 1 h. Finally, 10 ml of triethylamine was added to the solution under stirring for 2 h, prior to washing and drying of the final product. Interestingly, it was observed that both the surface area and pore volume increased after modification which was attributed to pore opening during the amine-functionalisation process, usually during modification processes, increasing the surface functionalisation results in pore blocking and a decreased surface area (Table 12). The modified ACs were then applied in batch and continuous adsorption studies (Section 6.1), and regeneration cycles (Section 7). Despite seeing an overall increase in the adsorption capacity of the modified ACs, a key limitation of this study is the industrial feasibility and cost of the modification method, requiring a large number of chemicals and reaction steps.

Biomacromolecules such as alginate and chitosan, can be grafted with other forms of CA, in addition to use as the adsorbent precursor, as discussed in Section 3.1. Hassan et al., synthesised calcium alginate/AC composite beads using the ionic gelation method to investigate the removal arsenic (Hassan et al., 2014). This was achieved by mixing 2 g of AC with 100 ml of deionised water and 200 ml of sodium alginate (1% wt/v). The subsequent mixture was stirred for 2 hr to achieve homogeneous solution. After which the solution was transferred to a burette and added dropwise to a solution of calcium chloride to achieve the final product which is denoted as GC. KOH activated ACs (C) and calcium alginate beads (G) were also prepared individually for comparison purposes. Although GC had a surface area of less than half of C, the arsenic adsorption capacity was found to be more than double. This was attributed to the significantly high affinity of alginate to divalent metal ions.

Chitosan-based adsorbents have been modified with glycidyl-methacrylate and diethylenetriamine grafting (Elwakeel and Guibal, 2015). Firstly, the chitosan-based adsorbent was combined with glycidyl-methacrylate in a mass ratio of 50% (w/w). The mixture was

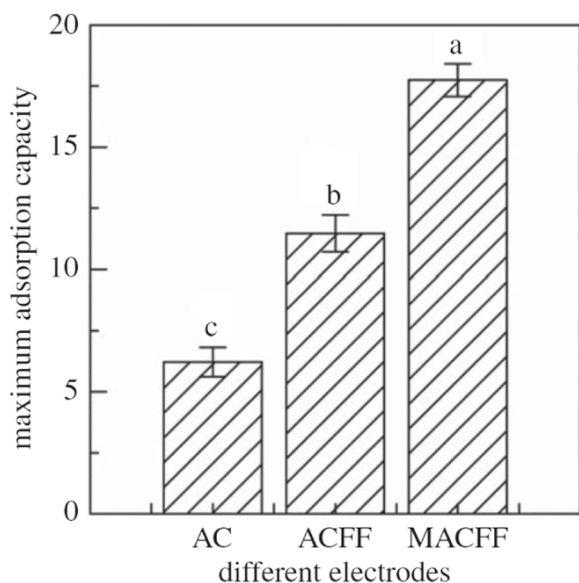


Fig. 17. Maximum adsorption capacity of different electrodes (activated carbon, activated carbon fibre felt and modified activated carbon fibre felt) for  $\text{Cr}^{6+}$  (300 mg/l) (Zhao et al., 2018).

Table 12  
Surface area and arsenic adsorption capacity of C, G and GC.

Sample	$S_{\text{BET}}$	Adsorption capacity (mg/L)
C	1621.0	26.3
G	32.9	39.4
GC	733.6	54.8

then agitated before adding 0.2 g of MBA and 0.1 g of Bz<sub>2</sub>O were then added as the crosslinking agent and indicator for the polymerisation reaction, respectively. Followed by the addition 1 g of magnetite. Finally, 3 ml of isopropyl alcohol and cyclohexane were added. The resulting solution was transferred to a flask containing 100 ml of 1% polyvinyl alcohol and heated in a water bath at 75 – 80 °C for 3 h under stirring. The resulting product was washed and air dried. Once dry the chitosan-based adsorbent was suspended in 70 ml of isopropyl alcohol, forming a suspension. Epichlorohydrin was then dissolved in an acetone/water mixture (1:1 v/v) and stirred for 24 at 60 °C. The final product was washed, treated with DETA and dried. The resulting adsorbent was applied to Hg(II) adsorption, achieving a maximum adsorption capacity of 2.02 mmol/g.

Chitosan has been grafted onto fly ash to investigate the adsorption of HMs (Adamczuk and Kołodyńska, 2015). This was achieved by dissolving chitosan into acetic acid and water under continuous agitation at 100 rpm for 24 h. Activated fly ash was then combined with various IR of chitosan, ranging from 4:1 – 8:1. The subsequent adsorbents were found to have an irregular and porous surface. In some cases, a plethora of modification techniques may be applied to achieve the desired adsorbent characteristics. For example, Ameen et al., developed CoFe<sub>2</sub>O<sub>4</sub>/NiO anchored microalgae-derived nitrogen-doped AC for the removal of azithromycin (Ameen et al., 2023). The synthesis of the microalgae-derived AC was achieved by mixing micro algae and glucose in a 2:1 mass ratio at 120 °C for 24 h in a Teflon-lined stainless-steel

autoclave reactor. The resultant biochar was washed with distilled water and ethanol followed by drying at 100 °C. CoFe<sub>2</sub>O<sub>4</sub>/NiO were synthesised using the co-precipitation method. The resulting particles were mixed with AC in a 1:3 ratio, which was ultrasonically dispersed in ethanol for 2 h, after which the dispersion was heated to 80 °C for 18 h. The resultant product was found to have a low surface area of 111.88 m<sup>2</sup>/g, despite this, a high removal efficiency of < 98% was achieved. This synthesis technique benefits from having an optimum pH range of 7, therefore being applicable at environmentally relevant conditions, however the complexity of the synthesis route would lead to increased costs in comparison to traditional modification techniques. Table 13.

#### 4. Application of adsorbents to remove pollutants generated by the aquaculture industry

Adsorption is a highly attractive separation technology, owing to being cheap, simple, and readily industrially scalable processes. This is particularly true for aqueous-phase adsorption, where it has been estimated that 80% of the AC globally is applied within aqueous media (Dias et al., 2007).

Removal efficiency directly relates to adsorbent’s surface area, pore size distribution and functionalisation. Increasing the microporosity of a material increases the total surface area; however, limits the accessibility to internal networks by larger molecules. In an aquatic setting,

**Table 13**  
Review of the modification technologies for CAs.

Precursor	Modification agent/ Concentration (M)	Modification Temperature (°C)	Modification Time (h)	S <sub>BET</sub> (m <sup>2</sup> /g)		V <sub>micro</sub> /V <sub>tot</sub> (cm <sup>3</sup> / g)		PZC		Functional Groups Introduced	ref
				CA	m-CA	CA	m-CA	CA	m-CA		
PAN-ACF cloth	HNO <sub>3</sub> /3	50	24	1123.3	1209.3	0.55/ 0.74	0.50/ 0.69	8.2	2.2		(Huang and Su, 2010)
Phenol- based ACFs	HNO <sub>3</sub> /0.1	20	1	1670	1550.0	0.64/ 0.68	0.62/ 0.65			Hydroxyl, carboxyl	(Oda et al., 2006)
ACF felt	HNO <sub>3</sub> /3.65	-	2	835.26	1104.5	0.26/-	0.32/-			carboxyl, hydroxyl and carbonyl	(Zhao et al., 2018)
GAC	HNO <sub>3</sub> /10	90	12	1392	48.0	-/0.93	-/0.4	5.8			(Qin et al., 2018)
AC	HNO <sub>3</sub> /15	90	2	1399	738.1	0.55/ 0.68	0.29/ 0.40	3.6	2.8	lactonic, phenolic, and carboxylic	(Demiral et al., 2021)
MWCNT	H <sub>2</sub> SO <sub>4</sub> /18 M HNO <sub>3</sub> /14 M 3:1 vol/vol	120	0.5							Carboxylic, carbonyl	(Khan et al., 2019)
AC	H <sub>3</sub> PO <sub>4</sub>	1. 180 2. 500	1. 0.75 2. 1		1230.6		0.50/ 0.62		4.1		(Turk Sekulic et al., 2019)
Viscose ACF	H <sub>2</sub> O <sub>2</sub>	Ambient	3	1223	1202	0.45/ 0.58	0.45/ 0.57			Pyridinic, pyrrolic quaternary-N	(Yang et al., 2012)
Raynon ACF	Thermal	500	0.55	1267	2121	0.46/ 0.60	0.68/ 0.90				(Rong et al., 2003)
PAN-ACF	HF/4	50	24	1239	979	0.42/ 0.43	0.21/ 0.31			Carboxylic hydroxyl	(Bai et al., 2015)
PAN-ACF	NaOCl/0.13	700	24	1910	1946	0.75/ 0.79	0.76/ 0.80	8.40	7.80	Carbonyl phenolic	(Guedidi et al., 2017)
Lyocell fibres	O <sub>2</sub> plasma	300 (W)	3	2121	1615	0.82/ 1.22	0.63/ 0.89			Phenolic, carboxylic	(Park and Kim, 2004)
Lyocell fibres	N <sub>2</sub> plasma	120 (W)	0.17	1003	1040	0.39/ 0.51	0.37/ 0.53			Pyridinic, pyrrolic quaternary-N	(Bai, Dec 15 et al., 2016)
MWCNT	HNO <sub>3</sub> /3 H <sub>2</sub> SO <sub>4</sub> /1	85	3	435	330	-/0.91	-/0.48			Acidic	(Lu and Chiu, 2008)
MWCNT	HNO <sub>3</sub>	85	3	435	256	-/0.91	-/0.35			Acidic	(Lu and Chiu, 2008)
MWCNT	KMnO <sub>4</sub>	85	3	435	283	-/0.91	-/0.37			Acidic	(Lu and Chiu, 2008)
MWCNT	NaClO	85	3	435	297	-/0.91	-/0.38			Acidic	(Lu and Chiu, 2008)

typically mesoporosity or hierarchical porosity is favoured since larger pores provide low-resistance transport pathways for a range of pollutants.

When considering the pollutants generated by the aquaculture industry, there are a range of organic and inorganics introduced, such as antibiotics, nutrients, hormones, anaesthetics and more (Section 2.1). However, due to their persistence and impacts on human and environmental health, antibiotics and HMs will be the key focus in this review paper.

#### 4.1. Single-component adsorption

##### 4.1.1. Batch adsorption

Batch adsorption is a simplistic method, used to identify the removal percentage, influence of various factors, equilibrium adsorption capacity (Section 4.1.1.1) and adsorption kinetics (Section 4.1.1.2) of a system. A known amount of CA is combined with a known concentration of adsorbate for a predetermined time, after which the final adsorbate concentration is measured (Aktar, 2021). Commonly investigated parameters for aqueous adsorption systems include pH, initial adsorbate concentration, adsorbent dose, and temperature.

Davidi et al. applied batch adsorption to investigate the adsorption of Zn(II) using  $H_3PO_4$ -ACs (Davidi et al., 2019). The parameters studied were pH, contact time and initial concentration which were ranged between 1 and 7, 5 – 360 min and 25 – 100 mg/L, respectively. Adsorption capacity was found to increase with increasing pH due to enhanced electrostatic interactions between the positively charged metal ion and negatively charged adsorbent surface. ACs have also been applied to adsorb TCs using NaOH-ACs. Batch adsorption studies were applied to determine investigate the effects of initial concentration and pH (Martins, Jan 15 et al., 2015). Lower pH (~3) favoured higher adsorption capacities of TC due to the di- and tri-valent species present which readily interact with the negatively charged adsorbent surface.

In recent years, some studies have turned to the application of X-ray fluorescence (XRF) to determine the maximum retention capacity over traditional adsorption isotherms (Aranda et al., 2013, 2016). The technique benefits from its ability for direct analysis of solid and liquid samples with minimum sample handling. However, aqueous phase analysis has some limitations such as short linear range, poor sensitivity and the requirement for precise standards to overcome matrix effects (Aranda et al., 2013). Aranda et al. determined the retention of As(V) on activated MWCNTs using XRF and found the total capacity retention was 150 mg/g (Fig. 18) (Aranda et al., 2016).

As can be seen from Table 14, CAs have been extensively applied to remediate pollutants such as antibiotics and HMs. However, for antibiotics in particular, understanding the mechanism of adsorption for

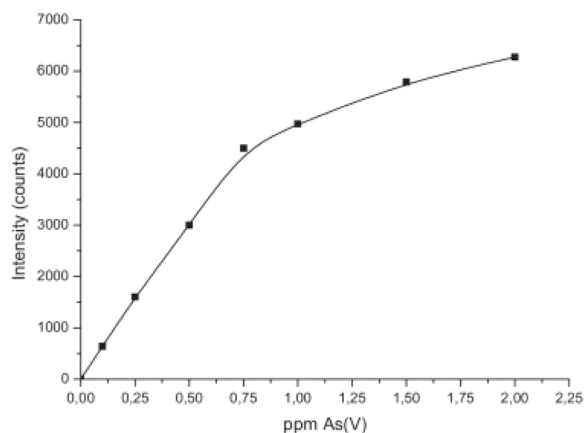


Fig. 18. Retention capacity of As(V) on activated MWCNTs (Aranda et al., 2016).

parent compounds and their subsequent degradation compounds can be difficult. Some studies are beginning to investigate the interaction mechanism via a computational approach, namely density functional theory Vienna Ab-initio simulation package (DFT-VASP), which allows for modelling of atomic scale materials (Ai et al., 2019; Wang, Jun 1 et al., 2021; Kan, Jul 1 et al., 2023). Wang et al. applied DFT-VASP with the Perdew-Burke-Ernzerh (PBE) parameterization of the generalized gradient approximation (GGA) to investigate the adsorption of three antibiotics TC, ofloxacin (OFO) and norfloxacin (NFO) onto AC (Wang, Jun 1 et al., 2021). The schematic depicted the laminae-trestle-laminae (L-T-L) structure (Fig. 19B) which was previously observed using SEM (Fig. 19A). The computational analysis identified that the L-T-L structure assisted with external diffusion, whilst hydrophilic nature of agarose is one of the key factors to aid adsorption. Furthermore, the adsorption models and energies were computed (Fig. 19C). The energies of adsorption were calculated to be  $-0.629$ ,  $-0.397$  and  $-0.385$  eV for LAC-OFO, LAC-TC and LAC-NFO, respectively. Lower energies of adsorption are favoured this suggesting that the highest adsorption capacities would be observed with OFO, which was in agreement with the experimental campaign, where the maximum adsorption capacities for TC, OFO and NFO were calculated to be of 537.63, 581.40 and 434.78 mg/g, respectively.

4.1.1.1. Adsorption isotherms. Adsorption isotherms are a fundamental technique, used to describe the equilibrium within an adsorption system by identifying the interactions between adsorbents and adsorbate molecules. There are numerous adsorption isotherms cited in literature which are typically divided depending on type of surface coverage (monolayer vs multilayer), whether adsorbates are mobile or localised, and the number of model parameters employed. The most commonly cited isotherms for liquid adsorption are Langmuir, Freundlich and Temkin isotherms, which have been discussed below.

The Langmuir adsorption isotherm (Eq. (5)) was one of the first proposed models and typically describes chemisorption phenomenon (Langmuir, 1918). The isotherm is based on several assumptions; adsorption occurs in a monolayer only, the surface of the adsorbent is homogeneous, and all sites are energetically equivalent, adsorption is irreversible, each active site only interacts with one adsorbent molecule and adsorbent molecules are localised, meaning there is no lateral interactions between adsorbent molecules.

$$q_e = \frac{K_L C_e}{1 + K_L C_e} \quad (5)$$

Where,  $q_e$  [mg/g] is the equilibrium adsorption capacity,  $K_L$  [L/mg] is the Langmuir constant, relating to rate of adsorption, and  $C_e$  [mg/L] is the concentration at equilibrium.

The Freundlich isotherm is an empirical adsorption model, which developed upon Langmuir's equation. The Freundlich model typically describes physisorption, meaning the reaction is reversible. Freundlich's assumptions allows for multilayer adsorption on a surface with asymmetric energy distribution, with a decreasing adsorption energy as more molecules are adsorbed, and accounts for surface heterogeneity.

$$q_e = K_F C_e^{1/n} \quad (6)$$

Where,  $K_F$  [L/g] is the Freundlich constant, and  $n$  is a correction factor for adsorption intensity. One disadvantage of the Freundlich isotherm is the fact that it cannot predict an adsorption maximum; however, researchers have often used the parameters  $K_F$  and  $1/n$  to draw conclusions.

The Temkin isotherm is another empirical isotherm which accounts for chemisorption. The isotherm is best suited to intermediate adsorbate concentrations. Due to adsorbate-adsorbent interactions, it is assumed that the heat of adsorption ( $\Delta H_{ads}$ ) of all adsorbate molecules within a layer decrease linearly as adsorption capacity increases.

**Table 14**  
Review of carbonaceous adsorbents to remediate aquaculture pollutants.

Sample	S <sub>BET</sub>	V <sub>micro</sub> / V <sub>tot</sub>	Pollutant	C <sub>0</sub> (mg/ L)	q <sub>e</sub> (mg/ g)	Optimum pH	Adsorption isotherm/R <sup>2</sup>	Kinetic model/ R <sup>2</sup>	Ref
AC	852	-/0.67	Ciprofloxacin		101.7	8.5	Langmuir/0.999	PSO/0.998	(Abbas et al., 2016)
AC	852	-/0.67	Norfloxacin		99.71	4.5	Langmuir/0.999	PSO/0.998	(Abbas et al., 2016)
AC	852	-/0.67	Levofloxacin		104.76	8.5	Langmuir/0.999	PSO/0.999	(Abbas et al., 2016)
m-AC (Thermal)	1013	0.34/ 0.66	Ciprofloxacin	20	300	7	Langmuir/0.995	PSO/0.981	(Carabineiro, 2011)
m-AC (H <sub>3</sub> PO <sub>4</sub> )	-	-	Ciprofloxacin	50	49.75	8	Langmuir/0.982	PSO/0.999	(Agboola, Olugbenga and, Bello S.)
CNTs (Thermal)	456	0/2.13	Ciprofloxacin	20	60	7	Langmuir/0.998	PSO/0.980	(Carabineiro, 2011)
AC	1524	0.65/ 0.83	Tetracycline	500	369.4	3	Temkin/0.980	Elovich/0.990	(Martins, Jan 15 et al., 2015)
m-AC (H <sub>2</sub> O <sub>2</sub> )	117.05	-/0.10	Tetracycline	500	42.45	9	Langmuir/0.991	PSO/0.947	(Tan et al., 2019)
ACF	1007.69	0.34/ 0.49	Tetracycline		249.02	2	Freundlich/0.999	PSO/0.999	(Huang et al., 2013)
ACF	1007.69	0.34/ 0.49	Oxytetracycline		249.00	2	Langmuir/0.998	PSO/0.999	(Huang et al., 2013)
AC	-	-	Oxytetracycline	10	17.99	9	Freundlich/0.980	PSO/0.990	(Nayeri et al., 2019)
MWCNT	-	-	Cu <sup>2+</sup>	10	28.49	5	Langmuir/0.982	-	(Li et al., 2003)
AC	9.71	-	Cu <sup>2+</sup>	90	34.85	4.77	Langmuir/0.984	PSO/0.943	(Liu et al., 2018)
m-AC	1100	-	Cu <sup>2+</sup>	37	38		Langmuir/0.990	-	(Monser and Adhoum, 2002)
([N(C <sub>4</sub> H <sub>9</sub> ) <sub>4</sub> ] <sup>+</sup> )									
m-AC	1100	-	Zn <sup>2+</sup>	27	9.9		Langmuir/0.990		(Monser and Adhoum, 2002)
([N(C <sub>4</sub> H <sub>9</sub> ) <sub>4</sub> ] <sup>+</sup> )									
m-MWCNT	297	-/0.38	Zn <sup>2+</sup>		3.268		Langmuir/0.999	PSO/0.999	(Lu and Chiu, 2008)
(NaClO)									
Raynon-ACF	2121	0.68/ 0.90	Formaldehyde		723		-	-	(Rong et al., 2003)

$$q_e = \frac{RT}{K_T} \ln A_T C_e \tag{7}$$

Where, K<sub>T</sub> is the Temkin isotherm constant, A<sub>T</sub> is the Temkin equilibrium binding constant, R is the universal gas constant and T is the temperature (K).

A number of other isotherm models have also been used to describe the adsorption process. A summary of these isotherm models is presented in Table S1.

Overall, adsorption isotherms are fundamental to understanding adsorbate-adsorbent interactions. As can be seen in Table 14, a large portion of aqueous-phase CAs are fitted to the Langmuir adsorption isotherm when considering adsorption of both antibiotics and HMs, suggesting that chemisorption is the main mechanism of adsorption.

**4.1.1.2. Adsorption thermodynamics.** The thermodynamics of adsorption is another key analysis technique to determine whether a process is favourable. This is calculated using the Gibbs free energy of adsorption (ΔG<sub>ads</sub>). For an adsorption process to be spontaneous, ΔG<sub>ads</sub> must be negative. In simple form, the equation is as follows:

$$\Delta G_{ads} = \Delta G_{non-electric} + \Delta G_{electric} \tag{8}$$

Where ΔG<sub>electric</sub> refers to the energy of columbic interactions and ΔG<sub>non-electric</sub> refers to all other interactions. In practice, the ΔG<sub>ads</sub> can be calculated using the Eqs. (9)–(12). The distribution coefficient (K<sub>d</sub>) can be calculated using Eq. (9):

$$K_d = \frac{q_{eq}}{C_{eq}} \tag{9}$$

Where, K<sub>d</sub> is a dimensionless constant. Often, isotherm constants can be substituted for K<sub>d</sub>, for example the Langmuir constant is typically expressed in L/mol units; by multiplying it by the number of moles of water in a litre of solution (55.5 mol/L), it can be recalculated as a dimensionless constant. Subsequently, the true ΔG value can be calculated using Eq. (10).

$$\Delta G^0 = -RT \ln K_d \tag{10}$$

Eq. (11) expresses the relationship between ΔG<sup>0</sup>, enthalpy/heat of

adsorption (ΔH<sup>0</sup>) and entropy change (ΔS<sup>0</sup>):

$$\Delta G^0 = \Delta H^0 - T \Delta S^0 \tag{11}$$

By substituting Eq. (10) into Eq. (11), the following linear equation is generated:

$$\ln K_d = -\frac{\Delta H^0}{RT} + \frac{\Delta S^0}{R} \tag{12}$$

Therefore, by plotting lnK<sub>d</sub> against the inverse temperature, ΔH<sup>0</sup> and ΔS<sup>0</sup> can be determined from the slope and intercept, respectively.

In addition to adsorption isotherms, thermodynamic calculations offer an insight into an adsorption mechanism. ΔH<sup>0</sup> can provide a host of information; for example, positive ΔH<sup>0</sup> values indicate an endothermic process and negative values indicate exothermic processes. Additionally, the magnitude of ΔH<sup>0</sup> indicates the adsorption mechanism with physisorption typically ranging between 2.1 and 20.9 kJ/mol and chemisorption ranging between 80 and 200 kJ/mol. Unfortunately, this technique is only accurate if K<sub>d</sub> has been calculated accurately, which is highly dependent on the adsorption system which has been discussed in depth elsewhere (Agboola, Olugbenga and, Bello S.; Liu, 2009).

Adamczuk et al. investigated the thermodynamics for the adsorption of HMs (Cr(III) Cr(VI), Cu(II), Zn(II) and As(V)) onto chitosan-coated fly ash (Adamczuk and Kołodyńska, 2015). The study found that the adsorption process was favourable and spontaneous for all HMs due to the negative ΔG<sup>0</sup> and positive ΔH<sup>0</sup>.

**4.1.1.3. Adsorption kinetics.** Adsorption kinetics are hugely important to determine the rate of adsorption, which ultimately provides information on adsorbent performance and is essential for the design of adsorption systems. This is typically influenced by factors such as pH, adsorbate concentration, flow rate, adsorbent dose, surface morphology, and functionalization. The most common kinetic models are the pseudo-first order, pseudo-second order, Elovich and intraparticle diffusion models. In addition, there are a number of other kinetic models that have been reported (although less frequently) in the literature. These models have been summarised in Table S2.

The PFO and PSO models are empirical models which are typically applied in batch adsorption systems (Wang and Guo, 2020). There are

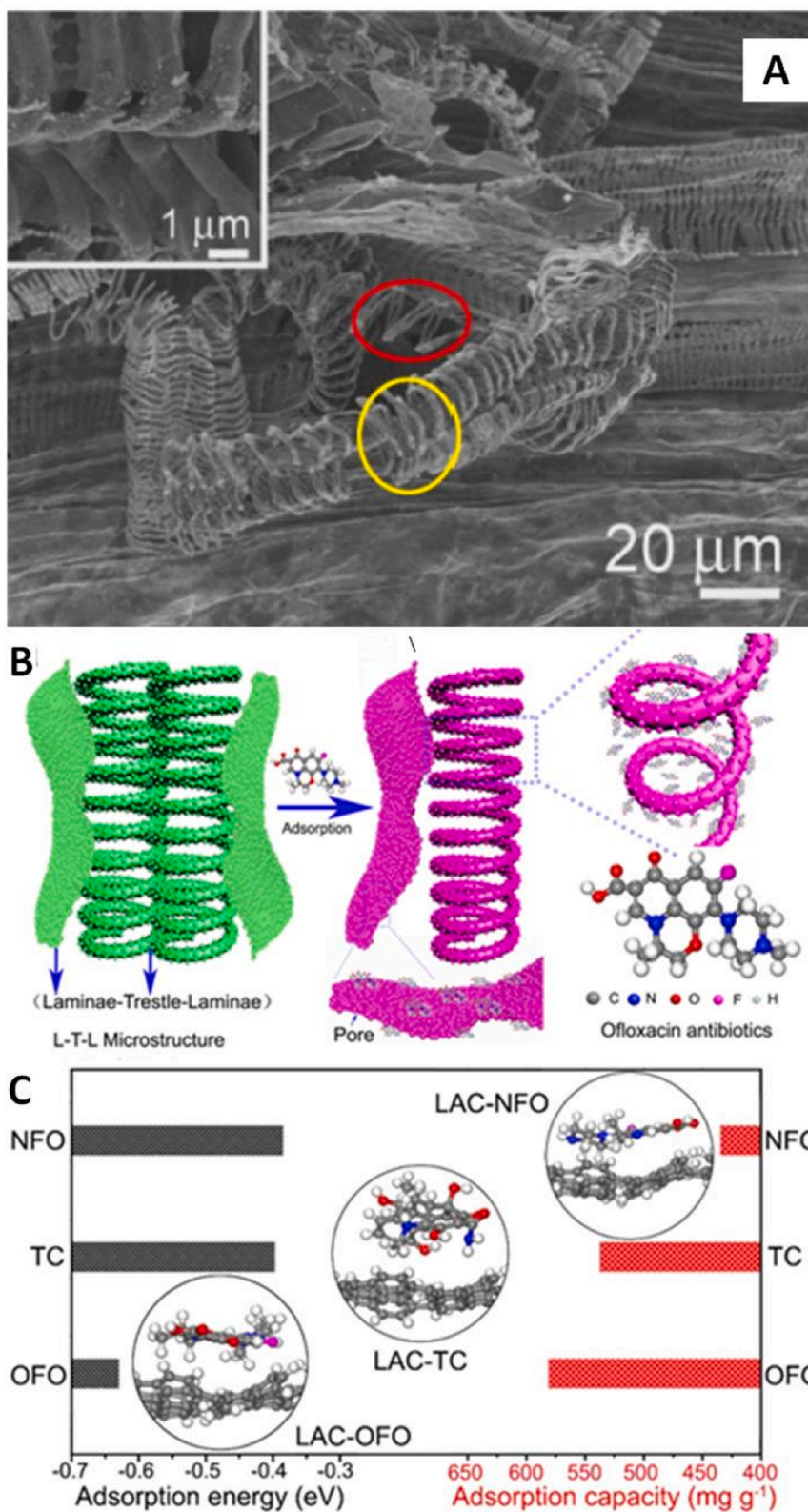


**Fig. 19.** (A) High resolution SEM images of the LAC. The upper left inset of (A) is an enlarged SEM image of the helix structure. (B) Schematic illustration of the adsorption process of LAC towards OFO. (C) The atomic adsorption model for NFO, TC and OFO adsorbed on LAC and the comparison of the corresponding adsorption energy (left axis) and capacity (right axis). Where, the grey, blue, red, pink and white balls represent carbon, nitrogen, oxygen, fluorine and hydrogen atoms, respectively.



some differences in the physical processes of each model. For example, PFO is suitable for systems where  $C_0$  is high, the process is in the initial stages of adsorption and there are few active sites. Whereas PSO is better suited to systems where  $C_0$  is low, adsorption occurs over a longer period and the adsorbent has abundant active sites. Linear regression of the models has been widely applied owing to its simplicity in calculating model parameters. However, linearization can introduce errors to both dependent and independent variables, through uncertainty and bias which ultimately leads to inaccurate estimations of the parameters (Wang and Guo, 2020).

In contrast, non-linear models provide more accurate estimations of model parameters, but are more complicated in practice. The method involves prediction of model parameters by applying a predefined objective function (OF), most commonly using the sum of squares of the differences between  $q_{e(cal)} and  $q_{e(exp)}$  (Eq. (13)).$

$$OF = \sum_{i=1}^n (y_i - \hat{y}_i)^2 \tag{13}$$

Where,  $n$  is the total number of observations,  $y_i$  is the experimental response of the  $i^{th}$  observation and  $\hat{y}_i$  is the calculated value of  $y_i$ .

Huang et al. applied PFO and PSO models in linear form to determine the adsorption kinetics of TC and OTC onto ACFs. The study found that the PSO model was best fitting for both TC and OTC, with correlation coefficients  $> 0.99$ , indicating that chemisorption may play a role in adsorption processes. This was further investigated using the process using the IPD multi-linearity method model,

Romero-Cano et al. investigated the adsorption kinetics of  $Cu^{2+}$  ions onto AC synthesised from fruit peels (Romero-Cano et al., 2017). The study applied PFO, PSO, Elovich and IPD models in non-linear form. For all models, the authors applied the Levenberg-Marquardt estimation algorithm, using statistical software (STATISTICA 7), to adjust the experimental data to fit them to non-linear equations. Analysis of the resulting data found that both the PFO and PSOs had the best fit, with  $R^2$  values  $> 0.99$ . However, it was concluded that PFO model best described the adsorption process since the  $q_{e(cal)}$  values were most similar to the  $q_{e(exp)}$ , meaning the adsorption mechanism was likely physical.

Similarly, to the adsorption isotherms, there is a clear trend in the adsorption kinetics of CAs, where PSO is most commonly assigned, suggesting that the rate-limiting step is surface adsorption involving chemisorption (Robati, 2013). Furthermore, as mentioned above PSO is

favoured at lower initial concentrations, which is typical of natural environments.

#### 4.1.2. Continuous adsorption

In industrial settings, continuous flow columns are commonly used via the employment of a dual-column system. This allows for continuous adsorption operations since one column can operate whilst the other is regenerated. In lab-scale research, continuous column operations can provide fundamental information regarding adsorbent properties such as the mass transfer zone and breakthrough curves.

Mass transfer describes the adsorption of a solution in a fixed bed. The kinetics of mass transfer can be summarised in four steps, namely, external mass transfer, internal mass transfer, surface diffusion and adsorption (de Haan, 2015). External mass transfer involves the diffusion of an adsorbate through the liquid film which surrounds the adsorbent. Internal mass transfer describes the movement of an adsorbent through the porous structure of an adsorbent. Surface diffusion occurs along the porous surface. Finally, the third step involves the adsorption of an adsorbate onto an active site. As the adsorption process continues, more fractions of the bed become saturated/used, resulting in the gradual migration of the mass transfer zone (MTZ) from the inlet ( $C_1 - C_3$ ) (Fig. 20) (Theodore and Ricci, 2011). Breakthrough curves are observed between the breakthrough and exhaustion points ( $C_3 - C_4$ ). The breakthrough point is defined, when the effluent concentration reaches 5% of the inlet concentration. The entire bed is considered to be saturated when the effluent concentration reaches 95% of the inlet concentration, which is known as the exhaustion point. From this data, the MTZ and breakthrough capacity (BC) can be determined using Eqs. (14) and (15), respectively (Theodore and Ricci, 2011).

$$MTZ = \left(1 - \frac{q_u}{q_{SAT}}\right)Z \tag{14}$$

$$BC = \frac{0.5(q_{SAT} \times MTZ) + q_{SAT}(Z - MTZ)}{Z} \tag{15}$$

Where,  $q_u$  and  $q_{SAT}$  [mg/g] are the useful adsorption capacity and the saturation capacity, respectively and  $Z$  is the bed length.

Numerous studies have been conducted to determine the uptake of pharmaceuticals and heavy metals in continuous flow mode (Table 15). Usually, batch adsorption studies will be undertaken prior to column experiments, to determine the optimum conditions such as pH and contact time (Section 6.1.1). Wang et al. investigated adsorption of

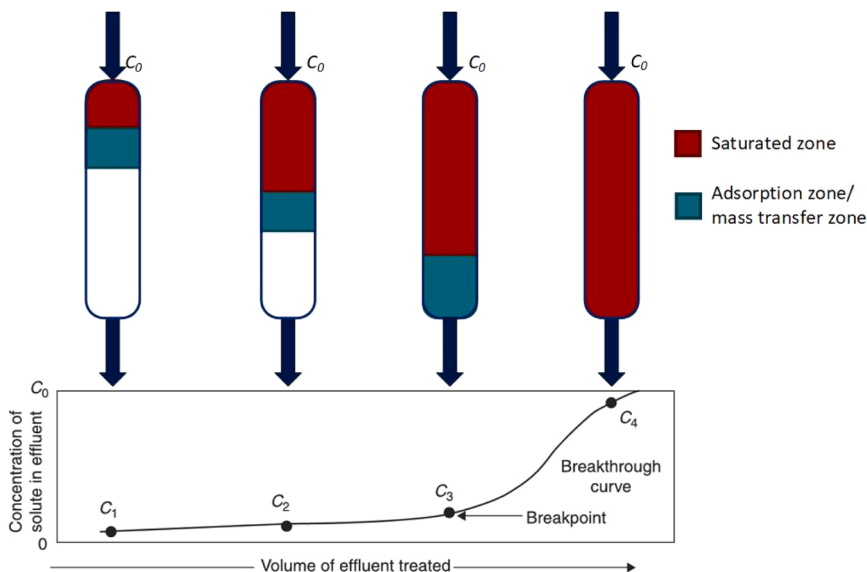


Fig. 20. – Schematic of continuous flow mode adsorption for the production of breakthrough curves.

**Table 15**  
Summary of literature employing lab-scale continuous adsorption experiments.

Adsorbent	$S_{BET}$ ( $m^2/g$ )	Adsorbate	Initial concentration (mg/L)	Column ID/L (mm)	Flow rate (ml/min)	Time (min)	$q_e$ (mg/g)	Ref
ACF	1499	CIP	10	50/200	10	60	191.8	(Wang et al., 2018)
ACF	1499	SDM	10	50/200	10	60	202.2	
AC	1029	AMX	50	11/300	6.67	10	274.1	(Moussavi et al., 2013)
AC	1259	SMX	1		3.5	60		(Zhou et al., 2021)
AC	1388	Zn(II)	100	2.5/30	10	1140	152	(Davidi et al., 2019)

ionisable antibiotics using ACF in continuous flow mode using electro-assisted adsorption (Wang et al., 2018). Voltages of  $-1.0$  ranging between  $1.0$  V were applied to the ACFs to enhance the adsorption of CIP and SDM, respectively. It was found that increasing the potential (positive or negative) increased the removal efficiency between 1.2 and 3.9 times, due to enhanced electrostatic interactions between the adsorbent surface and the ionised antibiotics (Fig. 21). The optimum pH for CIP and SDM were 7.4 and 6.1, respectively. At pH 7.4, CIP exists as  $CIP^{2+}$ , meaning an increased negative potential ( $-1.0$  V) leads to increased adsorption onto the deprotonated ACF surface. Whereas at pH 6.1, SDM exists as  $SDM^-$  meaning an increased positive potential ( $+1.0$  V) is favoured.

Zinc (II) adsorption has also been studied in continuous flow mode to assess the reusability of an adsorbent throughout three adsorption/desorption cycles (Davidi et al., 2019). The study was conducted using ACs derived from walnut shells which were chemically activated using  $H_3PO_4$ . The equilibrium adsorption capacity after one cycle was  $152$  mg/g, whilst the adsorption capacities of second and third cycles were reduced by 5%, and 29%, respectively. Furthermore, the subsequent cycles took less time to reach breakthrough, when compared to the first cycle (Fig. 22). This can be attributed to incomplete regeneration of the adsorbent between adsorption cycles, resulting in a reduction in available active sites and pore blocking.

## 4.2. Multi-component adsorption

### 4.2.1. Competition between pollutants

There are multiple potential pathways for pollutants in aquatic environments, which largely depends on the chemical characteristics of the pollutant in question. Yadav et al. investigated the adsorption of TC and sulfadiazine (SDZ) in both mono-component and multi-component systems using ACs derived from spent tea (Yadav et al., 2022). Batch adsorption studies were performed at  $25^\circ C$ . Similarly, to Section 4.1.1, preliminary mono-component adsorption was applied to investigate the impacts of various parameters such as pH (2 – 12), adsorbent dose (1 – 5 g/L), contact time (0 – 420 min) and initial concentration (5, 10, 25, 50 and 100 mg/L). Additionally, equilibrium and kinetic studies were

conducted. For multi-component adsorption, the optimum dosage was applied to solutions containing a mixture of TC and SDZ, having concentrations of 1 + 1, 5 + 5, 10 + 10, 25 + 25, 50 + 50 and 100 + 100 (mg/L, TC + SDZ). The competitive Langmuir isotherm was applied to determine the maximum adsorption capacity of both antibiotics within the system. An “antagonistic/synergistic” effect was observed where the adsorption of one component is suppressed by the other (Table 16). In this case, TC adsorption was improved, and SDZ suppressed when compared to the mono-component system.

Oxidised ACs have also been applied to investigate the simultaneous removal of TCs and Cu (II), consistently with above, monovalent solutions were investigated prior to divalent systems. An increased adsorption capacity was observed for both TC and Cu(II) in a binary system when compared to the individual component systems, indicating synergistic effects. This can be attributed to the formation of ternary complexes of AC-Cu(II)-TC and AC-TC-Cu(II).

### 4.2.2. Competition with salinity and other environmental matrices

In an environmental setting, the considerations for adsorption processes are much more complicated. The sea and natural waters are a complex mixture containing a myriad of environmental factors such as salinity, dissolved organic matter (DOM) and more, that will interfere with, or in some cases aid adsorption. This has been discussed below.

**4.2.2.1. Dissolved organic matter.** DOM is typically defined as the fraction of organic matter in aqueous phase, typically ranging between 1 and 450 nm in size (Gbadegesin et al., 2022). The natural prevalence of DOM originates from a wide range of sources such as leaching from rocks, crops, animal faeces and more. For this reason, DOM can have diverse chemical structures with a range of functional groups and molecular sizes, with humic-like, fulvic-like and tyrosine-like being identified as some of the most common forms of DOM in aquaculture (Nimptsch et al., 2015; Kamjunke et al., 2017). For this reason, a range of interaction mechanisms have been identified in literature, some frequent examples being complexation, covalent bonding,  $\pi$ - $\pi$  interactions, electrostatic interactions and van der Waals forces. For this reason, many forms of DOM can readily interact with adsorbent surfaces and

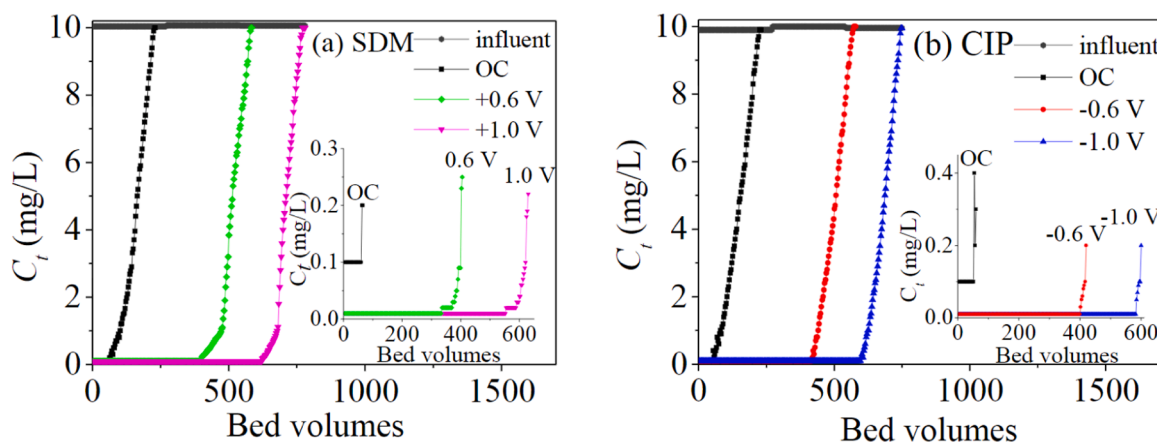


**Fig. 21.** Effluent concentrations ( $C_t$ ) of (a) SDM, (b) CIP, versus bed volume under different conditions. The inserts show magnified graphs of  $C_t$  in the range 0 to 0.4 mg/L (Wang et al., 2018).

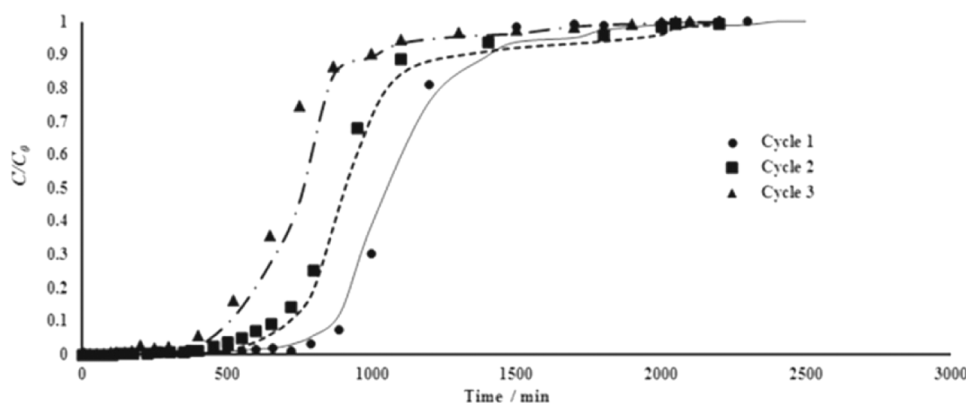


Fig. 22. The breakthrough curves for Zn(II)removal using OPAC activated carbon bed (Davidi et al., 2019).

Table 16

Equilibrium data of chicken feather derived biochars, in monocomponent and multicomponent systems.

System	Antibiotic	PAC			SAC		
		$q_m$	$K_L$	$R^2$	$q_m$	$K_L$	$R^2$
Monocomponent	TC	10.87	2.58	0.993	23.20	0.08	0.996
	SDZ	16.75	0.13	0.997	24.69	0.03	0.992
Multicomponent	TC	32.86	0.29	0.981	23.70	0.52	0.989
	SDZ	12.23	0.36	0.995	15.31	0.05	0.993

adsorbates. Numerous studies have identified direct site competition and pore blockage as the leading interference mechanisms of DOM, when considering the adsorption of pollutants onto carbonaceous materials (Gbadegesin et al., 2022; Wang et al., 2021b; Ebie et al., 2001; Guillossou et al., 2020).

In this case of DOM or other large environmental matrices, pore size exclusion is attractive to instantly limit a range of substances from entering a porous network. For example, DOM typically ranges from 1 to 450 nm in size (Murray et al., 2022). In comparison, the largest molecules applied in aquaculture are the tetracycline class antibiotics, which have a computationally simulated size of approximately  $1.48 \times 0.90 \times 0.75$  nm (Turk Sekulic et al., 2019). It has been well established that adsorption of molecules becomes more favourable when pore size is increased to approximately 1.7 times of a molecules second largest dimension (Pelekani and Snoeyink, 1999; Gun'ko, 2007). It is preferential for pores to be a similar size to the target adsorbate, to increase contact points between the molecule and adsorbent, and therefore the likelihood of interactions with active sites. However, pore sizes must be large enough to enable diffusion into the porous network. Therefore, by limiting pore sizes to 1.53 nm, large quantities of DOM can immediately be eliminated from the internal porous structure. However, this comes with some sacrifices; as previously mentioned in Section 4, mesoporosity or hierarchical porosity is attractive for aqueous phase adsorption due to reduced resistance and therefore, a compromise would need to be made between adsorption capacity of pollutants and exclusion of natural matter.

Guillossou et al. investigated the adsorption of 12 organic micropollutants (including some antibiotics) and DOM from wastewater effluents onto PAC (PB-170) purchased from DaCarb (Guillossou et al., 2020). The study first investigated the adsorption of DOM from wastewater. LC-OCD analysis identified humic-like substances, biopolymers, building blocks, low molecular weight neutrals and hydrophobic molecules as the main DOM components of the wastewater. The adsorption studies identified high selectivity in the adsorption of DOM with biopolymers and hydrophobic molecules being adsorbent in the greatest fractions (>30% removal). Despite humic acids being the most abundant, very low adsorption capacities were observed (2% removal). This phenomenon was attributed to the much larger molecules such as

biopolymers which may interfere with the diffusion of humic acids into the internal network. The researchers then investigated the adsorption of micropollutants from wastewater effluent, in the presence and absence of DOM. It was found that all DOM had a negative impact on adsorption kinetics, with all pollutants having a lower removal after 30 min when compared to those adsorbed in ultrapure water. This was attributed to limited diffusion and the formation of complexes between DOM and the pollutants. However, after 72 h, half of the pollutants tested had achieved similar adsorption capacities when compared to experiments conducted in ultrapure water.

Phosphoric acid-modified biochar synthesised from chicken feather have been applied to adsorb HMs in the presence of some DOM components, namely proline and glucose (Chen et al., 2019). The study consisted of a series of batch absorption experiments, which firstly investigated the adsorption capacity of the material as mono- and binary-component systems (Fig. 23a). From this data, a significant reduction in the adsorption capacity is observed in the dual system when compared to the mono-system, particularly for  $Cd^{2+}$ . The preferential adsorption of  $Pb^{2+}$  was attributed to several factors, namely the smaller hydrated radii, lower  $pK_H$ , and higher electronegativity of  $Pb^{2+}$ , when compared to  $Cd^{2+}$  (Table 17), which ultimately facilitates the diffusion of Pb into the porous network and increases the affinity toward polar functional groups.

**4.2.2.2. Salinity.** Salinity is a much more difficult factor to navigate, being composed of a number of ions, the most abundant being chloride ( $Cl^-$ ), sodium ( $Na^+$ ), sulphate ( $SO_4^{2-}$ ), magnesium ( $Mg^{2+}$ ), calcium ( $Ca^{2+}$ ) and potassium ( $K^+$ ) which make up approximately 99 wt% of all sea salts. Due to the small size of the ions, pore size exclusion is impossible. Additionally, ionic strength (IS) has been identified to have a major influence on adsorption processes. For this reason, there has been significant research into the potential interactions between adsorbent materials, ion-containing liquids (such as saline solutions) and adsorbates. The most cited mechanisms of adsorption in ion-containing liquids include ionic strength, salting-out effects, ion paring, intermolecular aggregation and sphere complexation which have been discussed in depth elsewhere (Zhang et al., 2019).

In summary, salting-out theory describes the enhanced hydrophobic

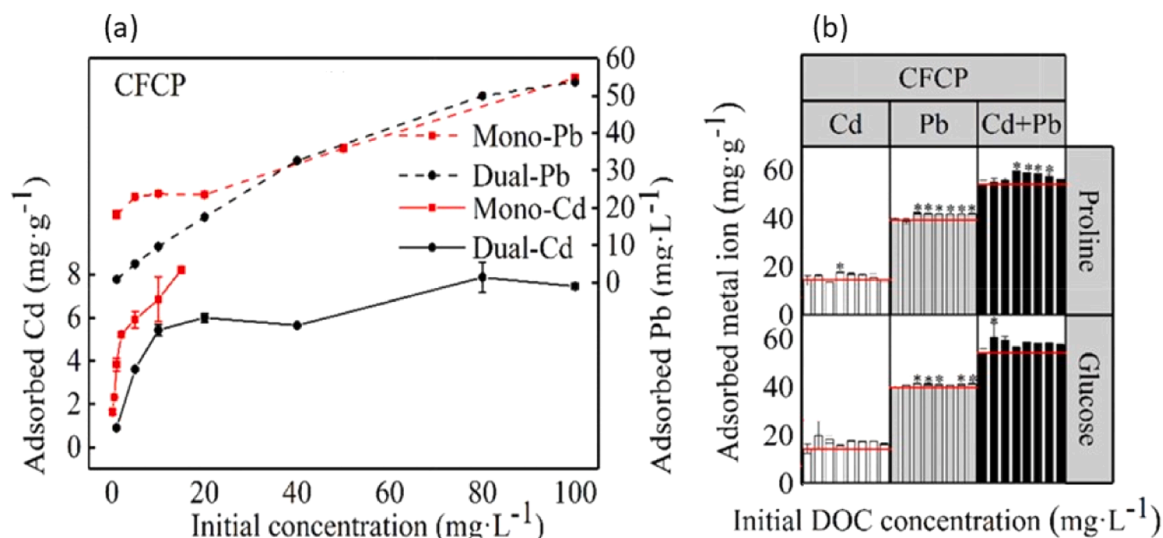


Fig. 23. The Cd<sup>2+</sup> and Pb<sup>2+</sup> adsorption by CFC2 in the single and binary metal systems (a), and the initial DOC concentrations for each column (left to right are 0, 1, 5, 10, 15, 30, 50, and 90 mg/L).

Table 17  
Physiochemical characteristics of Pb and Cd.

	Pb	Cd
Hydrated Radii (Å)	4.01	4.26
pK <sub>H</sub>	7.71	10.1
Electronegativity	2.33	1.69

effects between an adsorbent and adsorbate which is caused when increasing ion concentrations result in a reduction in the solubility of an adsorbent. The effect is commonly applied to describe the adsorption organic compounds containing benzene-like structures.

Ion pairing involves the partial association between two oppositely charged ions in solution via long-range electrostatic interactions (Fig. 24). For two ions to be considered a pair, they must interact at separation *r*, which must be smaller than the specified cut-off *R*. When *r* > *R*, ions are free. The distance between the molecules is also limited by the sum of the ionic radii of both oppositely charged ions  $\alpha$ , due to strong repulsive forces between outer electron shells. Therefore, to be considered as an ion pair, the following characteristics must apply,  $\alpha \leq r \leq R$ .

Intermolecular aggregation can describe several different effects, with cation bridging being most applicable to the pollutants in question. This has been discussed in depth in Section 6.2.2.1. where cation bridging is observed between the adsorbent, HMs and antibiotics. Similarly, in this situation, cation bridging can occur between the

adsorbate, divalent ions (Mg<sup>2+</sup>, Ca<sup>2+</sup> etc.), and antibiotics.

Sphere complexation largely describes interactions that are covalent in character and interact with water (Fig. 25). The phenomenon can be divided into inner sphere surface complexes, which describes the arrangement of water atoms in relation to the adsorbent-adsorbate system.

Xia et al. investigated the impacts of NaCl and CaCl<sub>2</sub> on the adsorption of antibiotics, sulfapyridine (SPY) and sulfadimethoxine (SDM) using four adsorbent materials, including ACs (F-400) and MWCNTs (Xia et al., 2013). When considering F-400 and MWCNT, at environmentally relevant pH, there was a positive correlation between adsorption capacity and salt concentration up to a salt concentration of 3 wt%, for all samples except F-400 when adsorbing SPY combined with CaCl<sub>2</sub>, where there was a negative correlation (Fig. 26). The increased adsorption capacity for the former three samples was attributed to three phenomena, salting out theory, binding of the Ca<sup>2+</sup> ions to the antibiotic, which interact with  $\pi$ -electrons or negatively charged surface groups within the adsorbent, and finally, the screening of surface charges which allow for the hydrophobic groups to more readily interact with the surface.

Song et al. investigated the impacts of salinity on the adsorption of TCs onto porous hexagonal boron nitride particles. The study found that increasing the NaCl concentration from 0 to 100 mmol/L led to a 13.39% increase in the adsorption of TCs (Song et al., 2017). This phenomenon can be attributed to salting out theory.

As can be seen from above, there has been research into the impacts

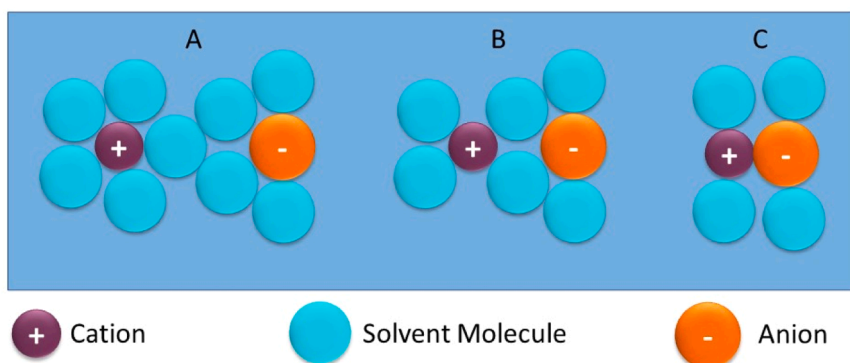


Fig. 24. Schematic representation of ion-pair types: (A) solvent separated (2SIP), (B) solvent shared (SIP), and (C) contact (CIP) (Ebie et al., 2001).

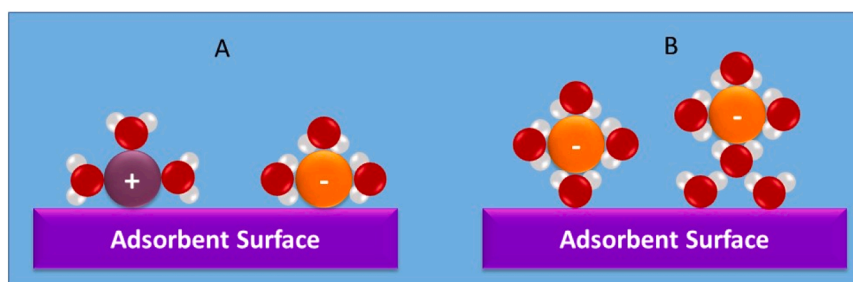


Fig. 25. Schematic picture of the (a) inner-sphere and (b) outer-sphere surface complexes. Adopted from Zhang et al. (2019).

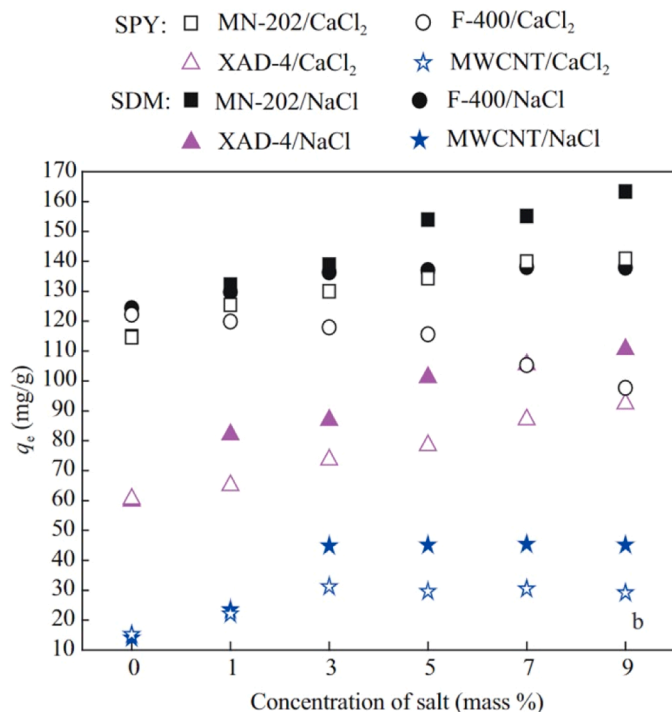


Fig. 26. Influence of ionic concentration (NaCl and CaCl<sub>2</sub>) on adsorbed amounts of sulfadimethoxine at 303 K pH of 8.0 and initial concentration of 100 mg/L (Xia et al., 2013).

of various ionic liquids individually, with the most researched being NaCl and CaCl<sub>2</sub>. However, there appears to be a gap in literature when focusing on environmentally relevant solutions composed of the common ions found in saline waters.

### 5. Leaching

As previously mentioned, low-cost is a fundamental aspect of adsorbent preparation. This makes the valorisation of waste materials an attractive route in the synthesis of adsorbents. However, using waste inevitably increases the likelihood of unknown chemical species being present within the adsorbent structure. Furthermore, adsorbates may leach from a spent adsorbent. It is imperative to determine which chemical species may be leached from an adsorbent, to prevent harm to ecosystems. There are two key stages where leaching potential should be assessed: during the lifetime of an adsorbent and during disposal of a spent adsorbent.

Typically, governmental organisations have standard protocols to determine leaching potential of a material, for example, the Leaching Environmental Assessment Framework (LEAF) and the UK landfill

directive published by the Environmental Protection Agency (EPA, USA) and the Environmental Agency (UK), respectively (Environmental Protection Agency, 2017; Environment Agency, 2003). Typically, these tests involve either simulating a specific environmental condition (e.g. salinity, pH, temperature, DOM etc.) or sequential chemical extraction tests to determine the subsequent leachates (Tiwari et al., 2015).

A one-stage batch leaching procedure is the simplest type of test, where an adsorbate is placed in a known volume of leachant solution, under agitation until chemical equilibrium is reached, the most commonly cited method being a toxicity characteristic leaching procedure (TCLP). Alternatively, column leaching tests can be applied, which involve percolating a leachant through a fixed bed of porous material, which provides results that better reflect real systems by simulating solute transport caused by fluid flow. However, the technique suffers from higher costs and more complex operations in comparison to batch testing (Tiwari et al., 2015). The subsequent leachates are typically analysed using a range of analytical techniques. For metal analysis techniques typically include AAS or ICP-OES, while HPLC is more commonly applied to assessment of organics.

Several studies have applied TCLP to determine the leaching behaviour of HMs, such as Cu, Fe, Zn and Al, from CAs (Wang et al., 2017; Mahedi et al., 2019). The method consists of preparing a stock solution of extraction fluid containing, 5.7 ml of glacial acetic acid and 64.3 ml of 1 M sodium hydroxide in 1 L of deionised water. The spent adsorbent was then combined with the extraction fluid in a 1:20 (w/v%) ratio for 18 h. The samples were then vacuum filtered and divided into two aliquots, one of which was acidified (pH<2) with 10% nitric acid. The resulting solution was analysed using ICP-OES to determine HM concentrations.

### 6. Regeneration

Reusability and recyclability of adsorbents is fundamental to make an adsorbent industrially viable and reduce the environmental impact of CAs, making regeneration studies a key aspect which must be studied. The aim is to desorb pollutants remaining on the adsorbent surface, without significant alteration to the porous structure of the adsorbent, to retain the original adsorption capacity (Dutta et al., 2019; Salvador et al., 2015). The effectiveness of a regeneration technique is typically determined using desorption efficiency (DE) and regeneration efficiency (RE).

DE - also known as cumulative heel - can be defined as the percentage of adsorbate desorbed with respect to total amount adsorbed within an exhausted structure. DE is commonly measured by comparing differences in weight of a CA, between the adsorption cycles (Eq. (17)) (Dutta et al., 2019; Jahandar Lashaki et al., 2016).

$$DE(\%) = \frac{M_{AA} - M_{BA}}{M_{VA}} \times 100 \tag{16}$$

Where, M<sub>AA</sub> and M<sub>BA</sub> are the masses of the adsorbent after and before an adsorption cycle, respectively. M<sub>VA</sub> is the mass of the virgin adsorbent.

RE involves comparing the adsorption capacities of the original CA with the regenerated CA, and can be determined using Eq. (18) (Salvador et al., 2015).

$$RE(\%) = \frac{q_{reg}}{q_{orig}} \times 100 \quad (17)$$

Where,  $q_{reg}$  and  $q_{orig}$  are the adsorption capacities of the regenerated and original CA, respectively.

Adsorbent regeneration typically can be divided into several categories, namely, thermal, chemical, vacuum and biological (Table 18). These can be further sub-divided into several categories. Of the techniques, vacuum regeneration isn't typically applicable in aqueous-phase adsorption due to the lack of high-pressure vessels, which would be economically unviable to implement, purely for regeneration purposes, therefore, this technique will not be discussed further in this review.

Thermal regeneration is an industrialised technique which provides energy via conventional heating or physical waves such as microwaves to break adsorbate-adsorbent bonds. Temperature swing adsorption is a commonly applied industrial technique. The apparatus requires a minimum of a two-column system, where one column is operational and the other is spent. The spent adsorption column is regenerated by purging with inert gas ( $N_2$ , Ar or He) whilst heating to temperatures  $< 300\text{ }^\circ\text{C}$ , to thermally decompose adsorbates on the adsorbent surface). However, for aqueous phase adsorption, this technique is not typically viable since the adsorbent would first need to be dried prior to the TSA being implemented, after which the column would need to be cooled to temperatures  $< 90\text{ }^\circ\text{C}$  to be applicable in aqueous media.

Alternatively, steam TSA can be employed as a thermal generation technique in aqueous media, which benefits from reduced temperatures ( $< 200\text{ }^\circ\text{C}$ ) and enhanced heat capacity of steam over inert gases (Salvador et al., 2015).

Electro-assisted regeneration.

### 7. End-of-life adsorbents

In order to maintain a sustainable approach for the management of pollution in aquaculture, proper end-of-life management of spent adsorbents is paramount. At present several potential pathways exist for EoL CAs, namely, incineration, landfill, regeneration or reactivation (Kozyatnyk et al., 2020; Baskar et al., 2022).

Kozyatnyk et al. investigated the disposal of three CAs, AC, hydrochar (HC) and biochar (BC). This was achieved by life cycle assessment approach to determine the environmental impacts of the four EoL pathways. Fig. 27 shows the environmental impacts of each EoL scenario, where it can be seen that regeneration has the lowest environmental impact for each of the adsorbent materials. As discussed in Section 6, there are numerous techniques to regenerate CAs, however, over numerous cycles the RE declines, eventually reaching a point where the adsorbent may not be industrially feasible. At this point, an alternative disposal route should be applied.

In order to landfill spent adsorbents, full regeneration and leaching tests are required, to prevent harmful adsorbates such as antibiotics and HMs from entering soils and waterways. It is recommended that antibiotic-laden CAs are disposed of in accordance with the WHO's guidelines for safe disposal of pharmaceuticals, which suggests they are incinerated at a temperature greater than  $1200\text{ }^\circ\text{C}$  (Kozyatnyk et al., 2020; Guidelines for safe disposal of unwanted pharmaceuticals in and after emergencies, 1999).

In recent years, several studies have aimed to promote reuse and recovery of spent adsorbents to provide long-term alternative solutions for waste disposal. A number of studies have investigated secondary uses of spent adsorbents (Rial and Ferreira, 2022; Liu et al., 2019; Shen et al., 2020; Huang et al., 2020). For example, Rial et al. investigated the photocatalytic degradation of methylene blue using  $Cd^{2+}$ -laden CAs, achieving a maximum degradation of 97.4% (Rial and Ferreira, 2022).

**Table 18**  
Comparison between regeneration technologies.

Regeneration Technique	Method	Advantages	Disadvantages
Thermal	Pyrolysis at high temperature to thermally desorb or decompose adsorbates. RE increases with temperature	Simple operation High RE Industrial scalability Suitable for adsorbents loaded with a heterogeneous mixture of adsorbates	Reduction in $S_{BET}$ due to decomposition High energy consumption
Solvent	Vary pH, temperature and/or ionic strength of solvent to desorb adsorbates. Can be conducted at supercritical or subcritical conditions.	Can be coupled with other degradation processes such as including Fenton degradation. Useful for organics with high concentrations and low boiling points Simple operation High RE	RE is dependent on the solubility of the adsorbate within the solvent. Residual solvent may cause pore blocking. Hazardous waste stream Solvents need to be recycled. Limited scalability Lack of knowledge, new technology Mass transfer limitations between electrodes can cause residual adsorbate at the cathode.
Electro-chemical	Application of an electrical current for electrochemical oxidation of adsorbates.	Simple operation Suitable for both inorganic and organic adsorbates Low adsorbent fouling Low energy consumption Quick High RE	
Microwave	Apply MW irradiation to thermally desorb or decompose adsorbates.	Enhanced homogeneity of desorption Can increase pore size and surface area. Quick Low energy consumption High RE	Expensive Better suited to fluidised bed systems Pore-blocking from decomposition products
Ultrasonic	Provide sonicating power to cause desorption via physical phenomena (i.e. micro-streaming/turbulence)	Low energy consumption Simple operation No attrition of adsorbent No secondary pollution	Only effective for physisorption (Yu et al., 2021) Low RE
Ozonation	Supply adsorbent with a continuous flow of an ozone-oxygen mixture, to remove adsorbates via ozonation or interactions with free radicals	Readily degrades organic adsorbates. Little degradation to $S_{BET}$ Can improve adsorption capacity of adsorbent	Modification of adsorbent surface Doesn't react with all molecules. Requires calculation of adsorbent before reuse
Biological	Application of microbials for biodegradation of adsorbates	Converts toxic pollutants into small non-toxic molecules	Limited scalability Fouling due to regeneration by-products More effective for chemically activated adsorbents than thermally activated (Omorogie et al., 2014).

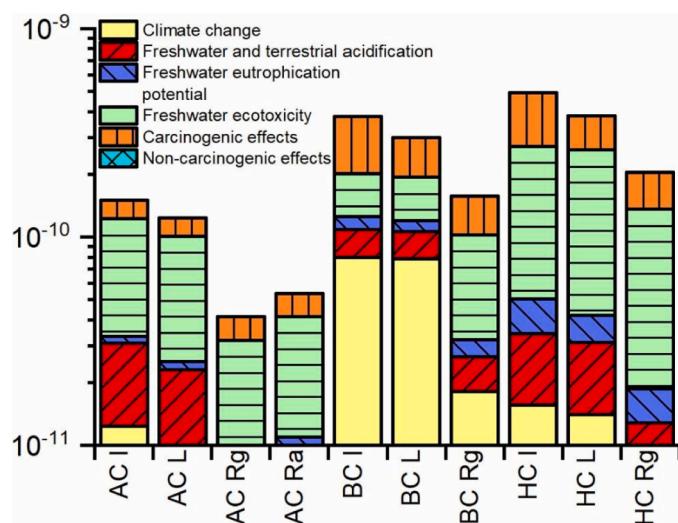


Fig. 27. Overall normalised environmental impacts of the ten end-of-life scenarios. AC – Activated Carbon; BC – Biochar; HC – Hydrochar. I – Incineration; L – Landfilling; Rg – Regeneration; Ra – Reactivation (Kozyatnyk et al., 2020).

However, more research is required within this area to create a circular economy for CAs.

## 8. Future prospectives

To improve the sustainability of aquaculture practices globally, better practices and management are required, particularly for CAs to be fully understood within an aquaculture setting, further research is required into competitive adsorption between pollutants and/or environmental matrices. Despite the wide range of lab-scale studies applying CAs to adsorb aquaculture pollutants such as antibiotics and HMs, there are much fewer articles applying real aquaculture effluents (Chen et al., 2020; Igwegbe et al., 2022). Although there is a lack of research in this area, current studies are promising. Igwegbe et al. applied bio-coagulation and adsorption kinetics characterisation techniques to investigate the purification of aquaculture effluent, using *Picralima nitida* seeds. The ACs were shown to be promising for the removal of turbidity, total suspended solids, chemical oxygen demand, biochemical oxygen demand and colour, achieving removal efficiencies of 90.35%, 88.84%, 82.38%, 82.11% and 65.77%, respectively. Furthermore, several review articles have highlighted adsorption as a promising technique for remediation of aquaculture effluents, however, at present there are few articles which apply CAs within this field (Li et al., 2023; Emenike et al., 2021b). Therefore, significant research is required in order to bridge this gap in literature.

Moreover, to enable a circular economy Of CAs, better EoL management is required. Further research should be conducted, particularly regarding high-value secondary uses of spent adsorbents such as catalysts, secondary adsorption or cement production etc (Rial and Ferreira, 2022).

## 9. Conclusions

In this paper the authors reviewed the sources and effects of various pollutants within the aquaculture industry, finding that antibiotics and HMs have shown the greatest ecotoxicological impacts on organisms and human health. However, at present, databases on chemical use in aquaculture are very limited, therefore better documentation and management is required to gain a better insight into the chemicals introduced into fish farms.

The authors then applied a cradle-to-grave approach to review CAs as a possible solution to remediate contaminated aquaculture waters,

finding them to be a promising candidate. Numerous studies have demonstrated that a wide range of carbonaceous precursors (such as biomass, CFs, CNTs etc.), can be successfully activated using physical or chemical methods to produce adsorbents with high specific surface areas (>500 mg/g), developed porosity and high adsorption capacities. Furthermore, CAs can be readily modified to increase selectivity, and therefore adsorption capacity toward target pollutants. It was found that CAs with mesoporous or hierarchical porosity and high concentrations of surface functionalities are typically favoured in aqueous phase adsorption, to facilitate the diffusion of the pollutants into the porous network and enhance the hydrophilicity of the material.

Several review articles have highlighted adsorption as a promising technique for aquaculture remediation, however few studies have applied CAs to real world aquaculture samples. For CAs to become integrated within the aquaculture industry as a purification technology, further research is required to fully understand the impacts of competitive adsorption between target pollutants and environmental matrices (e.g. DOM and salinity).

Since it was found that developing countries consume the largest quantities of antibiotics and heavy metals, costs should be limited where possible. Therefore, the authors suggested that waste valorisation should be applied for precursor materials, where possible and processing steps should be limited. Chemical activation was found to be a particularly attractive technique since carbonisation, activation and surface modification can occur in a one-step process, therefore keeping expenses to a minimum.

## Declaration of Competing Interest

The authors declare that they have no known competing financial interests or personal relationships that could have appeared to influence the work reported in this paper.

## Data availability

No data was used for the research described in the article.

## Acknowledgements

This work has been funded by the UK's Engineering and Physical Sciences Research Council (EPSRC), as part of the UKRI, via the EPSRC Doctoral Training Partnership (project reference EP/T518116/1). The authors would like to thank and acknowledge the undergraduate research assistants from the Department of Chemical Engineering at Brunel University London, namely, Anila Islami and Emily Diaz, for all their assistance during this project. Also, the authors would like to recognise the Experimental Techniques Centre (ETC) at Brunel University London and their scientific officers, Uchechukwu Onwukwe and Nicholas Nelson, for facilitating access to analytical equipment.

## Appendix A. Supporting information

Supplementary data associated with this article can be found in the online version at doi:10.1016/j.ecoenv.2023.115552.

## References

- Carabineiro, S.A.C., 2011. 'Thavorn-AT 'Oeurea, MFR 'Figueiredo, J.I'. Adsorption of ciprofloxacin on surface-modified carbon materials. *Water Res* 45 (15), 4583–4591.
- Abatal, M., Anastopoulos, I., Giannakoudakis, D.A., Olguin, M.T., 2020. Carbonaceous material obtained from bark biomass as adsorbent of phenolic compounds from aqueous solutions. *J. Environ. Chem. Eng.* 8 (3), 103784. Jun 1.
- Abbas, A.S., Ahmed, M.J., Darweesh, T.M., 2016. Adsorption of fluoroquinolones antibiotics on activated carbon by K<sub>2</sub>CO<sub>3</sub> with microwave assisted activation. *Iraqi J. Chem. Pet. Eng.* [Internet] 17 (2), 15–23. Jun 2016 [cited 2021 Feb 24]. (<https://ijcpe.uobaghdad.edu.iq/index.php/ijcpe/article/view/78/74>).

- Adamczuk, A., Kotolnyńska, D., 2015. Equilibrium, thermodynamic and kinetic studies on removal of chromium, copper, zinc and arsenic from aqueous solutions onto fly ash coated by chitosan. *Chem. Eng. J.* 274, 200–212. Aug 15.
- Adriano, W.S., Veredas, V., Santana, C.C., Gonçalves, L.R.B., 2005. Adsorption of amoxicillin on chitosan beads: Kinetics, equilibrium and validation of finite bath models. *Biochem. Eng. J.* 27 (2), 132–137. Dec 15.
- Agboola O.S., Oluغبenga &, Bello S. Enhanced adsorption of ciprofloxacin from aqueous solutions using functionalized banana stalk. [cited 2022 Nov 30]; Available from: <https://doi.org/10.1007/s13399-020-01038-9>.
- Ahmad, A., Sheikh Abdullah, S.R., Hasan, H.A., Othman, A.R., Ismail, N., 2021. 'Izzati. Aquaculture industry: Supply and demand, best practices, effluent and its current issues and treatment technology. *J. Environ. Manag.* 287, 112271.
- Ahmed, M., Loric, M.H., 2002. Improving developing country food security through aquaculture development—lessons from Asia. *Food Policy* 27 (2), 125–141.
- Ai, Y., Liu, Y., Huo, Y., Zhao, C., Sun, L., Han, B., et al., 2019. Insights into the adsorption mechanism and dynamic behavior of tetracycline antibiotics on reduced graphene oxide (RGO) and graphene oxide (GO) materials. *Environ. Sci. Nano* [Internet] 6 (11), 3336–3348. Nov 7 [cited 2023 Sep 5]. (<https://pubs.rsc.org/en/content/article/html/2019/en/c9en00866g>).
- Aik Chong Lua, Guo J., 2001. Preparation and characterization of activated carbons from oil-palm stones for gas-phase. *Adsorpt. Colloids Surf. A Physicochem. Eng. Asp.* 179 (2–3), 151–162. Jan 30.
- Aktar, J., 2021. Batch adsorption process in water treatment. *Intell. Environ. Data Monit. Pollut. Manag.* 1–24. Jan 1.
- Al-Degs, Y.S., El-Barghouti, M.I., El-Sheikh, A.H., Walker, G.M., 2008. Effect of solution pH, ionic strength, and temperature on adsorption behavior of reactive dyes on activated carbon. *Dyes Pigments* 77 (1), 16–23. Jan 1.
- Alkathiri, D.S.S., Sabri, M.A., Ibrahim, T.H., ElSayed, Y.A., Jumean, F., 2020. Development of activated carbon fibers for removal of organic contaminants. Dec 1 [cited 2021 Mar 3] *Int. J. Environ. Sci. Technol.* [Internet] 17 (12), 4841–4852. <https://doi.org/10.1007/s13762-020-02808-8>.
- Ameen, F., Mostafazadeh, R., Hamidian, Y., Erk, N., Sanati, A.L., Karaman, C., et al., 2023. Modeling of adsorptive removal of azithromycin from aquatic media by CoFe<sub>2</sub>O<sub>4</sub>/NiO anchored microalgae-derived nitrogen-doped porous activated carbon adsorbent and colorimetric quantifying of azithromycin in pharmaceutical products. *Chemosphere* 329, 138635. Jul 1.
- Amer, M., Elwardany, A., 2020. Biomass Carbonisation. In: al Qubeissi, M., El-kharouf, A., Serhad Soyhan, H. (Eds.), *Renewable Energy*. IntechOpen, London, pp. 211–232.
- Anderson J.L., Asche F., Garlock T., Chu J. Aquaculture: Its Role in the Future of Food, 2017.
- Aranda P.R., Colombo L., Perino E., De Vito I.E., Raba J. Solid-phase preconcentration and determination of mercury(II) using activated carbon in drinking water by X-ray fluorescence spectrometry. *X-Ray Spectrometry* [Internet]. 2013 Mar 1 [cited 2023 Sep 6];42(2):100–104. Available from: <https://onlinelibrary.wiley.com/doi/full/10.1002/xrs.2440>.
- Aranda, P.R., Llorens, I., Perino, E., De Vito, I., Raba, J., 2016. Removal of arsenic(V) ions from aqueous media by adsorption on multiwall carbon nanotubes thin film using XRF technique. *Environ. Nanotechnol. Monit. Manag.* 5, 21–26. May 1.
- Babaei, A.A., Lima, E.C., Takdastan, A., Alavi, N., Goudarzi, G., Vosoughi, M., et al., 2016. Removal of tetracycline antibiotic from contaminated water media by multi-walled carbon nanotubes: operational variables, kinetics, and equilibrium studies. *Water Sci. Technol.* 74 (5), 1202–1216. Sep 19.
- Baek, J., Lee, H.M., An, K.H., Kim, B.J., 2019. Preparation and characterization of highly mesoporous activated short carbon fibers from kenaf precursors. *Carbon Lett.* [Internet] 29 (4), 393–399. Aug 1 [cited 2023 Apr 9]. (<https://link.springer.com/article/10.1007/s42823-019-00042-y>).
- Bai, B.C., Kim, E.A., Lee, C.W., Lee, Y.S., Im, J.S., 2015. Effects of surface chemical properties of activated carbon fibers modified by liquid oxidation for CO<sub>2</sub> adsorption. *Appl. Surf. Sci.* 353, 158–164. Oct 30.
- Bai, B.C., Lee, H.U., Lee, C.W., Lee, Y.S., Im, J.S., 2016. N<sub>2</sub> plasma treatment on activated carbon fibers for toxic gas removal: Mechanism study by electrochemical investigation. *Chem. Eng. J.* 306, 260–268.
- Bardestani R., Patience G.S., Kaliaguine S. Experimental methods in chemical engineering: specific surface area and pore size distribution measurements—BET, BJH, and DFT. *Can J Chem Eng* [Internet]. 2019 Nov 1 [cited 2023 Feb 14];97(11): 2781–2791. Available from: <https://onlinelibrary.wiley.com/doi/full/10.1002/cjce.23632>.
- Baskar, A.V., Bolan, N., Hoang, S.A., Sooriyakumar, P., Kumar, M., Singh, L., et al., 2022. Recovery, regeneration and sustainable management of spent adsorbents from wastewater treatment streams: A review. *Sci. Total Environ.* 822, 153555. May 20.
- Bevan E., Fu J., Luberti M., Zheng Y. Challenges and opportunities of hydrothermal carbonisation in the UK; case study in Chirnside, 2021.
- Bhatnagar, A., Hogland, W., Marques, M., Sillanpää, M., 2013. An overview of the modification methods of activated carbon for its water treatment applications. *Chem. Eng. J.* 219, 499–511. Mar 1.
- Bhatt, P., Goe, A., 2017. Carbon fibres: production, properties and potential use. *Mater. Sci. Res. India* 14 (1), 52–57. Jun 28.
- Bills, T.D., Marking, L.L., King, E.L., Walker, C.R., Howell, J.H., Alien, J.L., et al., 1977. Formalin: its toxicity to nontarget aquatic organisms, persistence, and counteraction. *Investig. Fish. Control* 73, 1–7.
- Bîru, E.I., Iovu, H., 2018. Graphene Nanocomposites Studied by Raman Spectroscopy. *Raman Spectrosc.* [Internet]. Jan 26 [cited 2022 Jan 4]. (<https://www.intechopen.com/chapters/59012>).
- Boyd C.E., McNevin A.A. Chemicals in Aquaculture. *Aquaculture, Resource Use, and the Environment* [Internet]. 2014 Dec 26 [cited 2023 Jan 8];173–210. Available from: <https://onlinelibrary.wiley.com/doi/full/10.1002/9781118857915.ch9>.
- Boyd, C.E., McNevin, A.A., 2015. *Aquaculture, Resource Use, and the Environment*. Vol. 9780470959, Aquaculture, Resource Use, and the Environment. Wiley Blackwell,, pp. 1–337.
- Canales-Flores, R.A., Prieto-García, F., 2020. Taguchi optimization for production of activated carbon from phosphoric acid impregnated agricultural waste by microwave heating for the removal of methylene blue. *Diam. Relat. Mater.* 109, 108027. Nov 1.
- Chai, W.S., Cheun, J.Y., Kumar, P.S., Mubashir, M., Majeed, Z., Banat, F., et al., 2021. A review on conventional and novel materials towards heavy metal adsorption in wastewater treatment application. *J. Clean. Prod.* 296, 126589. May 10.
- Chanda S., Nath Paul B., Ghosh K. Dietary essentiality of trace minerals in aquaculture: A Review. *Agriculture Research Communication Centre* [Internet]. 2015 [cited 2023 Feb 7]; Available from: [www.arcjournals.com](http://www.arcjournals.com).
- Chen, H., Liu, S., Xu, X.R., Liu, S.S., Zhou, G.J., Sun, K.F., et al., 2015. Antibiotics in typical marine aquaculture farms surrounding Hailing Island, South China: Occurrence, bioaccumulation and human dietary exposure. *Mar Pollut Bull* 90 (1–2), 181–187.
- Chen, H., Li, W., Wang, J., Xu, H., Liu, Y., Zhang, Z., et al., 2019. Adsorption of cadmium and lead ions by phosphoric acid-modified biochar generated from chicken feather: Selective adsorption and influence of dissolved organic matter. *Bioresour. Technol.* 292, 121948. Nov 1.
- Chen, J.Y., 2016. *Activated Carbon Fibre and Textiles*. Elsevier Science & Technology,, pp. 08–25.
- Chen, Y., Yu, W., Zheng, R., Li, J.Y., Zhang, L., Wang, Q., et al., 2020. Magnetic activated carbon (MAC) mitigates contaminant bioavailability in farm pond sediment and dietary risks in aquaculture products. *Sci. Total Environ.* 736, 139185. Sep 20.
- Choi, Y.J., Kim, J.H., Lee, K.B., Lee, Y.S., Im, J.S., 2019. Correlation verification of process factors and harmful gas adsorption properties for optimization of physical activation parameters of PAN-based carbon fibers. *J. Ind. Eng. Chem.* 80, 152–159. Dec 25.
- Dao, T.M., Le Luu, T., 2020. Synthesis of activated carbon from macadamia nutshells activated by H<sub>2</sub>SO<sub>4</sub> and K<sub>2</sub>CO<sub>3</sub> for methylene blue removal in water. *Bioresour. Technol. Rep.* 12, 100583. Dec 1.
- Davidi S., Lashanizadegan A., Sharifard H. Walnut shell activated carbon: Optimization of synthesis process, characterization and application for Zn (II) removal in batch and continuous process. *Mater Res Express* [Internet]. 2019 May 24 [cited 2021 Feb 11];6(8):085621. Available from: <https://iopscience.iop.org/article/10.1088/2053-1591/ab213e>.
- Dawood, M.A.O., Koshio, S., 2016. Recent advances in the role of probiotics and prebiotics in carp aquaculture: A review. *Aquaculture* 454, 243–251. Mar 1.
- Demiral, İ., Samdan, C., Demiral, H., 2021. Enrichment of the surface functional groups of activated carbon by modification method. *Surf. Interfaces* 22, 100873. Feb 1.
- Dias, J.M., Alvim-Ferraz, M.C.M., Almeida, M.F., Rivera-Utrilla, J., Sánchez-Polo, M., 2007. Waste materials for activated carbon preparation and its use in aqueous-phase treatment: A review. *J. Environ. Manag.* 85 (4), 833–846. Dec 1.
- Din M., Ashraf S., progress A.I.-S., 2017 undefined. Comparative study of different activation treatments for the preparation of activated carbon: a mini-review. *journals.sagepub.com* [Internet]. 2017 Sep 1 [cited 2023 Jan 26];100(3):299–312. Available from: <https://journals.sagepub.com/doi/pdf/10.3184/003685017x14967570531606>.
- Doyo, A.N., Kumar, R., Barakat, M.A., 2023. Recent advances in cellulose, chitosan, and alginate based biopolymeric composites for adsorption of heavy metals from wastewater. *J. Taiwan Inst. Chem. Eng.* 151, 105095. Oct 1.
- Dqbrowski, A., 1999. Adsorption - Its development and application for practical purposes. Vol. 120 A, *Stud. Surf. Sci. Catal.* 3–68.
- Drakeford B.M. Notes: Fisheries & Aquaculture The role of aquaculture in economic growth, food security and poverty reduction.
- Dutta, T., Kim, T., Vellingiri, K., Tsang, D.C.W., Shon, J.R., Kim, K.H., et al., 2019. Recycling and regeneration of carbonaceous and porous materials through thermal or solvent treatment. *Chem. Eng. J.* 364, 514–529. May 15.
- Ebie, K., Li, F., Azuma, Y., Yuasa, A., Hagishita, T., 2001. Pore distribution effect of activated carbon in adsorbing organic micropollutants from natural water. *Water Res* 35 (1), 167–179. Jan 1.
- Edie, D.D., Dunham, M.G., 1989. Melt spinning pitch-based carbon fibers. *Carbon N. Y.* 27 (5), 647–655.
- El-Hendawy, A.N.A., Alexander, A.J., Andrews, R.J., Forrest, G., 2008. Effects of activation schemes on porous, surface and thermal properties of activated carbons prepared from cotton stalks. *J. Anal. Appl. Pyrolysis* 82 (2), 272–278. Jul 1.
- Elwakeel, K.Z., Guibal, E., 2015. Selective removal of Hg(II) from aqueous solution by functionalized magnetic-macromolecular hybrid material. *Chem. Eng. J.* 281, 345–359. Dec 1.
- EMA. OXYTETRACYCLINE, TETRACYCLINE, CHLORTETRACYCLINE - Summary Report (2) [Internet]. 1996b [cited 2023 Jan 5]. Available from: [https://www.ema.europa.eu/en/documents/mrl-report/oxytetracycline-tetracycline-chlortetracycline-summary-report-2-committee-veterinary-medical\\_en.pdf](https://www.ema.europa.eu/en/documents/mrl-report/oxytetracycline-tetracycline-chlortetracycline-summary-report-2-committee-veterinary-medical_en.pdf).
- EMA. OXYTETRACYCLINE, TETRACYCLINE, CHLORTETRACYCLINE - Summary Report (1) [Internet]. 1996a [cited 2023 Jan 5]. Available from: [https://www.ema.europa.eu/en/documents/mrl-report/oxytetracycline-tetracycline-chlortetracycline-summary-report-1-committee-veterinary-medical\\_en.pdf](https://www.ema.europa.eu/en/documents/mrl-report/oxytetracycline-tetracycline-chlortetracycline-summary-report-1-committee-veterinary-medical_en.pdf).
- Emenike E.C., Iwuozor K.O., Anidiobi S.U. Heavy Metal Pollution in Aquaculture: Sources, Impacts and Mitigation Techniques. *Biological Trace Element Research* 2021 200:10 [Internet]. 2021a Nov 23 [cited 2023 Feb 6];200(10):4476–92. Available from: <https://link.springer.com/article/10.1007/s12011-021-03037-x>.



- Emenike, E.C., Iwuozor, K.O., Anidiobi, S.U., 2021b. Heavy Metal Pollution in Aquaculture: Sources, Impacts and Mitigation Techniques. *Biol. Trace Elem. Res.* 2021 200:10 [Internet] 200 (10), 4476–4492. Nov 23 [cited 2023 Sep 12]. (<https://link.springer.com/article/10.1007/s12011-021-03037-x>).
- Environment Agency. Guidance on Monitoring of Landfill Leachate, Groundwater and Surface Water [Internet], 2003 [cited 2023 Feb 9]. Available from: ([www.environment-agency.wales.gov.uk](http://www.environment-agency.wales.gov.uk)).
- Environmental Protection Agency U. Leaching Environmental Assessment Framework (LEAF) How-To Guide, 2017.
- Ewis, D., Hameed, B.H., 2021. A review on microwave-assisted synthesis of adsorbents and its application in the removal of water pollutants. *J. Water Process Eng.* 41, 102006. Jun 1.
- Fenoradosa, T.A., Ali, G., Delattre, C., Laroche, C., Petit, E., Wadouachi, A., et al., 2010. Extraction and characterization of an alginate from the brown seaweed *Sargassum turbinarioides* Grunow. *J. Appl. Phycol.* [Internet] 22 (2), 131–137. Apr 14 [cited 2023 Sep 16]. (<https://link.springer.com/article/10.1007/s10811-009-9432-y>).
- Frank, E., Hermanutz, F., Buchmeiser, M.R., 2012. Carbon fibers: Precursors, manufacturing, and properties. *Macromol. Mater. Eng.* 297 (6), 493–501 (Jun).
- Fu S., Fang Q., Li A., Li Z., Han J., Dang X., et al. Accurate characterization of full pore size distribution of tight sandstones by low-temperature nitrogen gas adsorption and high-pressure mercury intrusion combination method. *Energy Sci Eng* [Internet]. 2021 Jan 1 [cited 2023 Feb 14];9(1):80–100. Available from: <https://onlinelibrary.wiley.com/doi/full/10.1002/ese3.817>.
- Gang, D., Uddin Ahmad, Z., Lian, Q., Yao, L., Zappi, M.E., 2021. A review of adsorptive remediation of environmental pollutants from aqueous phase by ordered mesoporous carbon. *Chem. Eng. J.* 403, 126286. Jan 1.
- Gao, Y., Yue, Q., Gao, B., Li, A., 2020. Insight into activated carbon from different kinds of chemical activating agents: A review. *Sci. Total Environ.* 746, 141094. Dec 1.
- Gbadejesin, L.A., Tang, X., Liu, C., Cheng, J., 2022. Transport of Veterinary Antibiotics in Farmland Soil: Effects of Dissolved Organic Matter. *Int J. Environ. Res Public Health* [Internet] 19 (3), 1702. Feb 1 [cited 2022 Dec 7]. (<https://www.mdpi.com/1660-4601/19/3/1702/html>).
- Ge, Y., Cheng, B., Wang, X., Zhao, T., 2020. Rapid Preparation of Activated Carbon Fiber Felt under Microwaves: Pore Structures, Adsorption of Tetracycline in Water, and Mechanism. *Ind. Eng. Chem. Res* [Internet] 59 (1), 146–153. Jan 8 [cited 2022 Nov 25]. (<https://pubs.acs.org/doi/abs/10.1021/acs.iecr.9b04259>).
- Goertzen, S.L., Thériault, K.D., Oickle, A.M., Tarasuk, A.C., Andreas, H.A., 2010. Standardization of the Boehm titration. Part I. CO<sub>2</sub> expulsion and endpoint determination. *Carbon N. Y* 48 (4), 1252–1261. Apr 1.
- Gorbounov, M., Taylor, J., Petrovic, B., Masoudi Soltani, S., 2022. To DoE or not to DoE? A Technical Review on & Roadmap for Optimisation of Carbonaceous Adsorbents and Adsorption Processes. *S Afr. J. Chem. Eng.* 41, 111–128. Jul 1.
- Guedidi, H., Reinert, L., Soneda, Y., Bellakhal, N., Duclaux, L., 2017. Adsorption of ibuprofen from aqueous solution on chemically surface-modified activated carbon cloths. *Arab. J. Chem.* 10, S3584–S3594. May 1.
- Guidelines for safe disposal of unwanted pharmaceuticals in and after emergencies, 1999.
- Guillossou, R., le Roux, J., Mailler, R., Pereira-Derome, C.S., Varrault, G., Bressy, A., et al., 2020. Influence of dissolved organic matter on the removal of 12 organic micropollutants from wastewater effluent by powdered activated carbon adsorption. *Water Res* 172, 115487. Apr 1.
- Gun'ko, V.M., 2007. Competitive adsorption. In: *Theoretical and Experimental Chemistry 2007* 43:3 [Internet], 43, pp. 139–183. May [cited 2022 Jan 25]. (<https://link.springer.com/article/10.1007/s11237-007-0020-4>). May [cited 2022 Jan 25].
- de Haan, A., 2015. Adsorption and ion exchange. *Process Technology: An Introduction* [Internet]. Walter de Gruyter, pp. 177–196 [cited 2023 Feb 10]. (<https://ebookcentral.proquest.com/lib/brunelu/reader.action?docID=1727164#>) [cited 2023 Feb 10].
- Hadi, P., To, M.H., Hui, C.W., Lin, C.S.K., McKay, G., 2015. Aqueous mercury adsorption by activated carbons. *Water Res* 73, 37–55. Apr 15.
- Han, Q., Wang, J., Goodman, B.A., Xie, J., Liu, Z., 2020. High adsorption of methylene blue by activated carbon prepared from phosphoric acid treated eucalyptus residue. *Powder Technol.* 366, 239–248. Apr 15.
- Hannesson, R., 2003. Aquaculture and fisheries. *Mar. Policy* 27 (2), 169–178. Mar 1.
- Hassan, A.F., Abdel-Mohsen, A.M., Elhadidy, H., 2014. Adsorption of arsenic by activated carbon, calcium alginate and their composite beads. *Int J. Biol. Macromol.* [Internet] 68, 125–130 [cited 2023 Sep 16]. (<https://pubmed.ncbi.nlm.nih.gov/24780567/>).
- Hassan, M.F., Sabri, M.A., Fazal, H., Hafeez, A., Shezad, N., Hussain, M., 2020. Recent trends in activated carbon fibers production from various precursors and applications—A comparative review. *J. Anal. Appl. Pyrolysis* 145, 104715. Jan 1.
- Heidari, M., Dutta, A., Acharya, B., Mahmud, S., 2019. A review of the current knowledge and challenges of hydrothermal carbonization for biomass conversion. *J. Energy Inst.* 92 (6), 1779–1799. Dec 1.
- Heidarnejad Z., Dehghani M.H., Heidari M., Javedan G., Ali I., Sillanpää M. Methods for preparation and activation of activated carbon: a review. *Environmental Chemistry Letters* 2020 18:2 [Internet]. 2020 Jan 4 [cited 2022 Oct 20];18(2):393–415. Available from: <https://link.springer.com/article/10.1007/s10311-019-00955-0>.
- Hermann, G., Hüttinger, K.J., 1986. Mechanism of water vapour gasification of carbon-A new model. *Carbon N. Y* 24 (6), 705–713.
- Hoseinzadeh Hesas, R., Arami-Niya, A., Wan Daud, W.M.A., Sahu, J.N., 2013. Preparation of granular activated carbon from oil palm shell by microwave-induced chemical activation: Optimisation using surface response methodology. *Chem. Eng. Res. Des.* 91 (12), 2447–2456. Dec 1.
- Huang, C.C., Su, Y.J., 2010. Removal of copper ions from wastewater by adsorption/electrosorption on modified activated carbon cloths. *J. Hazard Mater.* 175 (1–3), 477–483. Mar 15.
- Huang, D., Li, B., Ou, J., Xue, W., Li, J., Li, Z., et al., 2020. Megamerger of biosorbents and catalytic technologies for the removal of heavy metals from wastewater: Preparation, final disposal, mechanism and influencing factors. *J. Environ. Manag.* 261, 109879. May 1.
- (\*) Huang, L., Zhang, B., Niu, S., Gao, B., 2013. Characterization of activated carbon fiber by microwave heating and the adsorption of tetracycline antibiotics. *Sep. Sci. Technol.* 48 (19).
- Ighalo, J.O., Iwuozor, K.O., Igwegbe, C.A., Adeniyi, A.G., 2021. Verification of pore size effect on aqueous-phase adsorption kinetics: A case study of methylene blue. *Colloids Surf. A Physicochem Eng. Asp.* 626, 127119. Oct 5.
- Ighalo, J.O., Eletta, O.A.A., Adeniyi, A.G., 2022. Biomass carbonisation in retort kilns: Process techniques, product quality and future perspectives. *Bioresour. Technol.* Rep. 17, 109879. May 1.
- Igwegbe, C.A., Ovuoraye, P.E., Białowiec, A., Okpala, C.O.R., Onukwuli, O.D., Dehghani, M.H., 2022. Purification of aquaculture effluent using *Picalima nitida* seeds. *Sci. Rep.* 12 (1), 1–19. Dec 14 [cited 2023 Aug 31]. (<https://www.nature.com/articles/s41598-022-26044-x>).
- Illingworth, J.M., Rand, B., Williams, P.T., 2022. Understanding the mechanism of two-step, pyrolysis-alkali chemical activation of fibrous biomass for the production of activated carbon fibre matting. *Fuel Process. Technol.* 235, 107348. Oct 1.
- Ioannidou, O., Zabaniotou, A., 2007. Agricultural residues as precursors for activated carbon production—A review. *Renew. Sustain. Energy Rev.* 11 (9), 1966–2005. Dec 1.
- Jahandar Lashaki, M., Atkinson, J.D., Hashisho, Z., Phillips, J.H., Anderson, J.E., Nichols, M., 2016. The role of beaded activated carbon's pore size distribution on heel formation during cyclic adsorption/desorption of organic vapors. *J. Hazard Mater.* 315, 42–51. Sep 5.
- Jawad, A.H., Razuan, R., Appaturi, J.N., Wilson, L.D., 2019. Adsorption and mechanism study for methylene blue dye removal with carbonized watermelon (*Citrullus lanatus*) rind prepared via one-step liquid phase H<sub>2</sub>SO<sub>4</sub> activation. *Surf. Interfaces* 16, 76–84. Sep 1.
- Jorda M. High surface area carbon nanotubes prepared by chemical activation, 2002.
- Kamjunke, N., Nimptsch, J., Harir, M., Herzsprung, P., Schmitt-Kopplin, P., Neu, T.R., et al., 2017. Land-based salmon aquacultures change the quality and bacterial degradation of riverine dissolved organic matter. *Sci. Rep.* 7 (1), 1–15. Mar 3 [cited 2023 Jan 23]. (<https://www.nature.com/articles/srep43739>).
- Kan, Y., Zhang, R., Xu, X., Wei, B., Shang, Y., 2023. Comparative study of raw and HNO<sub>3</sub>-modified porous carbon from waste printed circuit boards for sulfadiazine adsorption: Experiment and DFT study. *Chin. Chem. Lett.* 34 (7), 108272.
- Kang S., Jian-chun J., Dan-dan C. Preparation of activated carbon with highly developed mesoporous structure from *Camellia oleifera* shell through water vapor gasification and phosphoric acid modification. *Biomass Bioenergy* [Internet]. 2011 Aug [cited 2022 Nov 19];35(8):3643–7. Available from: [https://www.researchgate.net/publication/251628937\\_Preparation\\_of\\_activated\\_carbon\\_with\\_highly\\_developed\\_mesoporous\\_structure\\_from\\_Camellia\\_oleifera\\_shell\\_through\\_water\\_vapor\\_gasification\\_and\\_phosphoric\\_acid\\_modification](https://www.researchgate.net/publication/251628937_Preparation_of_activated_carbon_with_highly_developed_mesoporous_structure_from_Camellia_oleifera_shell_through_water_vapor_gasification_and_phosphoric_acid_modification).
- Karimi-Maleh, H., Ayati, A., Davoodi, R., Tanhaei, B., Karimi, F., Malekmohammadi, S., et al., 2021. Recent advances in using of chitosan-based adsorbents for removal of pharmaceutical contaminants: A review. *J. Clean. Prod.* 291, 125880. Apr 1.
- Khan, I., Huang, S., Wu, C., Yarlagadda, V., Lin, G., Chong, Y., et al., 2019. Acid modified multiwalled carbon nanotubes condition by reflux [cited 2022 Nov 22] *Mater. Res Express* [Internet] 6, 115003. <https://doi.org/10.1088/2053-1591/ab4396>.
- Kim, K.-W., Lee, H.-M., Kang, S.-H., 2021. Kim B-J. Synthesis and Characterization of Activated Carbon Fibers Derived from Linear Low-Density Polyethylene Fibers Stabilized at a Low Temperature. *Polym. (Basel)* 13 (3918). Nov 12.
- Kodama, S., Sekiguchi, H., 2006. Estimation of point of zero charge for activated carbon treated with atmospheric pressure non-thermal oxygen plasmas. *Thin Solid Films* 506–507, 327–330. May 26.
- Kozyatnyk, I., Yacout, D.M.M., Van Caneghem, J., Jansson, S., 2020. Comparative environmental assessment of end-of-life carbonaceous water treatment adsorbents. *Bioresour. Technol.* 302, 122866. Apr 1.
- Kumar, M., Ando, Y., 2010. Chemical Vapor Deposition of Carbon Nanotubes: A Review on Growth Mechanism and Mass Production. *J. Nanosci. Nanotechnol.* 10 (6), 3739–3758 (Jun).
- Langmuir I. The adsorption of gases on plane surfaces of glass, mica and platinum. *J Am Chem Soc* [Internet]. 1918 Sep 1 [cited 2022 Nov 28];40(9):1361–1403. Available from: <https://pubs.acs.org/doi/abs/10.1021/ja02242a004>.
- Leal, Joana F., Maria Graça, P. M. S. Neves, Santos, B. H. Eduarda, Valdemar, I., 2018. Esteves Use of formalin in intensive aquaculture: properties, application and effects on fish and water quality, 2018 Jun 1 [cited 2023 Jan 9] *Rev Aquac* [Internet] 10 (2), 281–295. Available from: <https://onlinelibrary.wiley.com/doi/full/10.1111/raq.12160>.
- Lee, T., Ooi, C.-H., Othman, R., Yeoh, F.-Y., Lee, T., Ooi, C.-H., et al., 2014. Activated carbon fiber-the hybrid of carbon fiber and activated carbon. *Rev. Adv. Mater. Sci.* 36, 118–136.
- Lewis, I.C., 1982. Chemistry of carbonization. *Carbon N. Y.* 20 (6), 519–529. Jan 1.
- Li, H., Cui, Z., Cui, H., Bai, Y., Yin, Z., Qu, K., 2023. Hazardous substances and their removal in recirculating aquaculture systems: A review. *Aquaculture* 569, 739399. May 15.
- Li, Y.H., Ding, J., Luan, Z., Di, Z., Zhu, Y., Xu, C., et al., 2003. Competitive adsorption of Pb<sup>2+</sup>, Cu<sup>2+</sup> and Cd<sup>2+</sup> ions from aqueous solutions by multiwalled carbon nanotubes. *Carbon N. Y.* 41 (14), 2787–2792. Jan 1.

- Lillo-Ródenas, M.A., Cazorla-Amorós, D., Linares-Solano, A., 2003. Understanding chemical reactions between carbons and NaOH and KOH: An insight into the chemical activation mechanism. *Carbon* N. Y. 41 (2), 267–275. Feb 1.
- Liu, B., Du, C., Chen, J.J., Zhai, J.Y., Wang, Y., Li, H.L., 2021. Preparation of well-developed mesoporous activated carbon fibers from plant pulp fibers and its adsorption of methylene blue from solution. *Chem. Phys. Lett.* 771, 138535. May 16.
- Liu, M., Li, X., Du, Y., Han, R., 2019. Adsorption of methyl blue from solution using walnut shell and reuse in a secondary adsorption for Congo red. *Bioresour. Technol. Rep.* 5, 238–242.
- Liu, X., Chen, Z.Q., Han, B., Su, C.L., Han, Q., Chen, W.Z., 2018. Biosorption of copper ions from aqueous solution using rape straw powders: Optimization, equilibrium and kinetic studies. *Ecotoxicol. Environ. Saf.* [Internet] 150, 251–259. Apr 15 [cited 2022 Dec 5]. (<https://pubmed.ncbi.nlm.nih.gov/29288906/>).
- Liu Y. Is the Free Energy Change of Adsorption Correctly Calculated? *J Chem Eng Data* [Internet]. 2009 Jul 9 [cited 2022 Nov 30];55(7):1981–1985. Available from: <https://pubs.acs.org/doi/full/10.1021/je800661q>.
- Lu, A.H., Zheng, J.T., 2001. Study of microstructure of high-surface-area polyacrylonitrile activated carbon fibers. *J. Colloid Interface Sci.* 236 (2), 369–374. Apr 15.
- Lu, C., Chiu, H., 2008. Chemical modification of multiwalled carbon nanotubes for sorption of Zn<sup>2+</sup> from aqueous solution. *Chem. Eng. J.* 139 (3), 462–468. Jun 15.
- Lua A.C., Yang T. Effect of activation temperature on the textural and chemical properties of potassium hydroxide activated carbon prepared from pistachio-nut shell. *J Colloid Interface Sci* [Internet]. 2004 Jun 15 [cited 2022 Nov 10];274(2): 594–601. Available from: <https://pubmed.ncbi.nlm.nih.gov/15144834/>.
- Lua, Aik Chong, Guo, J., 2001. Preparation and characterization of activated carbons from oil-palm stones for gas-phase adsorption. *Colloids Surf. A Physicochem Eng. Asp.* 179 (2–3), 151–162. Jan 30.
- Lulijwa, R., Rupaia, E.J., Alfaro, A.C., 2020. Antibiotic use in aquaculture, policies and regulation, health and environmental risks: a review of the top 15 major producers. *Rev. Aquac.* [Internet] 12 (2), 640–663. May 1 [cited 2022 Dec 12]. (<https://onlinelibrary.wiley.com/doi/full/10.1111/raq.12344>).
- Maciá-Agulló, J.A., Moore, B.C., Cazorla-Amorós, D., Linares-Solano, A., 2004. Activation of coal tar pitch carbon fibres: Physical activation vs. chemical activation. *Carbon*. Elsevier Ltd., pp. 1367–1370.
- Maciá-Agulló, J.A., Moore, B.C., Cazorla-Amorós, D., Linares-Solano, A., 2007. Influence of carbon fibres crystallinities on their chemical activation by KOH and NaOH. *Microporous Mesoporous Mater.* 101 (3), 397–405. Apr 20.
- Mahedi, M., Cetin, B., Dayioglu, A.Y., 2019. Leaching behavior of aluminum, copper, iron and zinc from cement activated fly ash and slag stabilized soils. *Waste Manag.* 95, 334–355. Jul 15.
- Mahmood T., Saddique M.T., Naem A., Westerhoff P., Mustafa S., Alum A. Comparison of Different Methods for the Point of Zero Charge Determination of NiO. *Ind Eng Chem Res* [Internet]. 2011 Sep 7 [cited 2023 Feb 13];50(17):10017–10023. Available from: <https://pubs.acs.org/doi/abs/10.1021/ie200271d>.
- Marsh, H., Rodríguez-Reinoso, F., 2006a. Activation Processes (Thermal or Physical). *Activated Carbon* 243–321. Jan 1.
- Marsh, H., Rodríguez-Reinoso, F., 2006a. Characterization of Activated Carbon. *Act. Carbon* 143–242. Jan 1.
- Marsh, H., Rodríguez-Reinoso, F., 2006b. Activation Processes (Chemical). *Act. Carbon* 322–365. Jan 1.
- Martín-Gullón, I., Andrews, R., Jagtoyen, M., Derbyshire, F., 2001. PAN-based activated carbon fiber composites for sulfur dioxide conversion: Influence of fiber activation method. *Fuel* 80 (7), 969–977. May 1.
- Martins, A.C., Pezoti, O., Cazetta, A.L., Bedin, K.C., Yamazaki, D.A.S., Bandoch, G.F.G., et al., 2015. Removal of tetracycline by NaOH-activated carbon produced from macadamia nut shells: Kinetic and equilibrium studies. *Chem. Eng. J.* 260, 291–299.
- Melanitis N., Tetlow P.L., Galiotis C. Characterization of PAN-based carbon fibres with laser Raman spectroscopy. *Journal of Materials Science* 1996 31:4 [Internet]. 1996b Feb 1 [cited 2022 Jan 18];31(4):851–860. Available from: <https://link.springer.com/article/10.1007/BF00352882>.
- Melanitis, N., Tetlow, P.L., Galiotis, C., 1996a. Characterization of PAN-based carbon fibres with laser Raman spectroscopy Part I Effect of processing variables on Raman band profiles. *J. Mater. Sci.* 31, 860.
- Miranda C.D., Godoy F.A., Lee M.R. Current status of the use of antibiotics and the antimicrobial resistance in the Chilean salmon farms [Internet]. Vol. 9. *Frontiers in Microbiology*. Frontiers Media S.A.; 2018 [cited 2021 Jun 8]. p. 1284. Available from: [www.frontiersin.org](http://www.frontiersin.org).
- Mohamed A.R., Mohammadi M., Darzi G.N. Preparation of carbon molecular sieve from lignocellulosic biomass: A review. *Renewable and Sustainable Energy Reviews* [Internet]. 2010 [cited 2022 Nov 19];14(6):1591–9. Available from: <https://ideas.repec.org/a/eee/rensus/v14y2010i6p1591-1599.html>.
- Monser, L., Adhoum, N., 2002. Modified activated carbon for the removal of copper, zinc, chromium and cyanide from wastewater. *Sep Purif. Technol.* 26 (2–3), 137–146. Mar 1.
- Monteiro, S.H., Francisco, J.G., Campion, T.F., Pimpinato, R.F., Moura Andrade, G.C.R., Garcia, F., et al., 2015. Multiresidue antimicrobial determination in Nile tilapia (*Oreochromis niloticus*) cage farming by liquid chromatography tandem mass spectrometry. *Aquaculture* 447, 37–43. Oct 1.
- Moussavi, G., Alahabadi, A., Yaghmaei, K., Eskandari, M., 2013. Preparation, characterization and adsorption potential of the NH<sub>4</sub>Cl-induced activated carbon for the removal of amoxicillin antibiotic from water. *Chem. Eng. J.* 217, 119–128. Feb 1.
- Murray C.J., Ikuta K.S., Sharara F., Swetschinski L., Robles Aguilar G., Gray A., et al. Global burden of bacterial antimicrobial resistance in 2019: a systematic analysis. *The Lancet* [Internet]. 2022 Feb 12 [cited 2023 Feb 6];399(10325):629–55. Available from: <http://www.thelancet.com/article/S0140673621027240/fulltext>.
- (C) Nayeri, D., Mousavi, S.A., Mehrabi, A., 2019. Oxytetracycline removal from aqueous solutions using activated carbon prepared from corn stalks. *J. Appl. Res. Water Wastewater* 11.
- Nazraz M., Yamini Y., Asiabi H. Chitosan-based sorbent for efficient removal and extraction of ciprofloxacin and norfloxacin from aqueous solutions. *Microchimica Acta* [Internet]. 2019 Jul 1 [cited 2023 Sep 15];186(7):1–9. Available from: <https://link.springer.com/article/10.1007/s00604-019-3563-x>.
- Neme, I., Gonfa, G., Masi, C., 2022. Activated carbon from biomass precursors using phosphoric acid: A review. *Heliyon* 8 (12), e11940. Dec 1.
- Neolaka, Y.A.B., Lawa, Y., Naat, J., Riwu, A.A.P., Darmokoeseoemo, H., Widyaningrum, B. A., et al., 2021. Indonesian Kesambi wood (*Schleichera oleosa*) activated with pyrolysis and H<sub>2</sub>SO<sub>4</sub> combination methods to produce mesoporous activated carbon for Pb(II) adsorption from aqueous solution. *Environ. Technol. Innov.* 24, 101997. Nov 1.
- Neolaka, Y.A.B., Riwu, A.A.P., Aigbe, U.O., Ukhurebor, K.E., Onyancha, R.B., Darmokoeseoemo, H., et al., 2023. Potential of activated carbon from various sources as a low-cost adsorbent to remove heavy metals and synthetic dyes. *Results Chem.* 5, 100711. Jan 1.
- Nimptsch, J., Woelfl, S., Osorio, S., Valenzuela, J., Ebersbach, P., von Tuempling, W., et al., 2015. Tracing dissolved organic matter (DOM) from land-based aquaculture systems in North Patagonian streams. *Sci. Total Environ.* 537, 129–138. Dec 15.
- Njoku, V.O., Foo, K.Y., Asif, M., Hameed, B.H., 2014. Preparation of activated carbons from rambutan (*Nephelium lappaceum*) peel by microwave-induced KOH activation for acid yellow 17 dye adsorption. *Chem. Eng. J.* 250, 198–204. Aug 15.
- Noh, J.S., Schwarz, J.A., 1990. Effect of HNO<sub>3</sub> treatment on the surface acidity of activated carbons. *Carbon* N. Y. 28 (5), 675–682. Jan 1.
- Oda, H., Yamashita, A., Minoura, S., Okamoto, M., Morimoto, T., 2006. Modification of the oxygen-containing functional group on activated carbon fiber in electrodes of an electric double-layer capacitor. *J. Power Sources* 158 (2), 1510–1516. Aug 25.
- Oickle, A.M., Goertzen, S.L., Hopper, K.R., Abdalla, Y.O., Andreas, H.A., 2010. Standardization of the Boehm titration: Part II. Method of agitation, effect of filtering and dilute titrant. *Carbon* N. Y. 48 (12), 3313–3322. Oct 1.
- Okman, I., Karagöz, S., Tay, T., Erdem, M., 2014. Activated Carbons From Grape Seeds By Chemical Activation With Potassium Carbonate And Potassium Hydroxide. *Appl. Surf. Sci.* 293, 138–142. Feb 28.
- Omorige M.O., Babalola J.O., Unuabonah E.I. Regeneration strategies for spent solid matrices used in adsorption of organic pollutants from surface water: a critical review. *New pub: Balaban* [Internet]. 2014 Jan 8 [cited 2023 Apr 12];57(2):518–44. Available from: <https://www.tandfonline.com/doi/abs/10.1080/19443994.2014.967726>.
- Park, S.J., Kim, B.J., 2004. Influence of oxygen plasma treatment on hydrogen chloride removal of activated carbon fibers. *J. Colloid Interface Sci.* 275 (2), 590–595. Jul 15.
- Park, S.-J., Kim, K.-D., 2001. Influence of activation temperature on adsorption characteristics of activated carbon fiber composites. *Carbon* N. Y. 39, 1741–1746.
- Pauly, D., Froese, R., 2012. Comments on FAO's State of Fisheries and Aquaculture, or 'SOFIA 2010'. *Mar. Policy* 36 (3), 746–752. May 1.
- Pelekani, C., Snoeyink, V.L., 1999. Competitive adsorption in natural water: role of activated carbon pore size. *Water Res* 33 (5), 1209–1219. Apr 1.
- Peng, X., Hu, F., Zhang, T., Qiu, F., Dai, H., 2018. Amine-functionalized magnetic bamboo-based activated carbon adsorptive removal of ciprofloxacin and norfloxacin: A batch and fixed-bed column study. *Bioresour. Technol.* 249, 924–934. Feb 1.
- Pietrzak, R., Nowicki, P., Kaźmierczak, J., Kuszynska, I., Goscińska, J., Przepiórski, J., 2014. Comparison of the effects of different chemical activation methods on properties of carbonaceous adsorbents obtained from cherry stones. *Chem. Eng. Res. Des.* 92 (6), 1187–1191. Jun 1.
- Pradeepkiran J.A. Aquaculture role in global food security with nutritional value: a review. *Transl Anim Sci* [Internet]. 2019 Mar 1 [cited 2022 Oct 18];3(2):903–10. Available from: <https://academic.oup.com/tas/article/3/2/903/5487790>.
- Qin, Q., Wu, X., Chen, L., Jiang, Z., Xu, Y., 2018. Simultaneous removal of tetracycline and Cu(II) by adsorption and coadsorption using oxidized activated carbon. *RSC Adv.* [Internet] 8 (4), 1744–1752. Jan 5 [cited 2022 Mar 24]. (<https://pubs.rsc.org/en/content/articlehtml/2018/ra/c7ra12402c>).
- Rahman, A., Hango, H.J., Daniel, L.S., Uahengo, V., Jaime, S.J., Bhaskaruni, S.V.H.S., et al., 2019. Chemical preparation of activated carbon from *Acacia erioloba* seed pods using H<sub>2</sub>SO<sub>4</sub> as impregnating agent for water treatment: An environmentally benevolent approach. *J. Clean. Prod.* 237, 117689. Nov 10.
- Raychaudhuri, S. sen, Pramanick, P., Talukder, P., Basak, A., 2021. Polyamines, metallothioneins, and phytochelatin—Natural defense of plants to mitigate heavy metals. *Studies in Natural Products*. Chemistry 69, 227–261. Jan 1.
- Raymundo-Piñero, E., Azais, P., Cacciaguerra, T., Cazorla-Amorós, D., Linares-Solano, A., Béguin, F.K.O.H., 2005. and NaOH activation mechanisms of multiwalled carbon nanotubes with different structural organisation. *Carbon* N. Y. 43 (4), 786–795. Jan 1.
- Rehman A., Park M., Park S.-J. Current Progress on the Surface Chemical Modification of Carbonaceous Materials, 2019; Available from: ([www.mdpi.com/journal/coatings](http://www.mdpi.com/journal/coatings)).
- Rial, J.B., Ferreira, M.L., 2022. Potential applications of spent adsorbents and catalysts: Re-valorization of waste. *Sci. Total Environ.* 823, 153370. Jun 1.
- Rico A., Satapornvanit K., Haque M.M., Min J., Nguyen P.T., Telfer T.C., et al. Use of chemicals and biological products in Asian aquaculture and their potential environmental risks: a critical review. *Rev Aquac* [Internet]. 2012 Jun 1 [cited 2022 Dec 12];4(2):75–93. Available from: <https://onlinelibrary.wiley.com/doi/full/10.1111/j.1753-5131.2012.01062.x>.
- Rio, S., Faur-Brasquet, C., Coq, L., le Courcoux, P., Cloirec, P. le, 2005. Experimental design methodology for the preparation of carbonaceous sorbents from sewage sludge by chemical activation—application to air and water treatments. *Chemosphere* 58 (4), 423–437. Jan 1.

- Rio, S., le Coq, L., Faur, C., le Cloirec, P., 2006. Production of porous carbonaceous adsorbent from physical activation of sewage sludge: application to wastewater treatment. *Water Sci. Technol.* 53 (3), 237–244. Feb 1.
- Rivera-Utrilla, J., Sánchez-Polo, M., Gómez-Serrano, V., Álvarez, P.M., Alvim-Ferraz, M.C.M., Dias, J.M., 2011. Activated carbon modifications to enhance its water treatment applications. An overview. *J. Hazard Mater.* 187 (1–3), 1–23. Mar 15.
- Robati D. Pseudo-second-order kinetic equations for modeling adsorption systems for removal of lead ions using multi-walled carbon nanotube. *J. Nanostructure Chem* [Internet]. 2013 Dec 1 [cited 2023 Sep 6];3(1):1–6. Available from: <https://link.springer.com/article/10.1186/2193-8865-3-55>.
- Romero J., Feijóo C.G., Navarrete P. 6 Antibiotics in Aquaculture-Use, Abuse and Alternatives [Internet]. [cited 2021 Apr 7]. Available from: [www.intechopen.com](http://www.intechopen.com).
- Romero-Cano, L.A., García-Rosero, H., González-Gutierrez, L. v, Baldeño-Pérez, L.A., Carrasco-Marín, F., 2017. Functionalized adsorbents prepared from fruit peels: Equilibrium, kinetic and thermodynamic studies for copper adsorption in aqueous solution. *J. Clean. Prod.* 162, 195–204. Sep 20.
- Rong, H., Ryu, Z., Zheng, J., Zhang, Y., 2003. Influence of heat treatment of rayon-based activated carbon fibers on the adsorption of formaldehyde. *J. Colloid Interface Sci.* [Internet] 261 (2), 207–212. May 15 [cited 2023 Apr 10]. (<https://pubmed.ncbi.nlm.nih.gov/16256524/>).
- Ruiz-Fernández M., Alexandre-Franco M., Fernández-González C., Gómez-Serrano V. Development of activated carbon from vine shoots by physical and chemical activation methods. Some insight into activation mechanisms. *Adsorption* [Internet]. 2011 Jun 4 [cited 2023 Jan 25];17(3):621–9. Available from: <https://link.springer.com/article/10.1007/s10450-011-9347-1>.
- Sajjadi B., Chen W.Y., Egiebor N.O. A comprehensive review on physical activation of biochar for energy and environmental applications. *Reviews in Chemical Engineering* [Internet]. 2019 Aug 1 [cited 2023 Jan 25];35(6):735–76. Available from: <https://www.degruyter.com/document/doi/10.1515/revce-2017-0113/html>.
- Salvador, F., Martín-Sánchez, N., Sánchez-Hernández, R., Sánchez-Montero, M.J., Izquierdo, C., 2015. Regeneration of carbonaceous adsorbents. Part I: Thermal Regeneration. *Microporous Mesoporous Mater.* 202, 259–276. Jan 15.
- Sapkota, A., Sapkota, A.R., Kucharski, M., Burke, J., McKenzie, S., Walker, P., et al., 2008. Aquaculture practices and potential human health risks: Current knowledge and future priorities. *Environ. Int* 34 (8), 1215–1226. Nov 1.
- Şenturun-Shalaby, Ç., Uçak-Astarlıoğlu, M.G., Artok, L., Sarici, Ç., 2006 21. Preparation and characterization of activated carbons by one-step steam pyrolysis/activation from apricot stones. *Microporous Mesoporous Mater.* 88 (1–3), 126–134.
- Shah, K.A., Tali, B.A., 2016. Synthesis of carbon nanotubes by catalytic chemical vapour deposition: A review on carbon sources, catalysts and substrates. *Mater. Sci. Semicond. Process* 41, 67–82. Jan 1.
- Shen, W., Zhang, S., He, Y., Li, J., Fan, W., 2011. Hierarchical porous polyacrylonitrile-based activated carbon fibers for CO<sub>2</sub> capture. *J. Mater. Chem.* [Internet] 21 (36), 14036–14040. Sep 28 [cited 2021 Mar 4]. ([www.rsc.org/materials](http://www.rsc.org/materials)).
- Shen, X., Zhu, Z., Zhang, H., Di, G., Chen, T., Qiu, Y., et al., 2020. Carbonaceous composite materials from calcination of azo dye-adsorbed layered double hydroxide with enhanced photocatalytic efficiency for removal of Ibuprofen in water. *Environ. Sci. Eur.* [Internet]. 32 (1), 1–15. Dec 1 [cited 2023 Sep 8]. (<https://link.springer.com/articles/10.1186/s12302-020-00351-4>).
- Silva, T.L., Cazetta, A.L., Souza, P.S.C., Zhang, T., Asefa, T., Almeida, V.C., 2018. Mesoporous activated carbon fibers synthesized from denim fabric waste: Efficient adsorbents for removal of textile dye from aqueous solutions. *J. Clean. Prod.* 171, 482–490. Jan 10.
- Soliman, A.M., Elwy, H.M., Thiemann, T., Majedi, Y., Labata, F.T., Al-Rawashdeh, N.A.F., 2016. Removal of Pb(II) ions from aqueous solutions by sulphuric acid-treated palm tree leaves. *J. Taiwan Inst. Chem. Eng.* 58, 264–273. Jan 1.
- Song, Q., Fang, Y., Liu, Z., Li, L., Wang, Y., Liang, J., et al., 2017. The performance of porous hexagonal BN in high adsorption capacity towards antibiotics pollutants from aqueous solution. *Chem. Eng. J.* 325, 71–79. Oct 1.
- Strezov, V., Patterson, M., Zymła, V., Fisher, K., Evans, T.J., Nelson, P.F., 2007. Fundamental aspects of biomass carbonisation. *J. Anal. Appl. Pyrolysis* 79 (1–2), 91–100. May 1.
- Subasinghe R., Soto D., Jia J. Global aquaculture and its role in sustainable development. *Rev Aquac* [Internet]. 2009 Mar 1 [cited 2021 Feb 24];1(1):2–9. Available from: <http://doi.wiley.com/10.1111/j.1753-5131.2008.01002.x>.
- Sun J., Wang X., Wang C., Wang Q. Effects of activation time on the properties and structure of polyacrylonitrile-based activated carbon hollow fiber. *J Appl Polym Sci* [Internet]. 2006 Mar 5 [cited 2022 Jan 24];99(5):2565–2569. Available from: <https://onlinelibrary.wiley.com/doi/full/10.1002/app.22883>.
- Sun R., Chen J., Pan C., Sun Y., Mai B., Li Q.X. Antibiotics and food safety in aquaculture. *J Agric Food Chem* [Internet]. 2020 Oct 28 [cited 2022 Dec 12];68(43):11908–19. Available from: <https://pubs.acs.org/doi/pdf/10.1021/acs.jafc.0c03996>.
- Świątkowski, A., 1999. Industrial carbon adsorbents. *Stud. Surf. Sci. Catal.* 120, 69–94. Jan 1.
- Tan, I.A.W., Chan, J.C., Hameed, B.H., Lim, L.L.P., 2016. Adsorption behavior of cadmium ions onto phosphoric acid-impregnated microwave-induced mesoporous activated carbon. *J. Water Process Eng.* 14, 60–70. Dec 1.
- Tan Z., Zhang X., Wang L., Gao B., Luo J., Fang R., et al. Sorption of tetracycline on H2O2-modified biochar derived from rape stalk. <https://doi.org/101080/2639594020191607779> [Internet]. 2019 Jan 1 [cited 2023 Feb 2];31(1):198–207. Available from: <https://www.tandfonline.com/doi/abs/10.1080/26395940.2019.1607779>.
- Tavares-Dias M. Toxicity, physiological, histopathological and antiparasitic effects of the formalin, a chemotherapeutic of fish aquaculture. *Aquac Res* [Internet]. 2021 May 1 [cited 2023 Jan 9];52(5):1803–23. Available from: <https://onlinelibrary.wiley.com/doi/full/10.1111/are.15069>.
- Taylor J., Babamohammadi S., Troisi G., Masoudi Soltani S. Chemical Activation of Recycled Carbon Fibres for Application as Porous Adsorbents in Aqueous Media [Internet]. [cited 2022 Nov 17]. Available from: <https://ieeexplore.ieee.org/stamp/stamp.jsp?tp=&arnumber=9928646>.
- Theodore, L., Ricci, F., 2011. *Mass Transfer Operations for the Practicing Engineer*. John Wiley and Sons.
- Thilsted, S.H., Thorne-Lyman, A., Webb, P., Bogard, J.R., Subasinghe, R., Phillips, M.J., et al., 2016. Sustaining healthy diets: The role of capture fisheries and aquaculture for improving nutrition in the post-2015 era. *Food Policy* 61, 126–131. May 1.
- Tiwari, M.K., Bajpai, S., Dewangan, U.K., Tamrakar, R.K., 2015. Suitability of leaching test methods for fly ash and slag: A review. *J. Radiat. Res Appl. Sci.* 8 (4), 523–537. Oct 1.
- Turk Sekulic, M., Boskovic, N., Slavkovic, A., Garunovic, J., Kolakovic, S., Pap, S., 2019. Surface functionalised adsorbent for emerging pharmaceutical removal: Adsorption performance and mechanisms. *Process Saf. Environ. Prot.* 125, 50–63. May 1.
- Vakili, M., Deng, S., Cagnetta, G., Wang, W., Meng, P., Liu, D., et al., 2019. Regeneration of chitosan-based adsorbents used in heavy metal adsorption: A review. *Sep Purif. Technol.* 224, 373–387. Oct 1.
- Varun T.K., Senani S., Jayapal N., Chikkerur J., Roy S., Tekulapally V.B., et al. Extraction of chitosan and its oligomers from shrimp shell waste, their characterization and antimicrobial effect. *Vet World* [Internet]. 2017 Feb 12 [cited 2023 Sep 16];10(2): 170. Available from: <http://pmc/articles/PMC5352841/>.
- Wang, G., Yu, M., Feng, X., 2021a. Carbon materials for ion-intercalation involved rechargeable battery technologies. *Chem. Soc. Rev.* [Internet] 50 (4), 2388–2443. Mar 1 [cited 2022 Nov 21]. (<https://pubs.rsc.org/en/content/articlehtml/2021/cs/d0cs00187b>).
- Wang, J., Guo, X., 2020. Adsorption kinetic models: Physical meanings, applications, and solving methods. *J. Hazard Mater.* 390, 122156. May 15.
- Wang, J., Liu, T.L., Huang, Q.X., Ma, Z.Y., Chi, Y., Yan, J.H., 2017. Production and characterization of high quality activated carbon from oily sludge. *Fuel Process. Technol.* 162, 13–19. Jul 1.
- Wang, Q., Mitchell, R.L., Hofman, R., Yu, J., Yang, M., Rietveld, L.C., et al., 2021b. How properties of low molecular weight model competitors impact organic micropollutant adsorption onto activated carbon at realistically asymmetric concentrations. *Water Res* 202, 117443. Sep 1.
- Wang, S., Li, X., Zhao, H., Quan, X., Chen, S., Yu, H., 2018. Enhanced adsorption of ionizable antibiotics on activated carbon fiber under electrochemical assistance in continuous-flow modes. *Water Res* 134, 162–169. May 1.
- Wang, Z., Wang, G., Li, W., Cui, Z., Wu, J., Akpinar, I., et al., 2021. Loofah activated carbon with hierarchical structures for high-efficiency adsorption of multi-level antibiotic pollutants. *Appl. Surf. Sci.* 550, 149313.
- Watts J.E.M., Schreier H.J., Lanska L., Hale M.S. The Rising Tide of Antimicrobial Resistance in Aquaculture: Sources, Sinks and Solutions. *Mar Drugs* [Internet]. 2017 Jun 1 [cited 2022 Aug 1];15(6). Available from: <http://pmc/articles/PMC5484108/>.
- WEBSTER CD, LIM C. NUTRITION AND FISH HEALTH. [Internet]. CRC Press; 2019 [cited 2023 Feb 7]. 133–135 p. Available from: <https://www.routledge.com/Nutrition-and-Fish-Health/Webster-Lim/p/book/9780367397074>.
- World Health Organisation. Antimicrobial resistance [Internet]. 2021 [cited 2023 Feb 6]. Available from: <https://www.who.int/news-room/fact-sheets/detail/antimicrobial-resistance>.
- Xia, M., Li, A., Zhu, Z., Zhou, Q., Yang, W., 2013. Factors influencing antibiotics adsorption onto engineered adsorbents. *J. Environ. Sci.* 25 (7), 1291–1299. Jul 1.
- Xu, Y., Liu, Y., Chen, S., Ni, Y., 2020. Current Overview of Carbon Fibre: Toward Green Sustainable Raw Materials. *Bioresources* 15 (3), 7234–7259.
- Yadav, M.S.P., Sanjeev, N.O., Vallabha, M.S., Sekar, A., Valsan, A.E., Varghese, G.K., 2022. Competitive adsorption analysis of antibiotics removal from multi-component systems using chemically activated spent tea waste: effect of operational parameters, kinetics, and equilibrium study. *Environ. Sci. Pollut. Res.* [Internet] 1, 1–16. Aug 8 [cited 2023 Jan 16]. (<https://link.springer.com/article/10.1007/s11356-022-22323-2>).
- Yang, H., Liu, H., Zhou, K., Yan, Z.Q., Zhao, R., Liu, Z.H., et al., 2012. Oxidation path analysis of NO in the adsorption and removal process using activated carbon fibers. *J. Fuel Chem. Technol.* 40 (8), 1002–1008. Aug 1.
- Yang, I., Jung, M., Kim, M.S., Choi, D., Jung, J.C., 2021. Physical and chemical activation mechanisms of carbon materials based on the microdomain model. *J. Mater. Chem. A Mater.* [Internet] 9 (15), 9815–9825. Apr 20 [cited 2023 Jan 25]. (<https://pubs.rsc.org/en/content/articlehtml/2021/ta/d1ta00765c>).
- Yu, F., Li, Y., Han, S., Ma, J., 2016. Adsorptive removal of antibiotics from aqueous solution using carbon materials. *Chemosphere* 153, 365–385. Jun 1.
- Yu, J., Meng, Z., Chi, C., Gao, X., Chen, B., Zhu, B., et al., 2021. Low temperature pickling regeneration process for remarkable enhancement in Cu(II) adsorptivity over spent activated carbon fiber. *Chemosphere* [Internet] 281. <https://doi.org/10.1016/j.chemosphere.2021.130868>.
- Yue, Z., Economy, J., 2017a. Carbonization and activation for production of activated carbon fibers. *Act. Carbon Fiber Text.* 61–139.
- Yue, Z., Economy, J., 2017b. Carbonization and activation for production of activated carbon fibers. *Act. Carbon Fiber Text.* 61–139. Jan 1.
- Zhang, L., Zeng, Y., Cheng, Z., 2016. Removal of heavy metal ions using chitosan and modified chitosan: A review. *J. Mol. Liq.* 214, 175–191. Feb 1.
- Zhang, Y., Zhu, C., Liu, F., Yuan, Y., Wu, H., Li, A., 2019. Effects of ionic strength on removal of toxic pollutants from aqueous media with multifarious adsorbents: A review. *Sci. Total Environ.* 646, 265–279. Jan 1.

Zhao, N., He, C., Jiang, Z., Li, J., Li, Y., 2007. Physical activation and characterization of multi-walled carbon nanotubes catalytically synthesized from methane. *Mater. Lett.* 61 (3), 681–685. Feb 1.

Zhao X., Jia B., Sun Q., Jiao G., Liu L., She D. Removal of Cr<sup>6+</sup> ions from water by electrosorption on modified activated carbon fibre felt. *R Soc Open Sci* [Internet].

2018 Sep 1 [cited 2022 Nov 21];5(9). Available from: <https://royalsocietypublishing.org/doi/10.1098/rsos.180472>.

Zhou, C., Zhou, H., Yuan, Y., Peng, J., Yao, G., Zhou, P., et al., 2021. Coupling adsorption and in-situ Fenton-like oxidation by waste leather-derived materials in continuous flow mode towards sustainable removal of trace antibiotics. *Chem. Eng. J.* 420, 130370. Sep 15.